

Studies
on the Role of Cholesterol and Coronin 1
in Antigen-Presenting Cells

Inauguraldissertation

zur

Erlangung der Würde eines Doktors der Philosophie
vorgelegt der
Philosophisch-Naturwissenschaftlichen Fakultät
der Universität Basel

von

Imke Albrecht
aus Meissen, Deutschland

Basel, 2005

Genehmigt von der Philosophisch-Naturwissenschaftlichen Fakultät
auf Antrag von Prof. Dr. Jean Pieters und Prof. Dr. Antonius Rolink.

Basel, den 5. Juli 2005

Prof. Dr. Hans-Jakob Wirz
Dekan

Abstract

Antigen recognition and presentation to subsequently induce an appropriate host response is dependent on the action of antigen-presenting cells such as dendritic cells and macrophages. In this thesis, the function of cholesterol and coronin 1 in antigen-presenting cells was studied.

In the first part of this thesis, the delivery of exogenous antigens into the MHC class I pathway, termed cross-presentation, was investigated. Cross-presentation is important for the establishment of an immune response against viruses or tumour cells *in vivo*. Antigens to be cross-presented are frequently internalized via macropinocytosis. Here it is shown, that by cholesterol-depletion of antigen-presenting cells macropinosome formation was abolished resulting in an impaired cross-presentation of exogenous antigens. In accordance with a role of cholesterol in cross-presentation, modification of antigens by palmitoylation, a modification known to increase the affinity to cholesterol, resulted in a strongly enhanced uptake and improved cross-presentation of the antigen. Together, these results indicate that cholesterol plays an important role in macropinocytosis and in the subsequent delivery of antigens into the MHC class I pathway. To explore palmitoylation as a modification that would enhance cross-presentation of antigens, we found that such modification often results in the insolubility of the modified antigen. For specific antigens however the use of palmitoylation to improve cross-presentation of soluble proteins could be explored for the development of new vaccines.

The second part of this thesis focused on coronin 1, a member of the WD repeat protein family of actin-binding proteins termed coronins. In contrast to the other mammalian coronins, coronin 1 is expressed predominantly in leukocytes arguing for a role in leukocyte specific processes. To understand a function for coronin 1, the structure of coronin 1 was analyzed. Coronin 1 consists of three structural domains: a N-terminal region containing 5 WD40 repeats, which is connected by a linker region with a C-terminal coiled coil domain. Coronin 1 occurs *in vivo* as homotrimeric complexes, which associate with the plasma membrane and with the cytoskeleton via two distinct binding domains. It was found, that association of coronin 1 with the cytoskeleton was mediated by coiled coil induced trimerization of a stretch of positively charged residues within the linker region. In contrast, plasma membrane binding was independent of the oligomerization state of coronin 1 and required the presence of the N-terminal, WD repeat-containing domain. By bridging the F-actin cytoskeleton with the plasma membrane coronin1 may serve as a linker integrating outside signals with the remodelling of the F-actin cytoskeleton.

Table of Contents

Chapter 1: General Introduction.....	1
1.1. Abstract.....	2
1.2. The immune system.....	2
1.3. The basic mechanisms in adaptive immunity.....	3
1.4. The antigen-presenting cells.....	4
1.4.1. B-cells.....	4
1.4.2. Macrophages.....	4
1.4.3. Dendritic cells.....	5
1.5. The sampling of antigens.....	5
1.5.1. Receptor-mediated endocytosis.....	6
1.5.2. Phagocytosis.....	6
1.5.3. Macropinocytosis.....	6
1.6. Antigen-processing.....	7
1.6.1. The MHC class I pathway.....	7
1.6.2. The MHC class II pathway.....	8
1.7. Cross-presentation: The MHC class I pathway for exogenous antigens.....	10
1.7.1. The nature of the cross-presented antigen.....	10
1.7.2. The nature of the cross-presenting cell.....	11
1.7.3. The mechanism of cross-presentation.....	11
1.7.3.1. The TAP-independent pathway.....	11
1.7.3.2. The TAP-dependent pathway.....	12
1.7.3.2.1. MHC class I loading in the ER.....	13
1.7.3.2.2. MHC class I loading in the ER-phagosome.....	13
1.7.3.2.3. How does the cytosolic transport of antigens occur?.....	15
1.7.4. Regulation of cross-presentation.....	15
1.8. Antigen-presentation and T-cell activation.....	16
1.8.1. Formation of an immunological synapse at the contact site between T-cell and antigen-presenting cells.....	16
1.8.2. Role of lipid rafts and the cytoskeleton in formation of the immunological synapse.....	17
1.9. Coronin 1.....	18
1.10. Aims of this thesis.....	19
1.11. References.....	20
 Chapter 2: Materials and Methods.....	 31
2.1. Reagents.....	32
2.1.1. Chemicals.....	32
2.1.2. Kits.....	34
2.1.3. Peptides.....	35
2.2. General buffers and solutions.....	35
2.3. Bacterial media and supplements.....	36
2.4. Cell culture media and supplements.....	36
2.5. Vectors.....	38
2.6. Oligonucleotides.....	39
2.7. Antibodies / Dyes.....	40
2.8. Bacteria, culture conditions.....	41
2.9. Cells and cell lines, culture conditions.....	42
2.10. Molecular biology.....	43

2.10.1. Agarose gel electrophoresis.....	43
2.10.2. Preparation of electro-competent <i>E. coli</i> BL21.....	43
2.10.3. Preparation of ultra-competent <i>E. coli</i> DH10 β	43
2.10.4. Transformation.....	44
2.10.5. Cloning procedure.....	44
2.10.5.1. Polymerase chain reaction (PCR).....	44
2.10.5.2. Restriction digest of plasmid DNA/PCR fragments.....	45
2.10.5.3. Dephosphorylation of DNA.....	45
2.10.5.4. Purification of DNA from agarose gel.....	45
2.10.5.5. Ligation with T4 DNA ligase.....	45
2.10.5.6. Ligation of PCR products into pGEM [®] -T Easy Vector (Subcloning).....	46
2.10.5.7. Preparation of plasmid DNA from <i>E. coli</i> cultures.....	46
2.10.5.8. Ethanol precipitation of DNA.....	46
2.10.6. Site directed mutagenesis.....	47
2.10.7. Sequencing.....	47
2.11. Cell culture.....	48
2.11.1. Determination of cell numbers.....	48
2.11.2. Freezing and thawing of cells.....	48
2.11.3. Subculture and freezing of J774A.1 cells.....	48
2.11.4. Subculture and freezing of adherent cells.....	48
2.11.5. Preparation of L929-conditioned medium.....	49
2.11.6. Generation of murine bone marrow derived macrophages and dendritic cells.....	49
2.11.7. Isolation of total and CD8 ⁺ lymphocytes from OT-1 mice.....	49
2.11.8. Isolation of CD14 ⁺ monocytes and CD8 ⁺ T-cells from human peripheral blood.....	50
2.11.9. Generation of immature dendritic cells from CD14 ⁺ monocytes.....	50
2.11.10. Transient transfection of HEK293.....	51
2.11.11. Cholesterol depletion and replenishment.....	51
2.11.12. Cross-presentation.....	51
2.11.12.1. Proliferation assay.....	51
2.11.12.2. CTL induction.....	52
2.12. Flow cytometry.....	52
2.12.1. Testing of transgenic OT-1 mice.....	52
2.12.2. Quantification of IM (58-66) specific CD8 ⁺ T-cells by tetramer staining.....	52
2.12.3. Flow cytometry phagocytosis assay.....	53
2.12.4. Quantification of internalization of FITC labelled ovalbumin and palmitoylated ovalbumin.....	53
2.13. Microscopy.....	53
2.13.1. Indirect immunofluorescence and filipin staining of cells.....	53
2.13.2. Internalization of FITC-Dextran.....	54
2.13.3. Internalization and detection of horseradish peroxidase.....	54
2.13.4. Time-lapse video microscopy.....	55
2.14. Biochemical methods.....	55
2.14.1 Determination of protein concentration.....	55
2.14.2. Protein precipitation with trichloroacetic acid (TCA).....	55
2.14.3. Discontinuous SDS polyacrylamide gel electrophoresis (SDS-PAGE).....	56
2.14.4. Coomassie staining after SDS-PAGE.....	56
2.14.5. Semi-dry protein transfer onto nitrocellulose membranes and immunodetection.....	57
2.14.5.1. Transfer.....	57
2.14.5.2. Immunodetection.....	57
2.14.5.3. Stripping of antibody stained membranes for reprobing.....	57

2.14.6. Purification of the nuclear localization sequence (NLS)-mutant of the influenza matrix protein IM (1-164).....	58
2.14.7. Expression of recombinant Cor1 ^{L+C} in <i>E. coli</i> and purification.....	59
2.14.8. Preparation of total cell lysate.....	59
2.14.9. Homogenization of cells and preparation of membrane and cytosol.....	60
2.14.10. Isolation of cytoskeleton.....	60
2.14.11. Gel filtration of HEK293 cytosol.....	60
2.14.12. Metabolic labelling of cells using ³⁵ S-methionine / cysteine.....	61
2.14.13. Quantitation of horseradish peroxidase internalization.....	61
2.14.15. F-actin co-sedimentation assay.....	61
2.15. Synthesis of activated lipid substrates and protein modification.....	62
2.15.1. Preparation of the cholesterol-methyl- β -cyclodextrin inclusion complex.....	62
2.15.2. Synthesis of succinimidyl carbonate (SC)-farnesol.....	62
2.15.3. Synthesis of NHS esters of fatty acids.....	63
2.15.4. Palmitoylation of ovalbumin and horseradish peroxidase.....	63
2.15.5. Coupling of NHS-activated lipids to peptides.....	64
2.15.6. FITC labeling of ovalbumin and palmitoylated ovalbumin.....	64
2.16. Analytical methods.....	64
2.16.1. Nuclear magnetic resonance analysis (NMR).....	64
2.16.2. Mass spectrometry – sample preparation.....	64
2.16.3. Static light scattering (SLS).....	65
2.16.4. Thin layer chromatography (TLC).....	65
2.17. References.....	66

Chapter 3: Essential Role for Cholesterol in the Delivery of Exogenous Antigens to the MHC Class I Presentation Pathway..... 67

3.1. Abstract.....	68
3.2. Introduction.....	68
3.3. Results.....	71
3.3.1. Contribution of cholesterol to macropinosome formation.....	71
3.3.2. Role for cholesterol in cross-presentation.....	77
3.3.3. Modulation of internalization and cross-presentation of proteins by palmitoylation.....	80
3.4. Discussion.....	84
3.5. References.....	87

Chapter 4: Lipid Modification of Antigens to improve Cross-presentation..... 93

4.1. Abstract.....	94
4.2. Introduction.....	94
4.3. Results.....	95
4.3.1. Synthesis of activated lipids for protein modification.....	95
4.3.1.1. Activation of farnesol with succinimidyl carbonate (SC).....	95
4.3.1.2. Synthesis of lipid N-hydroxysuccinimide (NHS) ester.....	98
4.3.2. Coupling of activated lipids to peptides and proteins.....	99
4.3.3. Palmitoylation of exogenous proteins A general method to improve cross-presentation?.....	102
4.3.3.1. Expression and purification of influenza matrix protein.....	102
4.3.3.2. Cross-presentation of unmodified influenza matrix protein.....	102

4.3.3.3. Palmitoylation of influenza matrix protein.....	104
4.4. Discussion.....	105
4.5. References.....	106

Chapter 5: Characterisation of Coronin 1 Interaction Sites with the F-actin Cytoskeleton and the Plasma Membrane..... 109

5.1. Abstract.....	110
5.2. Introduction.....	110
5.3. Results.....	113
5.3.1. Subcellular localization of coronin 1 upon expression in HEK293 cells.....	113
5.3.2. Role of the coiled coil domain of coronin 1 in the interaction with the F-actin cytoskeleton.....	116
5.3.3. Role of the N-terminal β -propeller domain of coronin 1 in the interaction with the F-Actin cytoskeleton.....	120
5.3.4. Involvement of coronin 1 linker domain in the association with the F-actin cytoskeleton.....	122
5.3.5. Association of coronin 1 with the plasma membrane.....	125
5.4. Discussion.....	127
5.4.1. Interaction of coronin 1 with the F-actin cytoskeleton.....	128
5.4.2. Interaction of coronin 1 with the plasma membrane.....	130
5.4.3. What is the function of coronin 1 in immune cells?.....	130
5.5. References.....	131

Chapter 6: Summary..... 135

Appendix..... 139

Appendix I: Abbreviations.....	140
Appendix II: Acknowledgements.....	143
Appendix III: Curriculum vitae.....	144

- Chapter 1 -

General Introduction

1.1. Abstract

In this chapter the basic mechanisms involved in the generation of adaptive immunity are introduced. Antigen-presentation is dependent on the function of antigen-presenting cells such as macrophages and dendritic cells. It will be explained how these cells process and present antigens. Furthermore, cross-presentation, a mechanism important in the generation of immunity against viruses and tumour cells are discussed. Many functions in the immune system are dependent on the remodelling of the actin cytoskeleton including the interaction of antigen-presenting cells with T-cells. This results in the generation of a so-called immunological synapse, that represents the clustering of cytoskeletal elements with transmembrane receptors and signaling molecules. One protein, which may play a regulatory role in the formation of the immunological synapse is coronin 1. The final part of this chapter describes the current knowledge on coronin 1.

1.2. The immune system

Vertebrates are constantly exposed to microorganisms such as bacteria, viruses, fungi and parasites. However, they do not develop infections under normal conditions due to the presence of a protective system - the immune system -, which is involved in pathogen recognition and subsequent clearance of these pathogens from the body. In vertebrates, two different kinds of immunity exist and the generation of an effective immune response relies on both of them.

The early phase of host defence is controlled by the components of the so-called innate immune system. In this phase, removal of antigens relies mainly on the action of phagocytes such as macrophages and neutrophils. These cells express pattern-recognition receptors (PPR), which are germline-encoded and recognize conserved repetitive antigenic structures so-called PAMPs (pathogen-associated molecular patterns), (Janeway, 1989; Ezekowitz *at al.*, 1990; Janeway and Medzhitov, 2002). Recognition leads to internalization of the microbes and their products and subsequently to their degradation in the endosomal/lysosomal compartments.

In the later phase of host defence, when the pathogens have managed to evade the mechanisms of innate host defence and established an infection, the generation of a more

pathogen-specific immune response is required, resulting in the induction of an adaptive immune response. Adaptive immune responses can be induced against practically all foreign antigens and allows the generation of “memory”, which, in a second encounter with the antigen, generates a more efficient immune response.

1.3. The basic mechanisms of adaptive immunity

Antigen recognition in the adaptive immunity is based on the presence of a broad variety of highly diverse soluble and membrane-bound antigen receptors. This diversity is mainly generated by somatic rearrangement of germline-encoded receptor gene segments (Tonewaga, 1988). To be able to deal both with extracellular as well as with intracellular pathogens, two different types of adaptive immune responses exist, namely a humoral and a cellular response. The appropriate stimulation of these responses relies on the action of different effector cells; the antigen-presenting cell (APC) such as macrophages and dendritic cells, the B-cell and the T-cell.

Effector B-cells, the mediators of the humoral immune response, use membrane-bound receptors (immunoglobulins (Igs)) to recognize epitopes formed by the native-three dimensional structure of the antigen (Amit *et al.*, 1985, 1986; Colman *et al.*, 1987). Upon activation, B-cells secrete antibodies (= soluble Igs), which bind to soluble or membrane-associated antigens. Binding can lead to neutralization of extracellular pathogens and their products and facilitate uptake by phagocytic cells (Lanzavecchia, 1987).

T-cells, the mediators of the cellular immune response, recognize antigens (usually peptides) via a membrane-bound receptor, the T-cell receptor (TCR), only when antigens are bound to molecules of the major histocompatibility complex (MHC) and are presented on the surface of APC. Peptides, which are to be bound to MHC molecules are derived from proteins, which are intracellularly processed. Two processing pathways exist within the APC, generating ligands for the two different MHC subsets, the MHC class I and MHC class II molecules.

Peptides bound to MHC class I molecules are recognized by CD8⁺ (cytotoxic) T-cells. Antigen recognition induces effector CD8⁺ T-cells to rapidly kill the presenting cell by secretion (perforin/granzymes) or surface expression (Fas-ligand) of apoptosis inducing factors (Berke, 1997). In the case of an infection, pathogens residing in the cytosol are thereby either killed or released into the extracellular space. There they can be eliminated by

subsequent internalization in macrophages or by recognition by antibodies followed by complement-mediated lysis (Harty *et al.*, 2000).

Recognition of peptides bound to surface MHC class II molecules activates CD4⁺ (helper) T-cells. Effector CD4⁺ T-cells then produce soluble factors, which induce macrophage activation to enhance macrophage microbicidal capacity (T_{H1} T-cells) or to stimulate B-cells to produce antibodies (T_{H2} T-cells) (Abbas *et al.*, 1996; Ma *et al.*, 2003).

Taken together, whereas B-cells and CD4⁺ T-cells ensure the elimination of pathogens residing in the extracellular space, CD8⁺ T-cells are necessary for the clearance of pathogens residing in the cytosol of infected cells.

1.4. The antigen-presenting cells

Antigen-presenting cells (APCs) convert endogenous and exogenous proteins into peptides, which are then bound on MHC molecules presented to T-cells for T-cell activation. Professional APCs are distinct from every other MHC expressing cell, as they possess the unique ability to stimulate naïve T-cells. Stimulation of naïve T-cells upon their first encounter with an antigen requires an additional signal delivered from the APC (Bugeon and Dallman, 2000). Professional APCs such as B-cells, macrophages and dendritic cells express therefore high levels of co-stimulatory molecules of the B7 family, which act on the T-cell surface molecules CD28 and CTLA-4.

1.4.1. B-cells

Antigen-presentation in B-cells is mainly linked with their function to secrete antibodies. Antigen binding to their surface Igs, results in the internalization of the antigen and subsequent processing in the MHC class II pathway (Lanzavecchia, 1990; Watts, 1997).

1.4.2. Macrophages

Macrophages possess a high endocytic capacity, which accounts for their important role in clearance of invading microorganism during the early phase of host response (Aderem and Underhill, 1999). They can internalize virtually any form of antigen, including soluble as well as particulate antigens non-specifically or via specific receptors. The endosomal/lysosomal compartments of these cells ensure the efficient digestion of the endocytosed material. In addition, upon infection or inflammation macrophages become activated enhancing

their ability to kill internalized microbes by production of reactive oxygen (oxidative burst) and nitrogen radicals and by accelerating phagosomal/lysosomal fusion (Fang, 2004). Macrophages express MHC class I, MHC class II and co-stimulatory molecules. However, compared to dendritic cells and B-cells, the expression levels are lower and this could be one reason why macrophages are less efficient in priming of naïve T-cells compared to DCs and B-cells (Chang *et al.*, 1995; Mellman *et al.*, 1998; Banchereau and Steinman, 1998). Activation of T-cells by macrophages is thought to occur especially at the site of infections or inflammation (Trombetta and Mellman, 2005).

1.4.3 Dendritic cells

Due to their efficiency in antigen-presentation and their unique migration behaviour dendritic cells are regarded as the antigen-presenting cell responsible for the activation of naïve T-cells (Banchereau and Steinman, 1998; Engering, 1998). Indeed, mice lacking DCs show defects in the initiation of adaptive immune responses (Jung *et al.*, 2002). In the tissue, dendritic cells occur in an immature state. Similar to macrophages, immature dendritic cells have a large capacity to internalize a broad range of antigens using specific and non-specific uptake modes. Stimulation by cytokines or bacterial compounds causes dendritic cells to migrate from the periphery to the T-cell zones of draining lymph nodes, where naïve T-cells are located (Roake *et al.*, 1995; MacPherson *et al.*, 1995). During migration, dendritic cells undergo a profound phenotypical change converting into a professional antigen-presenting cell, a so-called mature cell. This maturation process is accompanied by downregulation of endocytic capacities, by upregulation of the expression of co-stimulatory molecules, by enhanced intracellular antigen-processing and transport of peptide loaded MHC class molecules to the cell surface (Sallusto and Lanzavecchia, 1994; Cella *et al.*, 1997; West *et al.*, 2000; Garrett *et al.*, 2000; Inaba *et al.*, 2000; Trombetta *et al.*, 2003).

Several different DCs subsets occur *in vivo*, classified by their progenitors, their tissue distribution and surface markers (Shortman and Liu, 2002).

1.5. The sampling of antigens

Three general types of endocytic routes used by APCs can be distinguished: receptor-mediated endocytosis, phagocytosis and macropinocytosis.

1.5.1. Receptor-mediated endocytosis

Receptor-mediated endocytosis allows the efficient internalization of antigens, which enables the APC to present antigens also then antigens occur at low concentrations (Lanzavecchia, 1990). A broad range of surface receptors including Fc receptors, scavenger receptors, lectins such as complement receptor, mannose receptor or DEC-205 are involved in the recognition of a variety of extracellular material. Internalization of ligand-receptor complexes is performed mainly by clathrin-coated pits and to a lesser extent also through caveolae (caveolin containing invaginations) (Mellman, 1996; Conner and Schmid, 2003).

1.5.2. Phagocytosis

The uptake of particulate antigens by phagocytosis not only serves antigen sampling but also represents an important innate host defence mechanism. Phagocytosis relies partially on the same receptors used for the uptake of soluble ligands, as these receptors can also recognize their ligands on the surface of microbes (Trombetta and Mellman, 2005). Beside extracellular microbes, cells killed upon infection represent a major source of exogenous antigens. For internalization of apoptotic bodies a large repertoire of surface receptors are used including Fc-receptors, scavenger receptors and integrins (Almeida and Linden, 2005). Phagosome formation is an actin-dependent process, in which particle binding induces receptor clustering and F-actin assembly resulting in pseudopod formation and finally particle engulfment.

1.5.3. Macropinocytosis

Macropinocytosis accounts for the random internalization of extracellular fluid and soluble antigens (Lanzavecchia, 1996; Steinman, 1995). Whereas immature dendritic cells carry out macropinocytosis constitutively, it can be induced in macrophages by treatment with phorbol esters or growth factors (Swanson, 1989; Racoosin and Swanson, 1989; Sallusto *et al.*, 1995). Macropinosome formation starts at the cell periphery by extension of a large planar membrane ruffle (lamellipodium) that folds back to form the vesicles of 0.5-2 μm size (Araki *et al.*, 1996; Amyere *et al.*, 2000; Rupper *et al.*, 2001).

Together, using different internalization pathway allows the antigen-presenting cell to sample a great variety of antigens.

1.6. Antigen-processing

Internalized antigens need to be further processed to generate peptide ligands for surface presentation on MHC molecules. Processing takes place within antigen-presenting cells via either the MHC class I or the MHC class II pathway.

1.6.1. The MHC class I pathway

MHC class I molecules are heterodimers consisting of a membrane-spanning heavy chain which is non-covalently associated with a β -chain, called microglobulin. The peptides bind in a cleft generated by the folding of the α_1 and α_2 domains of the heavy chain (Bjorkman *et al.*, 1987). MHC class I peptide ligands are normally 8-10 aa long and possess two anchor positions (Townsend *et al.*, 1989; Falk *et al.*, 1991). Typically, MHC class I binding peptides are derived from different sources including cytosolic self or foreign proteins, alternative translation products and defective ribosomal products (DRiPs), or proteins retro-translocated to the cytosol from the endoplasmic reticulum (Wang *et al.*, 1996; Bullock and Eisenlohr, 1996; Bacik *et al.*, 1997; Schild and Rammensee, 2000; Schubert *et al.*, 2000). Once in the cytosol, antigens are ubiquitinated thereby becoming substrates for the proteasome, a cytosolic multi-enzyme complex (Baumeister *et al.*, 1998) that has the capacity to cleave the ubiquitinated proteins into peptides of 10-20 aa length. Stimulation of cells with interferon- γ can modulate the activity of the proteasome by upregulation of a subset of proteasomal subunits (LMP2, LMP7, MECL-1, P28) to generate more antigenic peptides (Belich *et al.*, 1994; Gaczynska *et al.*, 1994; Realini *et al.*, 1994; Nandi *et al.*, 1996; Groettrup *et al.*, 1996). Subsequently the generated peptides are transported into the ER-lumen by the ATP-dependent transporter associated with antigen-processing, the TAP1/TAP2 heterodimer (Spies *et al.*, 1990; Androlewicz *et al.*, 1993; Neefjes *et al.*, 1993). In the ER-lumen, the N-termini of the peptides are further proteolytic processed by an ER amino peptidase (ERAP) prior to their loading onto the newly synthesized MHC class I molecules (Serwold *et al.*, 2002). MHC class I peptide binding occurs with the assistance of the ER chaperones calnexin, calreticulin and tapasin and the thiol oxidoreductase ERp57 (Sadasivan *et al.*, 1996; Vassilakos *et al.*, 1996; Hughes and Cresswell, 1998; Lindquist *et al.*, 1998; Morrice and Powis, 1998).

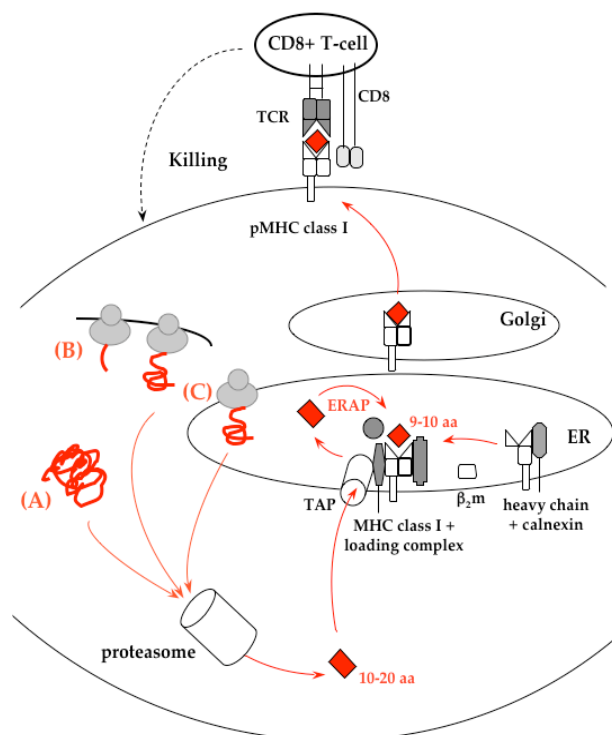


Figure 1.1. The MHC class I pathway

Pathogen-derived or self-proteins within the cytosol (A), DRiPS (B) or retro-translocated proteins from the ER (C) are degraded by the proteasome. Generated peptides of 10-20 aa length are transported by the TAP transporter into the endoplasmic reticulum (ER). In the ER-lumen, peptides are N-terminal trimmed by ER aminopeptidase (ERAP) prior to binding to newly synthesized MHC class I molecules [heavy chain + β_2 microglobulin (β_2m)]. Binding of peptides occurs with the assistance of ER chaperones, calreticulin (■), tapasin (†) and the ER-oxidoreductase ERp57 (●). Subsequently, the peptide-MHC class I complexes (pMHC class I) are transported via the Golgi complex to the plasma membrane. Recognition by $CD8^+$ T-cells results in killing of the presenting cell.

Peptide binding releases the MHC class I molecule for transport via the exocytic pathway to the cell surface (Townsend *et al.*, 1989). Peptides presented on MHC class I molecules are recognized by $CD8^+$ T-cells (figure 1.1.). Processing and presentation of MHC class I ligands occurs constitutively in all nucleated cells allowing protein expression to be monitored at all times.

1.6.2. The MHC class II pathway

Expression of MHC class II molecules is normally restricted to professional antigen-presenting cells. However, interferon- γ treatment can also lead to class II expression in other cell types (Steimle *et al.*, 1994). MHC class II molecules are composed of two transmembrane glycoproteins, the α - and β -chain. Due to the more open confirmation of the peptide binding site formed by the α_1 and β_1 domain of the two chains, the peptide length is not restricted and varies from 13 to 25 aa length (Brown *et al.*, 1993).

MHC class II peptide ligands are derived from endogenous proteins found in the endocytic compartment of the cell or from material that has gained access to this location upon internalization. For proteolytic processing, proteins are transported into the acidic lysosomal compartment where they are cleaved into shorter peptides by proteases, which include cysteine proteases, the cathepsins as well as asparaginyl endopeptidase (Chapman, 1998;

Manoury *et al.*, 1998). Subsequent MHC class II loading onto MHC class II molecules takes place in a specialized endocytic compartment, the so-called MHC class II compartment (MIIC) where the antigenic peptides encounter the MHC class II molecules coming from the ER (Peters *et al.*, 1991, Pieters *et al.*, 1991; Amigorena *et al.*, 1994; Tulp *et al.*, 1994, West *et al.*, 1994). Until peptide binding, the newly synthesized MHC class II molecules are complexed with the invariant chain (Ii) which occupies the peptide binding cleft of the MHC class II with its CLIP (class II linked invariant chain peptide) sequence. This prevents the unspecific binding of peptides in the ER (Roche and Cresswell, 1990; Teyton *et al.*, 1990; Eynon *et al.*, 1999). Furthermore the Ii targets the MHC class II molecules from the ER to the MIIC (Bakke *et al.*, 1990; Lotteau *et al.*, 1990; Pieters *et al.*, 1993).

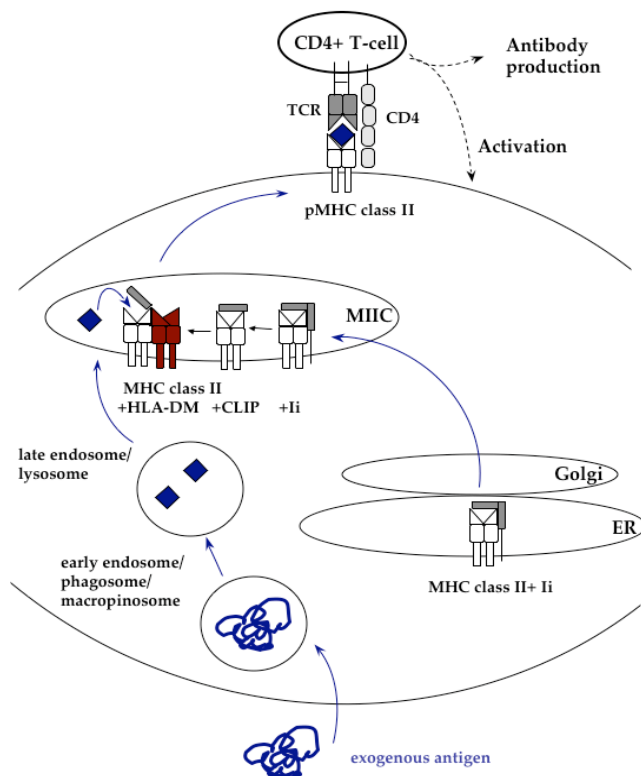


Figure 1.2. The MHC class II pathway.

Extracellular proteins/pathogens are internalized via receptor-mediated endocytosis, phagocytosis or macropinocytosis and are subsequently degraded in the endosomal/lysosomal system. MHC class II molecules are synthesized in the endoplasmic reticulum (ER), where they associate non-covalently with the invariant chain (Ii) to block binding of peptides to the MHC class II complex. The MHCII:Ii complex (one Ii trimer binds to three MHC class II molecules) is then transported via the Golgi complex, to the MHC class II loading compartment (MIIC), where the peptide loading takes place. First the Ii is degraded, giving rise to the CLIP peptide. Exchange of the CLIP peptide for antigenic peptides with the assistance of HLA-DM. After loading the peptide: MHC class II complex (pMHC class II) is transported to the plasma membrane, where they are recognized by CD4⁺ T-cells, which can then activate the presenting cell or mount an antibody response.

In the MIIC, the Ii is cleaved and the CLIP peptide bound to the MHC class II molecules is exchanged for high affinity antigenic peptides with the assistance of specific MHC class II like molecule HLA-DM (Mellins *et al.*, 1990; Kelly *et al.*, 1991; Denzin and Cresswell, 1995; Sloan *et al.*, 1995; Kropshofer *et al.*, 1996). Once loaded, the peptide-MHC class II complexes are transported to the surface of the antigen-presenting cell where they are recognized by CD4⁺ T-cells (figure 1.2.).

After development in the thymus, naïve CD4⁺ and CD8⁺ T-lymphocytes circulate in the blood system and the secondary lymphoid organs. As they are excluded from the periphery, generation of immunity against peripheral antigens depends on the action of antigen-presenting cells. These cells migrate from the periphery to the secondary lymphoid organs to present antigens internalized at the periphery to naïve T-cells.

1.7. Cross-presentation: The MHC class I processing pathway for exogenous antigens

For the generation of an immune response against viruses and tumour cells in the periphery, exogenous antigens have to gain access to the MHC class I processing pathway of antigen-presenting cells. Indeed, *in vivo* such a pathway exists and is referred to cross-presentation (Bevan, 1976).

Cross-presentation, first described in 1976 (Bevan, 1976) has two physiological outcomes. It can lead either to induction of tolerance against peripheral antigens (von Boehmer and Hafen, 1986; Kurts *et al.*, 1997; Heath and Carbone, 2001) or to stimulation of CD8⁺ T-cells. In the latter case, it ensures the generation of an anti-viral immune response when the professional APC is not infected by the virus itself (Sigal *et al.*, 1999; Prasad *et al.*, 2001) or when the virus interferes with the ability of professional APC to activate T-cells (Mueller *et al.*, 2002; Basta *et al.*, 2002; Gold *et al.*, 2002). Importantly, cross-presentation was also shown to be involved in the induction of an antitumour response (Huang *et al.*, 1994).

1.7.1. The nature of the cross-presented antigen

To date there appears to be no limitation to the types of antigens that can be cross-presented. In *in vitro* and *in vivo* studies, different types of exogenous antigens can gain access to the MHC class I processing pathway, including free peptides, peptides associated with heat-shock proteins, soluble proteins, immune complexes, exosomes, apoptotic bodies and material from both necrotic cells and live cells (Norbury *et al.*, 1995; Suto and Srivastava, 1995; Albert *et al.*, 1998; Regnault *et al.*, 1999; Harshyne *et al.*, 2001; Larsson *et al.*, 2001; Wolfers *et al.*, 2001; Andrieu *et al.*, 2003). One major source for the exogenous antigens *in vivo* might be cells killed in the course of an infection and their debris such as apoptotic bodies. It was shown that cell death leads to enhanced cross-presentation *in vivo* (Kurts *et al.*, 1998).

1.7.2. The nature of the cross-presenting cell

Several types of endocytic cells including L-cells, keratinocytes, macrophages, B-cells and dendritic cells have been shown to cross-present exogenous antigens *in vitro* (Ackerman and Cresswell, 2004). *In vivo*, dendritic cells are necessary and sufficient for cross-presentation. Of the different DC subsets *in vivo*, CD8⁺ DCs seem to be the predominant cross-presenting cells (Kurts *et al.*, 2001; Belz *et al.*, 2002; Jung *et al.*, 2002).

1.7.3. The mechanism of cross-presentation

The mechanism of cross-presentation can be influenced by the type of antigen and by the nature of the cross-presenting cell. Whereas some antigens directly traverse the plasma membrane and thereby gain access to the MHC class I processing pathway (Kim *et al.*, 1997; Jeannin *et al.*, 2000), in the majority of the cases, the antigens to be cross-presented are actively taken up by the APC via phagocytosis, macropinocytosis or receptor-mediated endocytosis (Reis e Sousa and Germain, 1995; Albert *et al.*, 1998; Norbury *et al.* 1995; Basu *et al.*, 2001). Studies of the subsequent processing of the internalized antigens led to the description of two different pathways, a TAP-independent and a TAP dependent pathway.

1.7.3.1. The TAP-independent pathway

After internalization, antigen can be processed in the endosomal/lysosomal compartment of the APC, generating peptides which either bind to recycling MHC class I molecules (Jondal *et al.*, 1996; Svensson *et al.*, 1997; Chefalo and Harding, 2001) or, after regurgitation, to empty MHC class I molecules on the cell surface (Harding and Song, 1994). This pathway is referred as the TAP-independent cross-presentation pathway (Campbell *et al.*, 2000; Chen and Jondal, 2004).

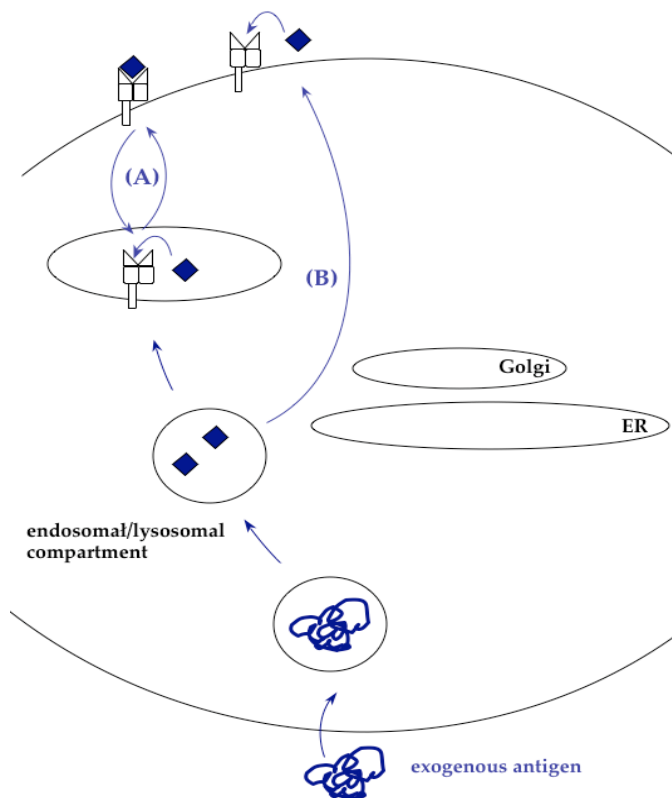


Figure 1.3. The TAP independent pathway

Exogenous antigens are processed after internalization in the endosomal/lysosomal compartment of the cell. Subsequent peptide loading onto recycling MHC class I molecules (A) occurs in the endosomal/lysosomal compartment. In addition, peptides can bind on empty MHC class I molecules at the cell surface after regurgitation (B).

In dendritic cells cross-presentation of exogenous antigens is not affected by inhibitors of lysosomal proteolysis or by chloroquine, which blocks acidification and thereby protein degradation in the endosomal/lysosomal system (Reis e Sousa and Germain, 1995; Kovacovic-Bankowski and Rock, 1995; Norbury *et al.*, 1995), indicating that this pathway does not play an important role in cross-presentation *in vivo*.

1.7.3.2. The TAP-dependent pathway

The major processing pathway, which is used for cross-presentation of most antigens relies on proteosomal degradation and TAP-dependent peptide MHC class I loading. The existence of such a pathway was first described in macrophages (Kovacovics-Bankowski and Rock, 1995; Norbury *et al.*, 1995; Reis e Sousa and Germain, 1995) and later also in dendritic cells (Shen *et al.*, 1997; Norbury *et al.*, 1997).

TAP dependency of antigen-processing is not restricted to the mode of antigen internalization and the type of antigen. Phagocytosis, macropinocytosis as well as receptor-mediated endocytosis are used for sampling of different kinds of antigens to be cross-presented via this pathway (Kovacovics-Bankowski and Rock, 1995; Rescigno *et al.*, 1998;

Svensson and Wick, 1999; Norbury *et al.*, 1995, 1997; Rodriguez *et al.*, 1999; Regnault *et al.*, 1999; Huang *et al.*, 1996; Miller *et al.*, 1998; Sigal *et al.*, 1999).

Concerning the underlying molecular basis, there are two major questions. First, where do antigens gain access to the cytosol and second, where does the TAP-dependent peptide loading onto MHC class I molecules take place.

1.7.3.2.1. MHC class I loading in the ER

After internalization and cytosolic transport, the antigen is degraded by the proteasome and the generated peptides are transported via the TAP complex into the ER. In the ER, peptides are loaded onto newly synthesized MHC class I molecules prior to the delivery to the cell surface for presentation (Heath and Carbone, 2001).

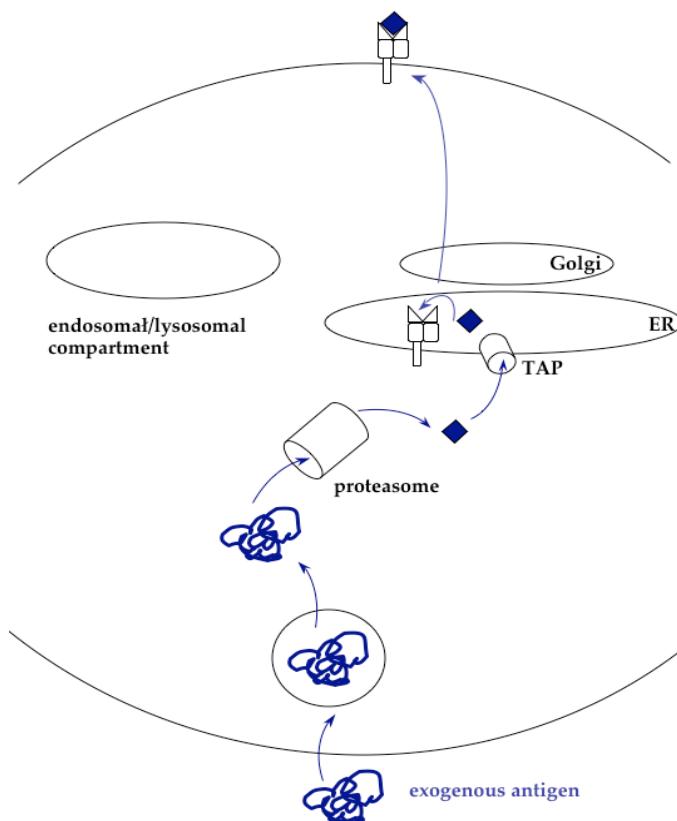


Figure 1.4. The TAP dependent pathway “ER loading”

After internalization, the exogenous antigens are transported via an unknown mechanism into the cytoplasm of the antigen-presenting cell. The subsequent processing of the antigens occurs via the classical MHC class I pathway.

1.7.3.2.2. MHC class I loading in the ER-phagosome

Recent work based on the finding that the ER contributes to phagosome formation (Garin *et al.*, 2001; Gagnon *et al.* 2002), led to the discovery of an ER-phagosome organelle (Ackerman *et al.*, 2003, Gueronprez *et al.*, 2003, Houde *et al.*, 2003). In addition to the endocytosed antigen, these “ER-phagosomes” contain newly synthesized MHC class I

molecules, TAP transporters and all components of the MHC class I loading complex. Furthermore, they associate with proteasomes at their cytoplasmic side (Ackerman *et al.*, 2003, Guernonprez *et al.*, 2003, Houde *et al.*, 2003). ER-phagosomes are sufficient for cross-presentation, fulfilling thereby a similar function as the ER in the classical MHC class I processing pathway. Shuttling of antigens to be cross-presented in an ER-like environment prior to the proteasomal degradation was also observed in dendritic cells where soluble proteins could gain access to the perinuclear lumen of the ER after internalization (Ackerman *et al.*, 2005).

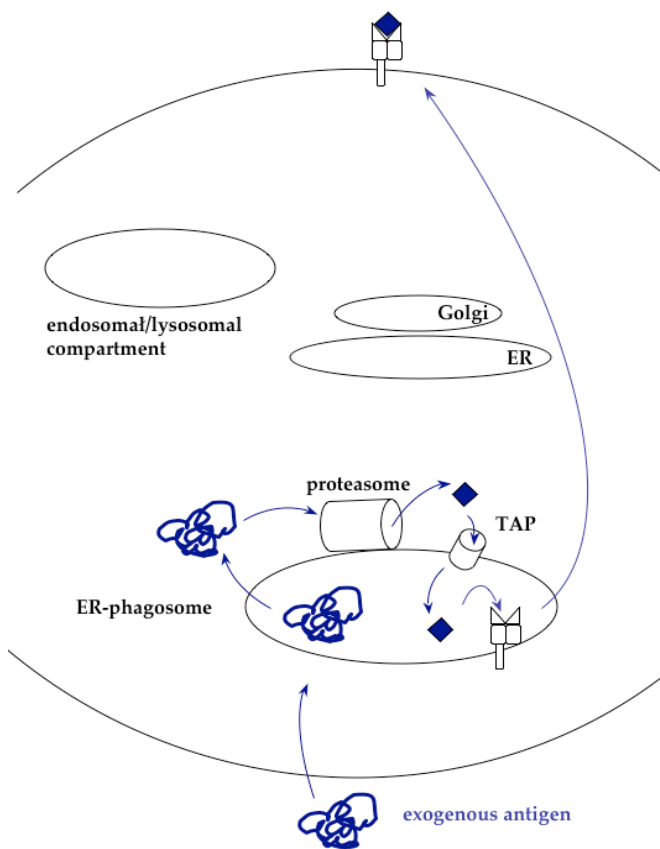


Figure 1.5. TAP-dependent pathway “ER-phagosome loading”

Exogenous antigens can gain access to an ER-like compartment during or immediately after internalization. These ER-phagosomes are fully competent to mediate cross-presentation. For subsequent proteasomal degradation, proteins are transported into the cytoplasm via an unknown mechanism. The generated peptides are transported back into the lumen of the ER-phagosome via the TAP transporter. After loading onto MHC class I molecules in the ER-phagosome, the peptide: MHC class I complexes are transported to the plasma membrane.

These studies suggest that after cytosolic transport, the proteins are proteolytically cleaved by the ER-phagosome-associated proteasome, then transported back into the ER-phagosome where loading on the MHC class I molecules takes place. How the generated peptide: MHC class I complexes are then transported to the cell surface is currently not well understood. As proteasomal products are relatively short-lived (Reits *et al.*, 2003), the compartmentalization of cross-presentation in ER-phagosomes may help to increase the efficiency of cross-presentation of the phagocytosed antigens.

1.7.3.2.3. How does the cytosolic transport of antigens occur?

In order to be efficiently cross-presented *in vivo*, the exogenous antigens have to reach the cytosol (Ackerman and Cresswell, 2004). It is not known how transport from the endosome to the cytosol occurs.

Early studies suggested that cytosolic transfer is a selective transport mechanism comprised of specific channels or translocators mediating the delivery by leakage or in a size dependent manner (Norbury *et al.* 1995; Rodriguez *et al.*, 1999; Ackerman *et al.*, 2004). The recent description of the functional intersection between the ER and the endocytic pathways led to the proposal that ER proteins could mediate the transport of antigens to the cytosol. Indeed, in the ER, there exists a pathway, termed ERAD (ER associated degradation) that is involved in the transport of misfolded proteins into the cytosol where the proteins are subjected to degradation (Tsai *et al.*, 2002). Cytosolic transport in the ERAD pathway is shown to occur by the same transporter used for the translocation of proteins into the ER, the Sec61 translocon (Wiertz *et al.*, 1996). Whether or not Sec61 mediates also the translocation of exogenous antigens from the endocytic compartment into the cytosol for cross-presentation remains to be proven (Koopmann *et al.*, 2000; Houde *et al.*, 2003; Imai *et al.*, 2005).

The human cytomegalovirus protein US11 induces the dislocation of the MHC class I heavy chain from the ER to the cytosol for subsequent degradation, thereby circumventing the induction of an immune response. Recent work by two groups (Lilley and Ploegh, 2004; Ye *et al.*, 2004) now identified an ER membrane protein, called Derlin-1, which is involved in this US11 mediated retro-translocation. Derlin-1 is proposed to be a component of the transport channel. Together with the cytosolic ATPase p97, which generates the driving force for the transport by ATP hydrolysis and targets the protein by ubiquitination for subsequent degradation, Derlin-1 might mediate also the transport of exogenous antigens into the cytosol.

1.7.4. Regulation of cross-presentation

Cross-presentation of exogenous antigens can be induced in dendritic cells by inflammatory compounds (Schulz *et al.*, 2005; Gil-Torregrose *et al.*, 2004; Datta *et al.*, 2003), by Fc receptor signaling (den Haan and Bevan, 2002), or by CD4⁺ T-cells (Machy *et al.*, 2002), raising the question whether cross-presentation is regulated perhaps similar to the presentation of MHC class II restricted antigens during DC maturation (Cella *et al.*, 1997; Pierre *et al.*, 1997).

The mechanisms underlying this regulation are not well understood. Enhancement of cross-presentation might be achieved by increased synthesis of MHC class I and components of the MHC class I loading complex (Gil-Torregrose *et al.*, 2004), by shifting the proteasomal activity from endogenous to exogenous protein processing (Lelouard *et al.*, 2002), by recruitment of MHC class I molecules to “cross-presentation” compartments (Lizee *et al.*, 2003) and by enhancement of the T-cell stimulatory capacity (Schulz *et al.*, 2005). Further investigations are necessary to completely understand how cross-presentation is regulated *in vivo*.

1.8. Antigen-presentation and T-cell activation

The peptide: MHC complexes presented on the surface of the APC are recognized by T-cells through their T-cell receptor (TCR). The TCR is a multimeric protein complex composed of the ligand binding TCR α and β -chain, the CD3 $\gamma\delta\epsilon$ chains and the homodimer CD3 ζ (Clefers *et al.*, 1988; Klausner *et al.*, 1990). Unlike the TCR chains, the CD3 components have long cytoplasmic tails containing double tyrosine based motifs, the so-called immune receptor tyrosine-based activation motifs (ITAM) which mediate the signal transduction through interaction with cytoplasmic proteins (Reth *et al.*, 1989). Signaling via the TCR results in the intracellular activation of transcription factors such as NF κ B, AP-1 and NF-AT (Cantrell, 1996). Together these factors promote transcription and secretion of the T-cell growth factor IL-2 and other cytokines, leading to T-cell proliferation, differentiation or induction of the effector function.

1.8.1. Formation of an immunological synapse at the contact site between T-cell and APC

Signaling by the TCR is accompanied with clustering of receptors, signaling molecules and cytoskeletal proteins in a so-called immunological synapse at the contact site between the APC and the T-cell (Monks *et al.*, 1998; Grakoui *et al.*, 1999). Formation of the immunological synapse is important to prolong signaling, for the regulation of signaling by successive recruitment of signaling molecules into the synapse and for receptor internalization (Monks *et al.*, 1998; Bunnell *et al.*, 2002; Huppa *et al.*, 2003). Furthermore, the close contact between APC and T-cell allows the targeted release of lytic granules and cytokines (Stinchcombe *et al.*, 2001; Reichert *et al.*, 2001).

In figure 1.6. a simplified scheme of an immunological synapse is shown. In the center of the synapse, the so-called centralized supramolecular activation cluster (cSMAC), peptide: MHC-TCR/CD3 complexes, the co-stimulatory molecules CD80/CD28 and the signaling molecules are aggregated. A rim, termed peripheral SMAC (pSMAC) formed by the adhesion receptors LFA-1/ICAM-1 and the cytoskeletal proteins surrounds the center of the immunological synapse and thereby stabilizing the junction (Bromley *et al.*, 2001).

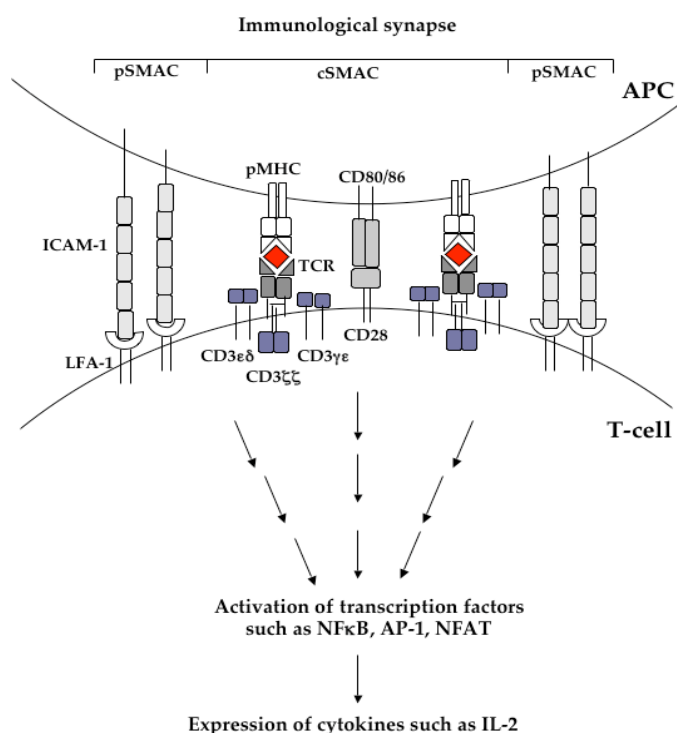


Figure 1.6. The immunological synapse

In the center of the synapse, the so-called centralized supramolecular activation cluster (cSMAC), TCR/CD3 complex and CD28 accumulate. A second group of molecules including the adhesion receptor LFA-1 which interacts with ICAM-1 on the opposing APC, form a ring around the cSMAC, termed peripheral SMAC. Signaling through the TCR results in the activation of transcription factors and subsequent expression of cytokines (adapted from Friedl and Storim, 2004).

1.8.2. Role of lipid rafts and the cytoskeleton in formation of the immunological synapse

The assembly of the immunological synapse depends on the interaction of lipid rafts and the F-actin cytoskeleton (Friedl and Storim, 2004; Meiri, 2004). Lipid rafts are glycosphingolipid and cholesterol enriched membrane microdomains, which are biochemically defined by their insolubility in nonionic detergents at 4°C (Simons and Ikonen, 1997). Protein localization in rafts is promoted by lipid anchors including glycosphosphatidylinositol (GPI) or myristoyl and palmitic acid moieties or by association with cholesterol (Brown and Rose, 1992;

Melkonian *et al.*, 1999). The immunological synapse represents a complex assemblage of rafts. Many proteins found in the immunological synapse are either constitutive raft proteins including CD4, CD28, CTLA-4 or can localize to rafts such as components of the TCR-CD3 complex, or the kinases ZAP-70 and PKC θ . Blockage of protein localization to rafts impairs TCR signaling supporting the importance of rafts in T-cell activation (Balamuth *et al.*, 2004; Bi *et al.*, 2001, Webb *et al.*, 2000).

The formation of the immunological synapse is accompanied with reorganization of the cortical F-actin cytoskeleton through the action of the small Rho GTPases Rac 1 and Cdc 42. Cdc 42 activates the Wiscott-Aldrich syndrome protein (WASP), which in turn controls the actin regulatory complex Arp2/3 (Snapper and Rosen, 1999; Rohatgi *et al.*, 1999). WASP plays a crucial role in T-cells as shown in Wiskott-Aldrich syndrome patients and WASP deficient mice. WASP deficiency leads to impairment of T-cell proliferation upon T-cell activation (Molina *et al.*, 1993; Gallego *et al.*, 1997; Zhang *et al.*, 1999). This indicates that the F-actin cytoskeleton not only exhibits a structural role in shaping the contact between APC and T-cell, but also contributes to TCR signaling for example through generation of scaffolds for the assembly of signaling complexes (Kaga *et al.*, 1998) or by supporting raft recruitment to the immunological (Harder and Simons, 1999). The molecular mechanisms underlying these processes are not well understood.

1.9. Coronin 1

A role in interaction between the plasma membrane and the F-actin cytoskeleton in immune cells could be fulfilled by coronin 1, also known as p57 or TACO. Coronin 1 belongs to the protein family of actin-binding WD40 repeat containing proteins, termed coronins (Rybakin and Clemen, 2005). In mammalian cells, up to seven coronin homologues are described (Okumura *et al.*, 1998; de Hostos, 1999; Rybakin *et al.*, 2004), whereby less is known about their function. Coronin 1 is predominantly expressed in leukocytes (Suzuki *et al.*, 1995; Ferrari *et al.*, 1999, Nal *et al.*, 2004), where it concentrates at sites of rearrangement of the cytoskeleton. In T-cells, upon activation of TCR-CD3 signaling, coronin 1 localizes to F-actin-rich areas of the immunological synapse (Nal *et al.*, 2004). In phagocytes, coronin 1 seems to be involved in early steps of phagosome formation (Yan *et al.*, 2005), accumulating at the cytosolic side of phagosomes. At later stages of phagocytosis, dissociation of

coronin 1 from the phagosome is required for further phagosome maturation (Itoh *et al.*, 2002). Pathogenic mycobacteria can actively retain coronin 1 at the phagosomal membrane allowing these bacteria to survive within macrophages (Ferrari *et al.*, 1999; Gatfield and Pieters, 2000). In neutrophils, coronin 1 interacts with a cytosolic subunit of the NADPH oxidase complex (Grogan *et al.*, 1997).

The precise role of coronin 1 in the remodelling of the cortical actin cytoskeleton or its regulation is however currently unknown.

1.10. Aims of this thesis

Part I (Chapter 3 and Chapter 4)

Cross-presentation plays an important role in the initiation of an immune response against intracellular pathogens and tumour cells. One way used by antigen-presenting cell to sample antigens to be cross-presented is through macropinocytosis.

To better understand the molecular mechanisms involved in macropinosome formation and in the subsequent delivery of macropinocytosed antigens to the cross-presentation pathway, the regulation of macropinocytosis in antigen-presenting cells was studied. The goal was to identify factors important for macropinosome formation and for the transport of internalized antigens into the cytosol. Furthermore, it was investigated whether specific targeting of exogenous antigens into the MHC class I pathway resulted in an improved cross-presentation and could provide a basis for the development of new vaccines against intracellular infectious agents and tumour cells.

Part II (Chapter 5)

Many functions in the immune system such as antigen-sampling, antigen-presentation and T-cell activation are inseparably associated with dynamic and specific changes of the cytoskeletal structures within immune cells. Coronin 1, whose role in the cell is not well defined, is one candidate involved in the remodelling of the F-actin cytoskeleton.

Similar to other members of the coronin family, coronin 1 possesses a three-domain structure, which mediates the interaction of the protein with the F-actin cytoskeleton and the plasma membrane. The goal in the second part of this thesis was to specify the role of the single coronin 1 domains, in order to better understand the function of coronin 1 in immune cells.

1.11. References

- Abbas, A.K., Murphy, K.M., Sher, A. Functional diversity of helper T lymphocytes. *Nature*. 1996, **383**: 787-93. Review.
- Ackerman, A.L., Kyritsis, C., Tampe, R., Cresswell, P. Access of soluble antigens to the endoplasmic reticulum can explain cross-presentation by dendritic cells. *Nat Immunol*. 2005, **6**: 107-13.
- Ackerman, A.L., Cresswell, P. Cellular mechanisms governing cross-presentation of exogenous antigens. *Nat Immunol*. 2004, **5**: 678-84. Review.
- Ackerman AL, Kyritsis C, Tampe R, Cresswell P. Early phagosomes in dendritic cells form a cellular compartment sufficient for cross presentation of exogenous antigens. *Proc Natl Acad Sci U S A*. 2003, **100**: 12889-94.
- Albert, M.L., Sauter, B., Bhardwaj, N. Dendritic cells acquire antigen from apoptotic cells and induce class I-restricted CTLs. *Nature*. 1998, **392**: 86-9.
- Almeida, C.J., Linden, R. Phagocytosis of apoptotic cells: a matter of balance. *Cell Mol Life Sci*. 2005.
- Amigorena, S., Drake, J.R., Webster, P., Mellman, I. Transient accumulation of new class II MHC molecules in a novel endocytic compartment in B lymphocytes. *Nature*. 1994, **369**: 113-20.
- Amit AG, Mariuzza RA, Phillips SE, Poljak RJ. Three-dimensional structure of an antigen-antibody complex at 2.8 Å resolution. *Science*. 1986, **233**: 747-53.
- Amit, A.G., Mariuzza, R.A., Phillips, S.E., Poljak, R.J. Three-dimensional structure of an antigen-antibody complex at 6 Å resolution. *Nature*. 1985, **313**: 156-8.
- Amyere, M., Payrastré, B., Krause, U., Van Der Smissen, P., Veithen, A., Courtoy, P.J. Constitutive macropinocytosis in oncogene-transformed fibroblasts depends on sequential permanent activation of phosphoinositide 3-kinase and phospholipase C. *Mol Biol Cell*. 2000, **11**: 3453-67.
- Aderem, A., Underhill, D.M. Mechanisms of phagocytosis in macrophages. *Annu Rev Immunol*. 1999, **17**: 593-623. Review.
- Andrieu, M., Desoutter, J.F., Loing, E., Gaston, J., Hanau, D., Guillet, J.G., Hosmalin, A. Two human immunodeficiency virus vaccinal lipopeptides follow different cross-presentation pathways in human dendritic cells. *J Virol*. 2003, **77**: 1564-70.
- Androlewicz, M.J., Anderson, K.S., Cresswell, P. Evidence that transporters associated with antigen processing translocate a major histocompatibility complex class I-binding peptide into the endoplasmic reticulum in an ATP-dependent manner. *Proc Natl Acad Sci U S A*. 1993, **90**: 9130-4.
- Araki, N., Johnson, M.T., Swanson, J.A. A role for phosphoinositide 3-kinase in the completion of macropinocytosis and phagocytosis by macrophages. *J Cell Biol*. 1996, **135**: 1249-60.
- Bacik, I., Snyder, H.L., Anton, L.C., Russ, G., Chen, W., Bennink, J.R., Urge, L., Otvos, L., Dudkowska, B., Eisenlohr, L., Yewdell, J.W. Introduction of a glycosylation site into a secreted protein provides evidence for an alternative antigen processing pathway: transport of precursors of major histocompatibility complex class I-restricted peptides from the endoplasmic reticulum to the cytosol. *J Exp Med*. 1997, **186**: 479-87.
- Bakke, O., Dobberstein, B. MHC class II-associated invariant chain contains a sorting signal for endosomal compartments. *Cell*. 1990, **63**: 707-16.

- Balamuth, F., Brogdon, J.L., Bottomly, K. CD4 raft association and signaling regulate molecular clustering at the immunological synapse site. *J Immunol.* 2004, **172**: 5887-92.
- Banchereau, J., Steinman, R.M. Dendritic cells and the control of immunity. *Nature.* 1998, **392**: 245-52. Review.
- Basta, S., Chen, W., Bennink, J.R., Yewdell, J.W. Inhibitory effects of cytomegalovirus proteins US2 and US11 point to contributions from direct priming and cross-priming in induction of vaccinia virus-specific CD8(+) T cells. *J Immunol.* 2002, **168**: 5403-8.
- Basu, S., Binder, R.J., Ramalingam, T., Srivastava, P.K. CD91 is a common receptor for heat shock proteins gp96, hsp90, hsp70, and calreticulin. *Immunity.* 2001, **14**: 303-13.
- Baumeister, W., Walz, J., Zuhl, F., Seemuller, E. The proteasome: paradigm of a self compartmentalizing protease. *Cell.* 1998, **92**: 367-80. Review.
- Belich, M.P., Glynn, R.J., Senger, G., Sheer, D., Trowsdale, J. Proteasome components with reciprocal expression to that of the MHC-encoded LMP proteins. *Curr Biol.* 1994, **4**: 769-76.
- Belz, G.T., Behrens, G.M., Smith, C.M., Miller, J.F., Jones, C., Lejon, K., Fathman, C.G., Mueller, S.N., Shortman, K., Carbone, F.R., Heath, W.R. The CD8 alpha(+) dendritic cell is responsible for inducing peripheral self-tolerance to tissue-associated antigens. *J Exp Med.* 2002, **96**: 1099-104.
- Berke, G. Killing mechanisms of cytotoxic lymphocytes. *Curr Opin Hematol.* 1997, **4**: 32-40. Review.
- Bevan, M.J. Minor H antigens introduced on H-2 different stimulating cells cross-react at the cytotoxic T cell level during in vivo priming. *J Immunol.* 1976, **117**: 2233-8.
- Bi, K., Tanaka, Y., Coudronniere, N., Sugie, K., Hong, S., van Stipdonk, M.J., Altman, A. Antigen-induced translocation of PKC-theta to membrane rafts is required for T cell activation. *Nat Immunol.* 2001, **2**: 556-63.
- Bjorkman, P.J., Saper, M.A., Samraoui, B., Bennett, W.S., Strominger, J.L., Wiley, D.C. Structure of the human class I histocompatibility antigen, HLA-A2. *Nature.* 1987, **329**: 506-12.
- Bromley, S.K., Burack, W.R., Johnson, K.G., Somersalo, K., Sims, T.N., Sumen, C., Davis, M.M., Shaw, A.S., Allen, P.M., Dustin, M.L. The immunological synapse. *Annu Rev Immunol.* 2001, **19**: 375-96. Review.
- Brown, J.H., Jardetzky, T.S., Gorga, J.C., Stern, L.J., Urban, R.G., Strominger, J.L., Wiley, D.C. Three-dimensional structure of the human class II histocompatibility antigen HLA-DR1. *Nature.* 1993, **364**: 33-9.
- Brown, D.A., Rose, J.K. Sorting of GPI-anchored proteins to glycolipid-enriched membrane subdomains during transport to the apical cell surface. *Cell.* 1992, **68**: 533-44.
- Bugeon, L., Dallman, M.J. Costimulation of T cells. *Am J Respir Crit Care Med.* 2000, **162**: S164-8. Review.
- Bullock, T.N., Eisenlohr, L.C. Ribosomal scanning past the primary initiation codon as a mechanism for expression of CTL epitopes encoded in alternative reading frames. *J Exp Med.* 1996, **184**: 1319-29.
- Bunnell, S.C., Hong, D.I., Kardon, J.R., Yamazaki, T., McGlade, C.J., Barr, V.A., Samelson, L.E. T cell receptor ligation induces the formation of dynamically regulated signaling assemblies. *J Cell Biol.* 2002, **158**: 1263-75.
- Campbell, D.J., Serwold, T., Shastri, N. Bacterial proteins can be processed by macrophages in a transporter associated with antigen processing-independent, cysteine protease-dependent manner for presentation by MHC class I molecules. *J Immunol.* 2000, **164**: 168-75.

- Cantrell, D. T cell antigen receptor signal transduction pathways. *Annu Rev Immunol.* 1996, **14**: 259-74. Review.
- Cella, M., Engering, A., Pinet, V., Pieters, J., Lanzavecchia, A. Inflammatory stimuli induce accumulation of MHC class II complexes on dendritic cells. *Nature.* 1997, **388**: 782-787.
- Chang, M.D., Stanley, E.R., Khalili, H., Chisholm, O., Pollard, J.W. Osteopetrotic (op/op) mice deficient in macrophages have the ability to mount a normal T-cell-dependent immune response. *Cell Immunol.* 1995, **162**: 146-52.
- Chapman, H.A. Endosomal proteolysis and MHC class II function. *Curr Opin Immunol.* 1998, **10**: 93-102. Review.
- Chen, L., Jondal, M. Alternative processing for MHC class I presentation by immature and CpG-activated dendritic cells. *Eur J Immunol.* 2004, **34**: 952-60.
- Chefalo, P.J., Harding, C.V. Processing of exogenous antigens for presentation by class I MHC molecules involves post-Golgi peptide exchange influenced by peptide-MHC complex stability and acidic pH. *J Immunol.* 2001, **167**: 1274-82.
- Clevers, H., Alarcon, B., Wileman, T., Terhorst, C. The T cell receptor/CD3 complex: a dynamic protein ensemble. *Annu Rev Immunol.* 1988, **6**: 629-62. Review.
- Colman, P.M., Laver, W.G., Varghese, J.N., Baker, A.T., Tulloch, P.A., Air, G.M., Webster, R.G. Three-dimensional structure of a complex of antibody with influenza virus neuraminidase. *Nature.* 1987, **326**: 358-63.
- Conner, S.D., Schmid, S.L. Regulated portals of entry into the cell. *Nature.* 2003, **422**: 37-44. Review.
- Datta, S.K., Redecke, V., Prilliman, K.R., Takabayashi, K., Corr, M., Tallant, T., DiDonato, J., Dziarski, R., Akira, S., Schoenberger, S.P., Raz, E. A subset of Toll-like receptor ligands induces cross-presentation by bone marrow-derived dendritic cells. *J Immunol.* 2003, **170**: 4102-10.
- de Hostos, E.L. The coronin family of actin-associated proteins. *Trends Cell Biol.* 1999, **9**: 345-50. Review.
- den Haan, J.M., Bevan, M.J. Constitutive versus activation-dependent cross-presentation of immune complexes by CD8(+) and CD8(-) dendritic cells in vivo. *J Exp Med.* 2002, **196**: 817-27.
- Denzin, L.K., Cresswell, P. HLA-DM induces CLIP dissociation from MHC class II alpha beta dimers and facilitates peptide loading. *Cell.* 1995, **82**: 155-65.
- Engering, A.J. Regulation of Major Histocompatibility Complex class II-Restricted Antigen Presentation by human Dendritic Cells. Vrije Universiteit, Amsterdam, 1998.
- Eynon, E.E., Schlax, C., Pieters, J. A secreted form of the major histocompatibility complex class II-associated invariant chain inhibiting T cell activation. *J Biol Chem.* 1999, **274**: 26266-71.
- Ezekowitz, R.A., Sastry, K., Bailly, P., Warner, A. Molecular characterization of the human macrophage mannose receptor: demonstration of multiple carbohydrate recognition-like domains and phagocytosis of yeasts in Cos-1 cells. *J Exp Med.* 1990, **172**: 1785-94.
- Falk, K., Rotzschke, O., Stevanovic, S., Jung, G., Rammensee, H.G. Allele-specific motifs revealed by sequencing of self-peptides eluted from MHC molecules. *Nature.* 1991, **351**: 290-6.
- Fang, F.C. Antimicrobial reactive oxygen and nitrogen species: concepts and controversies. *Nat Rev Microbiol.* 2004, **2**: 820-32. Review.
- Ferrari, G., Langen, H., Naito, M., Pieters, J. A coat protein on phagosomes involved in the intracellular survival of mycobacteria. *Cell.* 1999, **97**: 435-47.

- Friedl, P., Storim, J. Diversity in immune-cell interactions: states and functions of the immunological synapse. *Trends Cell Biol.* 2004, **14**: 557-67. Review.
- Gaczynska, M., Rock, K.L., Spies, T., Goldberg, A.L. Peptidase activities of proteasomes are differentially regulated by the major histocompatibility complex-encoded genes for LMP2 and LMP7. *Proc Natl Acad Sci U S A.* 1994, **91**: 9213-7.
- Gagnon, E., Duclos, S., Rondeau, C., Chevet, E., Cameron, P.H., Steele-Mortimer, O., Paiement, J., Bergeron, J.J., Desjardins, M. Endoplasmic reticulum-mediated phagocytosis is a mechanism of entry into macrophages. *Cell.* 2002, **110**: 119-31.
- Gallego, M.D., Santamaria, M., Pena, J., Molina, I.J. Defective actin reorganization and polymerization of Wiskott-Aldrich T cells in response to CD3-mediated stimulation. *Blood.* 1997, **90**: 3089-97.
- Garin, J., Diez, R., Kieffer, S., Dermine, J.F., Duclos, S., Gagnon, E., Sadoul, R., Rondeau, C., Desjardins, M. The phagosome proteome: insight into phagosome functions. *J Cell Biol.* 2001, **152**: 165-80.
- Garrett, W.S., Chen, L.M., Kroschewski, R., Ebersold, M., Turley, S., Trombetta, S., Galan, J.E., Mellman, I. Developmental control of endocytosis in dendritic cells by Cdc42. *Cell.* 2000, **102**: 325-34.
- Gatfield, J., Pieters, J. Essential role for cholesterol in entry of mycobacteria into macrophages. *Science.* 2000, **288**: 1647-50.
- Gil-Torregrosa, B.C., Lennon-Dumenil, A.M., Kessler, B., Guermonprez, P., Ploegh, H.L., Fruci, D., van Endert, P., Amigorena, S. Control of cross-presentation during dendritic cell maturation. *Eur J Immunol.* 2004, **34**: 398-407.
- Gold, M.C., Munks, M.W., Wagner, M., Koszinowski, U.H., Hill, A.B., Fling, S.P. The murine cytomegalovirus immunomodulatory gene m152 prevents recognition of infected cells by M45-specific CTL but does not alter the immunodominance of the M45-specific CD8 T cell response in vivo. *J Immunol.* 2002, **169**: 359-65.
- Grakoui, A., Bromley, S.K., Sumen, C., Davis, M.M., Shaw, A.S., Allen, P.M., Dustin, M.L. The immunological synapse: a molecular machine controlling T cell activation. *Science.* 1999, **285**: 221-7.
- Groettrup, M., Soza, A., Eggers, M., Kuehn, L., Dick, T.P., Schild, H., Rammensee, H.G., Koszinowski, U.H., Kloetzel, P.M. A role for the proteasome regulator PA28alpha in antigen presentation. *Nature.* 1996, **381**: 166-8.
- Grogan, A., Reeves, E., Keep, N., Wientjes, F., Totty, N.F., Burlingame, A.L., Hsuan, J.J., Segal, A.W. Cytosolic phox proteins interact with and regulate the assembly of coronin in neutrophils. *J Cell Sci.* 1997, **110**: 3071-81.
- Guermonprez, P., Saveanu, L., Kleijmeer, M., Davoust, J., Van Endert, P., Amigorena, S. ER-phagosome fusion defines an MHC class I cross-presentation compartment in dendritic cells. *Nature.* 2003, **425**: 397.
- Harder, T., Simons, K. Clusters of glycolipid and glycosylphosphatidylinositol-anchored proteins in lymphoid cells: accumulation of actin regulated by local tyrosine phosphorylation. *Eur J Immunol.* 1999, **29**: 556-62.
- Harding, C.V., Song, R. Phagocytic processing of exogenous particulate antigens by macrophages for presentation by class I MHC molecules. *J Immunol.* 1994, **153**: 4925-33.
- Harshyne, L.A., Watkins, S.C., Gambotto, A., Barratt-Boyes, S.M. Dendritic cells acquire antigens from live cells for cross-presentation to CTL. *J Immunol.* 2001, **166**: 3717-23.
- Harty, J.T., Tvinnereim, A.R., White, D.W. CD8+ T cell effector mechanisms in resistance to infection. *Annu Rev Immunol.* 2000, **18**: 275-308. Review.

- Heath, W.R., Carbone, F.R. Cross-presentation in viral immunity and self-tolerance. *Nat Rev Immunol.* 2001, **1**: 126-34. Review.
- Houde, M., Bertholet, S., Gagnon, E., Brunet, S., Goyette, G., Laplante, A., Princiotta, M.F., Thibault, P., Sacks, D., Desjardins, M. Phagosomes are competent organelles for antigen cross-presentation. *Nature.* 2003, **425**: 402-6.
- Huang, A.Y., Bruce, A.T., Pardoll, D.M., Levitsky, H.I. In vivo cross-priming of MHC class I-restricted antigens requires the TAP transporter. *Immunity.* 1996, **4**: 349-55.
- Huang AY, Golumbek P, Ahmadzadeh M, Jaffee E, Pardoll D, Levitsky H. Role of bone marrow-derived cells in presenting MHC class I-restricted tumor antigens. *Science.* 1994, **264**: 961-5.
- Hughes, E.A., Cresswell, P. The thiol oxidoreductase ERp57 is a component of the MHC class I peptide-loading complex. *Curr Biol.* 1998, **8**: 709-12.
- Huppa, J.B., Gleimer, M., Sumen, C., Davis, M.M. Continuous T cell receptor signaling required for synapse maintenance and full effector potential. *Nat Immunol.* 2003, **4**: 749-55.
- Imai, J., Hasegawa, H., Maruya, M., Koyasu, S., Yahara, I. Exogenous antigens are processed through the endoplasmic reticulum-associated degradation (ERAD) in cross-presentation by dendritic cells. *Int Immunol.* 2005, **17**: 45-53.
- Inaba, K., Turley, S., Iyoda, T., Yamaide, F., Shimoyama, S., Reis e Sousa, C., Germain, R.N., Mellman, I., Steinman, R.M. The formation of immunogenic major histocompatibility complex class II-peptide ligands in lysosomal compartments of dendritic cells is regulated by inflammatory stimuli. *J Exp Med.* 2000, **191**: 927-36.
- Itoh, S., Suzuki, K., Nishihata, J., Iwasa, M., Oku, T., Nakajin, S., Nauseef, W.M., Toyoshima, S. The role of protein kinase C in the transient association of p57, a coronin family actin-binding protein, with phagosomes. *Biol Pharm Bull.* 2002, **25**: 837-44.
- Janeway, C.A. Jr, Medzhitov, R. Innate immune recognition. *Annu Rev Immunol.* 2002, **20**: 197-216. Review.
- Janeway, C.A. Jr. Approaching the asymptote? Evolution and revolution in immunology. *Cold Spring Harb Symp Quant Biol.* 1989, **54 Pt 1**: 1-13. Review.
- Jeannin, P., Renno, T., Goetsch, L., Miconnet, I., Aubry, J.P., Delneste, Y., Herbault, N., Baussant, T., Magistrelli, G., Soulas, C., Romero, P., Cerottini, J.C., Bonnefoy, J.Y. OmpA targets dendritic cells, induces their maturation and delivers antigen into the MHC class I presentation pathway. *Nat Immunol.* 2000, **1**: 502-9.
- Jondal, M., Schirmbeck, R., Reimann, J. MHC class I-restricted CTL responses to exogenous antigens. *Immunity.* 1996, **5**: 295-302. Review.
- Jung, S., Unutmaz, D., Wong, P., Sano, G., De los Santos, K., Sparwasser, T., Wu, S., Vuthoori, S. Ko K., Zavala, F., Pamer, E.G., Littman, D.R., Lang, R.A. In vivo depletion of CD11c(+) dendritic cells abrogates priming of CD8(+) T cells by exogenous cell-associated antigens. *Immunity.* 2002, **17**: 211-20.
- Kaga, S., Ragg, S., Rogers, K.A., Ochi, A. Stimulation of CD28 with B7-2 promotes focal adhesion-like cell contacts where Rho family small G proteins accumulate in T cells. *J Immunol.* 1998, **160**: 24-7.
- Kelly, A.P., Monaco, J.J., Cho, S.G., Trowsdale, J. A new human HLA class II-related locus, DM. *Nature.* 1991, **353**: 571-3.
- Klausner, R.D., Lippincott-Schwartz, J., Bonifacino, J.S. The T cell antigen receptor: insights into organelle biology. *Annu Rev Cell Biol.* 1990, **6**: 403-31. Review.

- Kim, D.T., Mitchell, D.J., Brockstedt, D.G., Fong, L., Nolan, G.P., Fathman, C.G., Engleman, E.G., Rothbard, J.B. Introduction of soluble proteins into the MHC class I pathway by conjugation to an HIV tat peptide. *J Immunol.* 1997, **159**: 1666-8.
- Koopmann, J.O., Albring, J., Huter, E., Bulbuc, N., Spee, P., Neefjes, J., Hammerling, G.J., Momburg, F. Export of antigenic peptides from the endoplasmic reticulum intersects with retrograde protein translocation through the Sec61p channel. *Immunity.* 2000, **13**: 117-27.
- Kovacsovics-Bankowski, M., Rock, K.L. A phagosome-to-cytosol pathway for exogenous antigens presented on MHC class I molecules. *Science.* 1995, **267**: 243-6.
- Kurts, C., Cannarile, M., Klebba, I., Brocker, T. Dendritic cells are sufficient to cross-present self-antigens to CD8 T cells in vivo. *J Immunol.* 2001, **166**: 1439-42.
- Kurts, C., Miller, J.F., Subramaniam, R.M., Carbone, F.R., Heath, W.R. Major histocompatibility complex class I-restricted cross-presentation is biased towards high dose antigens and those released during cellular destruction. *J Exp Med.* 1998, **188**: 409-14.
- Kurts, C., Kosaka, H., Carbone, F.R., Miller, J.F., Heath, W.R. Class I-restricted cross-presentation of exogenous self-antigens leads to deletion of autoreactive CD8(+) T cells. *J Exp Med.* 1997, **186**: 239-45.
- Kropshofer, H., Vogt, A.B., Moldenhauer, G., Hammer, J., Blum, J.S., Hammerling, G.J. Editing of the HLA-DR-peptide repertoire by HLA-DM. *EMBO J.* 1996, **15**: 6144-54.
- Lanzavecchia, A. Mechanisms of antigen uptake for presentation. *Curr Opin Immunol.* 1996, **8**: 348-54. Review.
- Lanzavecchia, A. Receptor-mediated antigen uptake and its effect on antigen presentation to class II-restricted T lymphocytes. *Annu Rev Immunol.* 1990, **8**: 773-93. Review.
- Lanzavecchia, A. Antigen uptake and accumulation in antigen-specific B cells. *Immunol Rev.* 1987, **99**: 39-51. Review.
- Larsson, M., Fonteneau, J.F., Somersan, S., Sanders, C., Bickham, K., Thomas, E.K., Mahnke, K., Bhardwaj, N. Efficiency of cross presentation of vaccinia virus-derived antigens by human dendritic cells. *Eur J Immunol.* 2001, **31**: 3432-42.
- Lelouard, H., Gatti, E., Cappello, F., Gresser, O., Camosseto, V., Pierre, P. Transient aggregation of ubiquitinated proteins during dendritic cell maturation. *Nature.* 2002, **417**: 177-82.
- Lilley, B.N., Ploegh, H.L. A membrane protein required for dislocation of misfolded proteins from the ER. *Nature.* 2004, **429**: 834-40.
- Lindquist, J.A., Jensen, O.N., Mann, M., Hammerling, G.J. ER-60, a chaperone with thiol-dependent reductase activity involved in MHC class I assembly. *EMBO J.* 1998, **17**: 2186-95.
- Lizee, G., Basha, G., Tiong, J., Julien, J.P., Tian, M., Biron, K.E., Jefferies, W.A. Control of dendritic cell cross-presentation by the major histocompatibility complex class I cytoplasmic domain. *Nat Immunol.* 2003, **4**: 1065-73.
- Lotteau, V., Teyton, L., Peleraux, A., Nilsson, T., Karlsson, L., Schmid, S.L., Quaranta, V., Peterson, P.A. Intracellular transport of class II MHC molecules directed by invariant chain. *Nature.* 1990, **348**: 600-5.
- Ma, J., Chen, T., Mandelin, J., Ceponis, A., Miller, N.E., Hukkanen, M., Ma, G.F., Konttinen, Y.T. Regulation of macrophage activation. *Cell Mol Life Sci.* 2003, **60**: 2334-46. Review.
- Machy, P., Serre, K., Baillet, M., Leserman, L. Induction of MHC class I presentation of exogenous antigen by dendritic cells is controlled by CD4+ T cells engaging class II molecules in cholesterol-rich domains. *J Immunol.* 2002, **168**: 1172-80.

- MacPherson, G.G., Jenkins, C.D., Stein, M.J., Edwards, C. Endotoxin-mediated dendritic cell release from the intestine. Characterization of released dendritic cells and TNF dependence. *J Immunol.* 1995, **154**: 1317-22.
- Manoury, B., Hewitt, E.W., Morrice, N., Dando, P.M., Barrett, A.J., Watts, C. An asparaginyl endopeptidase processes a microbial antigen for class II MHC presentation. *Nature.* 1998, **396**: 695-9.
- Melkonian, K.A., Ostermeyer, A.G., Chen, J.Z., Roth, M.G., Brown, D.A. Role of lipid modifications in targeting proteins to detergent-resistant membrane rafts. Many raft proteins are acylated, while few are prenylated. *J Biol Chem.* 1999, **274**: 3910-7.
- Mellman, I., Turley, S.J., Steinman, R.M. Antigen processing for amateurs and professionals. *Trends Cell Biol.* 1998, **8**: 231-7. Review.
- Mellman, I. Endocytosis and molecular sorting. *Annu Rev Cell Dev Biol.* 1996, **12**: 575-625. Review.
- Mellins, E., Smith, L., Arp, B., Cotner, T., Celis, E., Pious, D. Defective processing and presentation of exogenous antigens in mutants with normal HLA class II genes. *Nature.* 1990, **343**: 71-4.
- Meiri, K.F. Membrane/cytoskeleton communication. *Subcell Biochem.* 2004, **37**: 247-82. Review.
- Miller, J.F., Kurts, C., Allison, J., Kosaka, H., Carbone, F., Heath, W.R. Induction of peripheral CD8+ T-cell tolerance by cross-presentation of self antigens. *Immunol Rev.* 1998, **165**: 267-77. Review.
- Molina, I.J., Sancho, J., Terhorst, C., Rosen, F.S., Remold-O'Donnell, E. T cells of patients with the Wiskott-Aldrich syndrome have a restricted defect in proliferative responses. *J Immunol.* 1993, **151**: 4383-90.
- Monks, C.R., Freiberg, B.A., Kupfer, H., Sciaky, N., Kupfer, A. Three-dimensional segregation of supramolecular activation clusters in T cells. *Nature.* 1998, **395**: 82-6.
- Morrice, N.A., Powis, S.J. A role for the thiol-dependent reductase ERp57 in the assembly of MHC class I molecules. *Curr Biol.* 1998, **8**: 713-6.
- Mueller, S.N., Jones, C.M., Smith, C.M., Heath, W.R., Carbone, F.R. Rapid cytotoxic T lymphocyte activation occurs in the draining lymph nodes after cutaneous herpes simplex virus infection as a result of early antigen presentation and not the presence of virus. *J Exp Med.* 2002, **95**: 651-6.
- Nal, B., Carroll, P., Mohr, E., Verthuy, C., Da Silva, M.I., Gayet, O., Guo, X.J., He, H.T., Alcover, A., Ferrier, P. Coronin-1 expression in T lymphocytes: insights into protein function during T cell development and activation. *Int Immunol.* 2004, **16**: 231-40.
- Nandi, D., Jiang, H., Monaco, J.J. Identification of MECL-1 (LMP-10) as the third IFN-gamma-inducible proteasome subunit. *J Immunol.* 1996, **156**: 2361-4.
- Neefjes, J.J., Momburg, F., Hammerling, G.J. Selective and ATP-dependent translocation of peptides by the MHC-encoded transporter. *Science.* 1993, **261**: 769-71.
- Norbury, C.C., Chambers, B.J., Prescott, A.R., Ljunggren, H.G., Watts, C. Constitutive macropinocytosis allows TAP-dependent major histocompatibility complex class I presentation of exogenous soluble antigen by bone marrow-derived dendritic cells. *Eur J Immunol.* 1997, **27**: 280-8.
- Norbury, C.C., Hewlett, L.J., Prescott, A.R., Shastri, N., Watts, C. Class I MHC presentation of exogenous soluble antigen via macropinocytosis in bone marrow macrophages. *Immunity.* 1995, **3**: 783-91.
- Okumura, M., Kung, C., Wong, S., Rodgers, M., Thomas, M.L. Definition of family of coronin-related proteins conserved between humans and mice: close genetic linkage between coronin-2 and CD45-associated protein. *DNA Cell Biol.* 1998, **17**: 779-87.

- Peters, P.J., Neeffjes, J.J., Oorschot, V., Ploegh, H.L., Geuze, H.J. Segregation of MHC class II molecules from MHC class I molecules in the Golgi complex for transport to lysosomal compartments. *Nature*. 1991, **349**: 669-76.
- Pierre, P., Turley, S.J., Gatti, E., Hull, M., Meltzer, J., Mirza, A., Inaba, K., Steinman, R.M., Mellman, I. Developmental regulation of MHC class II transport in mouse dendritic cells. *Nature*. 1997, **388**: 787-792.
- Pieters, J., Bakke, O., Dobberstein, B. The MHC class II-associated invariant chain contains two endosomal targeting signals within its cytoplasmic tail. *J Cell Sci*. 1993, **106**: 831-46.
- Pieters, J., Horstmann, H., Bakke, O., Griffiths, G., Lipp, J. Intracellular transport and localization of major histocompatibility complex class II molecules and associated invariant chain. *J Cell Biol*. 1991, **115**: 1213-23.
- Prasad, S.A., Norbury, C.C., Chen, W., Bennink, J.R., Yewdell, J.W. Cutting edge: recombinant adenoviruses induce CD8 T cell responses to an inserted protein whose expression is limited to nonimmune cells. *J Immunol*. 2001, **166**: 4809-12.
- Racoosin, E.L., Swanson, J.A. Macrophage colony-stimulating factor (rM-CSF) stimulates pinocytosis in bone marrow-derived macrophages. *J Exp Med*. 1989, **170**: 1635-48.
- Realini, C., Dubiel, W., Pratt, G., Ferrell, K., Rechsteiner, M. Molecular cloning and expression of a gamma-interferon-inducible activator of the multicatalytic protease. *J Biol Chem*. 1994, **269**: 20727-32.
- Regnault, A., Lankar, D., Lacabanne, V., Rodriguez, A., Thery, C., Rescigno, M., Saito, T., Verbeek, S., Bonnerot, C., Ricciardi-Castagnoli, P., Amigorena, S. Fcgamma receptor-mediated induction of dendritic cell maturation and major histocompatibility complex class I-restricted antigen presentation after immune complex internalization. *J Exp Med*. 1999, **189**: 371-80.
- Reth, M. Antigen receptor tail clue. *Nature*. 1989, **338**: 383-4.
- Reichert, P., Reinhardt, R.L., Ingulli, E., Jenkins, M.K. Cutting edge: in vivo identification of TCR redistribution and polarized IL-2 production by naive CD4 T cells. *J Immunol*. 2001, **166**: 4278-81.
- Reis e Sousa, C., Germain, RN. Major histocompatibility complex class I presentation of peptides derived from soluble exogenous antigen by a subset of cells engaged in phagocytosis. *J Exp Med*. 1995, **182**: 841-51.
- Reits, E., Griekspoor, A., Neijssen, J., Groothuis, T., Jalink, K., van Veelen, P., Janssen, H., Calafat, J., Drijfhout, J.W., Neeffjes, J. Peptide diffusion, protection, and degradation in nuclear and cytoplasmic compartments before antigen presentation by MHC class I. *Immunity*. 2003, **18**: 97-108.
- Rescigno, M., Citterio, S., Thery, C., Rittig, M., Medaglini, D., Pozzi, G., Amigorena, S., Ricciardi-Castagnoli, P. Bacteria-induced neo-biosynthesis, stabilization, and surface expression of functional class I molecules in mouse dendritic cells. *Proc Natl Acad Sci U S A*. 1998, **95**: 5229-34.
- Roake, J.A., Rao, A.S., Morris, P.J., Larsen, C.P., Hankins, D.F., Austyn, J.M. Dendritic cell loss from nonlymphoid tissues after systemic administration of lipopolysaccharide, tumor necrosis factor, and interleukin 1. *J Exp Med*. 1995, **181**: 2237-47.
- Roche, P.A., Cresswell, P. Invariant chain association with HLA-DR molecules inhibits immunogenic peptide binding. *Nature*. 1990, **345**: 615-8.
- Rodriguez, A., Regnault, A., Kleijmeer, M., Ricciardi-Castagnoli, P., Amigorena, S. Selective transport of internalized antigens to the cytosol for MHC class I presentation in dendritic cells. *Nat Cell Biol*. 1999, **1**: 362-8.

- Rohatgi, R., Ma, L., Miki, H., Lopez, M., Kirchhausen, T., Takenawa, T., Kirschner, M.W. The interaction between N-WASP and the Arp2/3 complex links Cdc42-dependent signals to actin assembly. *Cell*. 1999, **97**: 221-31.
- Rybakin, V., Clemen, C.S. Coronin proteins as multifunctional regulators of the cytoskeleton and membrane trafficking. *Bioessays*. 2005, **27**: 625-632.
- Rybakin, V., Stumpf, M., Schulze, A., Majoul, I.V., Noegel, A.A., Hasse, A. Coronin 7, the mammalian POD-1 homologue, localizes to the Golgi apparatus. *FEBS Lett*. 2004, **573**: 161-7.
- Rupper, A., Lee, K., Knecht, D., Cardelli, J. Sequential activities of phosphoinositide 3-kinase, PKB/Aakt, and Rab7 during macropinosome formation in Dictyostelium. *Mol Biol Cell*. 2001, **12**: 2813-24.
- Sadasivan, B., Lehner, P.J., Ortmann, B., Spies, T., Cresswell, P. Roles for calreticulin and a novel glycoprotein, tapasin, in the interaction of MHC class I molecules with TAP. *Immunity*. 1996, **5**: 103-14.
- Sallusto, F., Cella, M., Danieli, C., Lanzavecchia, A. Dendritic cells use macropinocytosis and the mannose receptor to concentrate macromolecules in the major histocompatibility complex class II compartment: downregulation by cytokines and bacterial products. *J Exp Med*. 1995, **182**: 389-400.
- Sallusto, F., Lanzavecchia, A. Efficient presentation of soluble antigen by cultured human dendritic cells is maintained by granulocyte/macrophage colony-stimulating factor plus interleukin 4 and downregulated by tumor necrosis factor alpha. *J Exp Med*. 1994, **179**: 1109-18.
- Schild, H., Rammensee, H.G. Perfect use of imperfection. *Nature*. 2000, **404**: 709-10.
- Schubert, U., Anton, L.C., Gibbs, J., Norbury, C.C., Yewdell, J.W., Bennink, J.R. Rapid degradation of a large fraction of newly synthesized proteins by proteasomes. *Nature*. 2000, **404**: 770-4.
- Schulz, O., Diebold, S.S., Chen, M., Naslund, T.I., Nolte, M.A., Alexopoulou, L., Azuma, Y.T., Flavell, R.A., Liljestrom, P., Reis e Sousa, C. Toll-like receptor 3 promotes cross-priming to virus-infected cells. *Nature*. 2005, **433**: 887-92.
- Serwold, T., Gonzalez, F., Kim, J., Jacob, R., Shastri, N. ERAAP customizes peptides for MHC class I molecules in the endoplasmic reticulum. *Nature*. 2002, **419**: 480-3.
- Shen, Z., Reznikoff, G., Dranoff, G., Rock, K.L. Cloned dendritic cells can present exogenous antigens on both MHC class I and class II molecules. *J Immunol*. 1997, **158**: 2723-30.
- Shortman, K., Liu, Y.J. Mouse and human dendritic cell subtypes. *Nat Rev Immunol*. 2002, **2**: 151-61. Review.
- Sigal, L.J., Crotty, S., Andino, R., Rock, K.L. Cytotoxic T-cell immunity to virus-infected non-haematopoietic cells requires presentation of exogenous antigen. *Nature*. 1999, **398**: 77-80.
- Simons, K., Ikonen, E. Functional rafts in cell membranes. *Nature*. 1997, **387**: 569-72. Review.
- Sloan, V.S., Cameron, P., Porter, G., Gammon, M., Amaya, M., Mellins, E., Zaller, D.M. Mediation by HLA-DM of dissociation of peptides from HLA-DR. *Nature*. 1995, **375**: 802-6.
- Snapper, S.B., Rosen, F.S. The Wiskott-Aldrich syndrome protein (WASP): roles in signaling and cytoskeletal organization. *Annu Rev Immunol*. 1999, **17**: 905-29. Review.
- Steinman, R.M., Swanson, J. The endocytic activity of dendritic cells. *J Exp Med*. 1995, **182**: 283-8. Review.
- Steimle, V., Siegrist, C.A., Mottet, A., Lisowska-Groszpiere, B., Mach, B. Regulation of MHC class II expression by interferon-gamma mediated by the transactivator gene CIITA. *Science*. 1994, **265**: 106-9.

- Stinchcombe, J.C., Bossi, G., Booth, S., Griffiths, G.M. The immunological synapse of CTL contains a secretory domain and membrane bridges. *Immunity*. 2001, **15**: 751-61.
- Suto, R., Srivastava, P.K. A mechanism for the specific immunogenicity of heat shock protein-chaperoned peptides. *Science*. 1995, **269**: 1585-8.
- Suzuki, K., Nishihata, J., Arai, Y., Honma, N., Yamamoto, K., Irimura, T., Toyoshima, S. Molecular cloning of a novel actin-binding protein, p57, with a WD repeat and a leucine zipper motif. *FEBS Lett*. 1995, **364**: 283-8.
- Spies, T., Bresnahan, M., Bahram, S., Arnold, D., Blanck, G., Mellins, E., Pious, D., DeMars, R. A gene in the human major histocompatibility complex class II region controlling the class I antigen presentation pathway. *Nature*. 1990, **348**: 744-7.
- Svensson, M., Wick, M.J. Classical MHC class I peptide presentation of a bacterial fusion protein by bone marrow-derived dendritic cells. *Eur J Immunol*. 1999, **29**: 180-8.
- Svensson, M., Stockinger, B., Wick, M.J. Bone marrow-derived dendritic cells can process bacteria for MHC-I and MHC-II presentation to T cells. *J Immunol*. 1997, **158**: 4229-36.
- Swanson, J.A. Phorbol esters stimulate macropinocytosis and solute flow through macrophages. *J Cell Sci*. 1989, **94**: 135-42.
- Teyton, L., O'Sullivan, D., Dickson, P.W., Lotteau, V., Sette, A., Fink, P., Peterson, P.A. Invariant chain distinguishes between the exogenous and endogenous antigen presentation pathways. *Nature*. 1990, **348**: 39-44.
- Tonegawa, S. Somatic generation of immune diversity. *Biosci Rep*. 1988, **8**: 3-26. Review.
- Townsend, A., Ohlen, C., Bastin, J., Ljunggren, H.G., Foster, L., Karre, K. Association of class I major histocompatibility heavy and light chains induced by viral peptides. *Nature*. 1989, **340**: 443-8.
- Trombetta, E.S., Mellman, I. Cell biology of antigen processing in vitro and in vivo. *Annu Rev Immunol*. 2005, **23**: 975-1028.
- Trombetta, E.S., Ebersold, M., Garrett, W., Pypaert, M., Mellman, I. Activation of lysosomal function during dendritic cell maturation. *Science*. 2003, **299**: 1400-3.
- Tsai, B., Ye, Y., Rapoport, T.A. Retro-translocation of proteins from the endoplasmic reticulum into the cytosol. *Nat Rev Mol Cell Biol*. 2002, **3**: 246-55. Review.
- Tulp, A., Verwoerd, D., Dobberstein, B., Ploegh, H.L., Pieters, J. Isolation and characterization of the intracellular MHC class II compartment. *Nature*. 1994, **369**: 120-6.
- Vassilakos, A., Cohen-Doyle, M.F., Peterson, P.A., Jackson, M.R., Williams, D.B. The molecular chaperone calnexin facilitates folding and assembly of class I histocompatibility molecules. *EMBO J*. 1996, **15**: 1495-506.
- von Boehmer, H., Hafen, K. Minor but not major histocompatibility antigens of thymus epithelium tolerize precursors of cytolytic T cells. *Nature*. 1986, **320**: 626-8.
- Wang, R.F., Parkhurst, M.R., Kawakami, Y., Robbins, P.F., Rosenberg, S.A. Utilization of an alternative open reading frame of a normal gene in generating a novel human cancer antigen. *J Exp Med*. 1996, **183**: 1131-40.
- Watts, C. Capture and processing of exogenous antigens for presentation on MHC molecules. *Annu Rev Immunol*. 1997, **15**: 821-50. Review.

- Webb, Y., Hermida-Matsumoto, L., Resh, MD. Inhibition of protein palmitoylation, raft localization, and T cell signaling by 2-bromopalmitate and polyunsaturated fatty acids. *J Biol Chem.* 2000, **275**: 261-70.
- West, M.A., Prescott, A.R., Eskelinen, E.L., Ridley, A.J., Watts, C. Rac is required for constitutive macropinocytosis by dendritic cells but does not control its downregulation. *Curr Biol.* 2000, **10**: 839-48.
- West, M.A., Lucocq, J.M., Watts, C. Antigen processing and class II MHC peptide-loading compartments in human B-lymphoblastoid cells. *Nature.* 1994, **369**: 147-51.
- Wiertz, E.J., Tortorella, D., Bogyo, M., Yu, J., Mothes, W., Jones, T.R., Rapoport, T.A., Ploegh, H.L. Sec61-mediated transfer of a membrane protein from the endoplasmic reticulum to the proteasome for destruction. *Nature.* 1996, **384**: 432-8.
- Wolfers, J., Lozier, A., Raposo, G., Regnault, A., Thery, C., Masurier, C., Flament, C., Pouzieux, S., Faure, F., Tursz, T., Angevin, E., Amigorena, S., Zitvogel, L. Tumor-derived exosomes are a source of shared tumor rejection antigens for CTL cross-priming. *Nat Med.* 2001, **7**: 297-303.
- Yan, M., Collins, R.F, Grinstein, S., Trimble, W.S. Coronin-1 Function Is Required for Phagosome Formation. *Mol Biol Cell.* 2005.
- Ye, Y., Shibata, Y., Yun, C., Ron, D., Rapoport, T.A. A membrane protein complex mediates retrotranslocation from the ER lumen into the cytosol. *Nature.* 2004, **429**: 841-7.
- Zhang, J., Shehabeldin, A., da Cruz, L.A., Butler, J., Somani, A.K., McGavin, M., Kozieradzki, I., dos Santos, A.O., Nagy, A., Grinstein, S., Penninger, J.M., Siminovitch, K.A. Antigen receptor-induced activation and cytoskeletal rearrangement are impaired in Wiskott-Aldrich syndrome protein-deficient lymphocytes. *J Exp Med.* 1999, **190**: 1329-42.

- Chapter 2 -

Materials and Methods

2.1. Reagents

2.1.1. Chemicals

acetic acid	Merck
acetone	Merck
acrylamide	Bio-Rad
agarose (LE)	Roche Diagnostics
adenosine-5'-triphosphate (ATP)	Boehringer Mannheim
albumin, bovine, 96% pure	Sigma
albumin, chicken egg grade V, minimum 98 % purity	Sigma
aluminum oxide, type 5016A, basic [Al ₂ O ₃]	Fluka
ammonium persulfate (APS)	Bio-Rad
ammonium sulfate [(NH ₄) ₂ SO ₄]	Merck
ampicillin	Sigma
antipain	Fluka
aprotinin	Merck
Bacto-Tryptone	Difco
Bacto-Yeast	Difco
bicinchoninic acid (BCA)	Pierce
bisacrylamide (N',N-methylen bisacrylamide)	Bio-Rad
boric acid	Merck
bromophenol blue	Merck
calcium chloride [CaCl ₂ x H ₂ O]	Sigma
cerium (VI)-sulfate [Ce(SO ₄) ₂ x 4H ₂ O]	Fluka
cholesterol, 98% pure	Avanti Polar-Lipids, Inc.
chloroform	Merck
chymostatin	Merck
Coomassie brilliant blue G-250	Bio-Rad
Coomassie brilliant blue R-250	Bio-Rad
deoxycholate	Sigma
desoxynucleotides (dNTP)	Roche Diagnostics
deuterated chloroform [CDCl ₃]	Dr. Glaser
dextran fluorescein, anionic, lysine fixable (MW 2 000 000)	Molecular Probes
3,3'-diaminobenzidine tetrahydrochloride (DAB)	Sigma
o-dianisidine	Sigma
dichloromethane	Merck
dicyclohexyl carbodiimide (DCC)	Sigma
4-(dimethylamino)-pyridine (DMAP)	Sigma
3,3'-dimethoxybenzidine, dihydrochloride (o-Dianisidine)	Sigma
N,N-dimethylformamide (DMF)	Merck
dimethylsulfoxide (DMSO)	Fluka
1,4-dioxane	Sigma
N,N'-disuccinimidyl carbonate (DSC)	Sigma
dithiothreitol (DTT)	Sigma
DNA standards	Roche Diagnostics
T4 DNA Ligase	New England Biolabs
EBSS (10x)	Gibco BRL
ethylene glycol-bis(β-aminoethylether)-tetraacetic acid (EGTA)	Sigma

elastase	Roche Diagnostics
ethanol	Merck
ethidium bromide	Sigma
ethyl acetate	Acros Organic
ethylenediamine tetraacetate (EDTA), sodium salt	Fluka
<i>trans, trans</i> -farnesol, 96% pure	Sigma
fatty acids	Sigma
ferric chloride [FeCl ₃]	Sigma
Ficoll-Paque	Pharmacia
FluoroGuard Antifade Reagent	Bio-Rad
Hi-Di™ Formamide	Applied Biosystems
5-bromo-4-chloro-3-indolyl-beta-D-galactopyranoside (X-Gal)	Appli Chem
gel filtration molecular weight standards	Biorad
D(+)-glucose	Fluka
glutaraldehyde, 50% aqueous solution	Sigma
glycine	Fluka
glycerol	Fluka
hydroxyethylpiperidine-ethanesulfonic acid (HEPES)	AppliChem
horseradish peroxidase (HRP)	Sigma
H ₂ O ₂ , 30 %, p.a.	Fluka
hydroxylamine hydrochloride	Fluka
hydrochloric acid (HCl)	Merck
imidazole	Fluka
iodine	Amersham
isopropyl-thiogalactoside (IPTG)	AppliChem
lactacystin, synthetic	Calbiochem
leupeptin	Fluka
lipofectin	Gibco BRL
lovastatin	Calbiochem
lipopolysaccharide (LPS)	Sigma
lysine	Sigma
lysis buffer (Facs™ Lysing Solution)	Becton Dickinson
lysozyme	Sigma
manganese chloride [MnCl ₂]	Sigma
magnesium chloride [MgCl ₂]	Sigma
magnesium sulfate [MgSO ₄]	Sigma
mevalonic acid	Sigma
methanol	Merck
methylacetate	Fluka
methyl-β-cyclodextrin	Sigma
mevalonic acid	Sigma
Mircoscient™ 40	Packard
ammonium molybdat-tetrahydrat [Mo ₇ O ₂₄ x 4H ₂ O]	Fluka
2-(N-morpholin) ethansulfonic acid (MES)	Fluka
N-hydroxysuccinimide (NHS)	Perbio
n-octylglucopyranoside	Sigma
oregon Green-NHS	Molecular Probes
palmitic acid-N-hydroxy succinimidester (NHS-palmitic acid)	Sigma
paraformaldehyde, powder, 95% pure	Aldrich
pepstatin	Fluka

petrol ether (40-60°C)	Fluka
phenylmethylsulfonylfluoride (PMSF)	Sigma
piperazine-1,4-bis(2-ethanesulfonic acid) (PIPES)	Sigma
phosphoric acid	Fluka
phorbol-1.2-myrisate, 1.3-acetate (PMA)	Sigma
Polyfect	QIAGEN
Ponceau S	Sigma
potassium chloride [KCl]	Sigma
potassium hydroxide [KOH]	Sigma
potassium dihydrogen phosphate [KH ₂ PO ₄]	Merck
2-propanol	Merck
restriction enzymes	New England Biolabs
saponin (from Quillaja Burk)	Sigma
SDS-PAGE molecular weight standards	Bio-Rad
shrimp alkaline phosphatase (SAP)	Roche Diagnostics
sodium acetate	Fluka
sodium chloride [NaCl]	Merck
sodium dihydrogen phosphate [NaH ₂ PO ₄]	Fluka
sodium dodecylsulfate (SDS)	Bio-Rad
sodium hydroxide [NaOH]	Merck
di-sodium hydrogenphosphate [Na ₂ HPO ₄]	Fluka
sucrose	BDH
sulfuric acid [H ₂ SO ₄]	Fluka
N,N,N',N'-tetramethylenethyldiamine (TEMED)	Bio-Rad
[methyl- ³ H]-thymidine	Amersham
trichloroacetic acid (TCA)	Merck
triethanolamine	Fluka
trifluoroacetic acid (TFA)	Fluka
tris(hydroxymethyl)aminomethane (Tris / Trizma base)	Sigma
Triton X-100	Boehringer Mannheim
trypan blue	Gibco BRL
trypsin-EDTA in HBSS	Gibco BRL
Tween 20	Merck
xylene cyanol FF	Sigma

2.1.2. Kits

Big Dye1.1 [®] Terminator v 1.1 Cycle Sequencing Kit	Applied Biosystems
BCA protein detection kit	Pierce
Enhanced Chemoluminescence (ECL) kit	Amersham
Expand Long Template PCR System Kit	Roche Diagnostics
Plasmid DNA Mini/Maxi-prep kit	QIAGEN
PolyFect [®] Transfection Reagent	QIAGEN
QIAquick Gel Extraction kit	QIAGEN
QIAquick Nucleotide Removal kit	QIAGEN
QIAquick PCR Purification kit	QIAGEN
pGEM [®] -T-Easy Vector kit	Promega

2.1.3. Peptides

GSGSGSK(Acetyl)	Peptide Specialty Laboratories, Germany
GILGFVTLTV [IM (58-66)]	Neosystem, Strasbourg,
YKLVVVGAG [Ras (4-12)]	Neosystem, Strasbourg,

SIINFEKL and Palm-SIINFEKL were synthesized using Fmoc-chemistry on peptide synthesizer AMS 422 (Abimed).

2.2. General buffers and solutions

DNA loading buffer (6x)	0.25% bromophenol blue 0.25% xylene cyanol FF 1 mM EDTA pH 8.0 30% glycerol
Homogenization buffer (HB)	10 mM triethanolamine 10 mM acetic acid 1 mM EDTA 0.25 M sucrose adjusted of pH 7.4 with NaOH
Lysis buffer (10x)	200 mM HEPES pH 7.4 1 M NaCl 50 mM MgCl ₂ 10% Triton X-100
PBS	137 mM NaCl 2.7 mM KCl 8 mM Na ₂ HPO ₄ 1.5 mM KH ₂ PO ₄
PBST	PBS + 0.2% (v/v) Tween 20
PD-buffer	7 mM Na-phosphate pH 7.4 137 mM NaCl 3 mM KCl
SDS-PAGE electrophoresis buffer, (10x)	1.9 M glycine 250 mM Tris SDS was added to the 1x buffer to a final conc. of 0.1% before use

SDS-PAGE reducing sample buffer, (5x)	10% (w/v) SDS 20% (v/v) glycerol 500 mM DTT (as powder) 300 mM Tris/HCl pH 6.8 0.015% (w/v) bromphenol blue
Semi-dry transfer buffer, 10x	480 mM Tris 390 mM glycine 0.375% (w/v) SDS 20% (v/v) methanol was added to the 1x buffer before use
10x TBE	108 g Tris 55 g Boric acid 40 ml of 0.5 M Na ₂ EDTA (pH 8.0) filled up to 1L with dH ₂ O
100x CLAAP	100 µg/ml chymostatin 100 µg/ml leupeptin 100 µg/ml aprotinin 100 µg/ml antipain 100 µg/ml pepstatin
100x PMSF	1 mM PMSF in 100 % ethanol

2.3. Bacterial media and supplements

Luria-Bertani Media (LB)	10 g tryptone (Difco) 5 g yeast extract (Difco) 10 g NaCl dissolved in 1L H ₂ O and autoclaved
ampicilin	Sigma, stock 100 mg/ml, use at 100 µg/ml
kanamycin	Sigma, stock 50 mg/ml, use 50 µg/ml

2.4. Cell culture media and supplements

DMEM powder	Gibco BRL
DMEM	Gibco BRL
RPMI 1640 w/o L-arginine, L-cysteine, L-methionine Inositol, glucose, L-glutamine	Gibco BRL
IMDM	Gibco BRL
Fetal calf serum (FCS)	Gibco BRL
Horse serum	Gibco BRL
Human serum	Blutspendezentrum, Basel, Switzerland

L-glutamine (200 mM)	Gibco BRL
β -mercaptoethanol (50 mM)	Gibco BRL
Sodium pyruvate (100 mM)	Gibco BRL
MEM (non-essential amino acids)	Gibco BRL
HEPES (1 M)	Gibco BRL
Penicillin/Streptomycin (10.000 U/ml, 10.000 μ g/ml)	Gibco BRL
Kanamycin (10.000 U/ml)	Gibco BRL
Trypsin/EDTA in HBBS	Gibco BRL
GM-CSF	Genzyme, Diagnostic
Lactacystin, synthetic	Calbiochem
Interleukin 2 (IL-2), recombinant, murine	PharMingen
Interleukin 4, (IL-4), recombinant, murine	R&D Systems
Interleukin 4 (IL-4), human	.. Dr. Lanzavecchia, Bellinzona, Switzerland

2.5. Vectors

Name (kb)	Vector	Insert; cloning site	Constructor (reference)	Application
pGEM [®] -T Easy (3kb)	pGEM [®] -T Easy amp ^r	—	Promega	subcloning
pCB6 (6.2kb)	pCB6, amp ^r , neo ^r	—	obtained through P. van der Sluijs Utrecht University, Netherlands	eukaryotic expression vector cloning
pCB6-Cor1-HA (7.6kb)	pCB6, amp ^r , neo ^r	Cor1-HA via EcoR1	J. Gatfield	expression of Cor1-HA in HEK293 cells
pCB-Cor1 Δ ACC-HA (7.5kb)	pCB6, amp ^r , neo ^r	Cor1-HA lacking aa 433-461; via EcoR1	J. Gatfield	expression of Cor1- Δ ACC-HA in HEK293 cells
pCB6-Cor1 Δ 400-416 (7.5kb)	pCB6, amp ^r , neo ^r	Cor1-HA lacking aa 400-416; via EcoR1	I. Albrecht, this thesis	expression of Cor1- Δ 400-416-HA in HEK293 cells
pCB6-Cor1- Δ 361-422 (7.4kb)	pCB6, amp ^r , neo ^r	Cor1-HA lacking aa 361-422; via EcoR1	I. Albrecht, this thesis	expression of Cor1- Δ 400-416-HA in HEK293 cells
pCB-Cor1 ^{L+C} -HA (6.5kb)	pCB6, amp ^r , neo ^r	Cor1-HA lacking aa 1-355; via EcoR1	B. Zanolari / I. Albrecht, this thesis	expression of Cor1 ^{L+C} -HA in HEK293 cells
pEGFP-N1 (4.7 kb)	pEGFP-N1 kan ^r , neo ^r	—	BD Biosciences Clontech	expression of EGFP and of c-terminal tagged EGFP fusionproteins in eukaryotic cells
pEGFP-N1-CC _{coronin1} (4.8kb)	pEGFP-N1 kan ^r , neo ^r	Cor1 lacking aa 1-428; via Xho I and Bam HI	B. Zanolari	expression Cor1-CC-EGFP fusion protein in HEK293 cells
pEGFP-N1-CC _{matrilin 4} (4.8kb)	pEGFP-N1 kan ^r , neo ^r	Mat4 coiled-coil (aa 574-619) via Bgl II and Bam HI	I. Albrecht, this thesis	expression Mat4-CC-EGFP fusion protein in HEK293 cells
pET22b-Cor1 ^{L+C} (5.8kb)	pET22b amp ^r (Novagen),	Cor1 lacking aa 1-355; via NdeI and XhoI, no tag	I. Albrecht, this thesis	expression of Cor1 ^{L+C} in <i>E. coli</i>
pET16-NLS-IM- (1-252) (6.4kb)	pET16b amp ^r (Novagen)	NLS-mutant of IM 1-252, via Xho I and BglIII	from F. Baudin, EMBL Grenoble	expression of NLS-mutated influenza matrix protein (1-252) in <i>E. coli</i>

2.6. Oligonucleotides

Name	Sequence (5'-3')	Source of sequence	Application
pET 22, F2.2	<i>GGG AAT CCC ATA TGT CGG ACC TGT TCC AGG AGG ACC TG</i>	Cor1-cDNA, bp 1066-1089	generation of of Cor1 ^{L+C} , coding
pET 22 R2.2	<i>CCG CTC GAG CTA CTA CTT GGC CTG AAC AGT CTC CTC CAG</i>	Cor1-cDNA bp 1360-1386	generation of Cor1 ^{L+C} , reverse
Dom I start	<i>GTG AAT TCC ATG AGC CGG CAG GTG GTT CG</i>	Cor1-cDNA, bp 1-20	site-directed mutagenesis, deletion of aa 400-416 and of aa 361-422
Dom II start	<i>GTG AAT TCC ATG TCG GAC CTG TTC CAG GAG</i>	Cor1-cDNA, bp 1066-1083	generation of Cor1 ^{L+C} -HA, coding
Dom III HA stop	<i>GAG GAT CCC TAA GCG TAA TCT GGA <u>ACA TCG TAT GGG TAC TTG GCC TGA</u> ACA GTC TCC</i>	Cor1-cDNA, bp 1365-1383	- generation of Cor1 ^{L+C} -HA, reverse - site-directed mutagenesis, deletion of aa 400-416 and of aa 361-422
Cor1M1198-1249- F	<i>GGC TAC GTG CCC CCA // GCT ACA CCA GAG CCC AGC GGC A</i>	Cor1-cDNA, bp 1184-1197 // 1249- 1270	site-directed mutagenesis, deletion of aa 400-416
Cor1M1198-1249- R	<i>GGG CTC TGG TGT AGC // TGG GGG CAC GTA GCC ATC CTT G</i>	Cor1-cDNA, bp 1176-1197// 1249- 1263	site-directed mutagenesis, deletion of aa 400-416
Cor1M1081-1266 - F	<i>GGA CCT GTT CCA G // GG CAC GCC CAG</i>	Cor1-cDNA, bp 1068-1080 //1267- 1277	site-directed mutagenesis, deletion of aa 361-422
Cor1M1081-1266- R	<i>CTG GGC GTG CC // C TGG AAC AGG TCC</i>	Cor1-cDNA, bp 1068-1080 //1267- 1277	site-directed mutagenesis, deletion of aa 361-422
Mat4-1612	<i>GAT CTG AGC TTC GGA GCC CAT GCG AA</i>	hMatrilin4 cDNA, variant 1, bp 1612-1632	generation of CC _{matrilin 4} construct, introduction for restriction sites, reverse
Mat4-Stop-R	<i>CGC GGA TCC TCA CTT CTG GTT GGC CAG CTG</i>	hMatrilin4 cDNA, variant 1, bp 1735-1755	generation of CC _{matrilin 4} construct, introduction of restriction sites, coding
Mat4T-1612	<i>GAG CTT CGG AGC CCA TGC GAA TGC GAA AGC CTC GTG GAG TTC CAG GGC CGC ACG CTG GGG GCG CTC GAG AGC CTG ACG CTG AAC CTG</i>	hMatrilin4 cDNA, variant 1, bp 1612-1699	generation of CC _{matrilin 4} construct template for PCR, coding
Mat4T-1669	<i>TCA CTT CTG GTT GGC CAG CTG GTT CTC CAG ATC CTC CAG GCG CGC CGT CAG CTG GGC CAG GTT CAG CGT CAG GCT CTC GAG CGC CCC C</i>	hMatrilin4 cDNA, variant 1, bp 1668-1755	generation of CC _{matrilin 4} construct, template for PCR, reverse

Remarks: coding sequence in italics, // marks deletion, sequence for HA-tag is underlined
All primers were obtained from Microsynth GmbH, Switzerland.

2.7. Antibodies / Dyes

Name	Isotype	Antigen / Target	Source	Application (dilution)
antiserum 1002	rabbit	GST-coronin 1, (mouse)	J. Gatfield	native immunoprecipitation immunofluorescence (1:1000)
antiserum 560	rabbit	VVRSSKFRHVFGQ PAK (coronin 1, aa 5-20) (mouse)	G. Ferrari BII	immunoblotting (1:1000)
12CA5 (anti-HA) (0.2 mg/ml)	mouse IgG _{2b}	YDYPVPDYA (hemagglutinintag)	Boehringer Mannheim	immunofluorescence (5 µg/ml)
HA.11 (anti-HA)	mouse IgG ₁	CYPYDVPDYASL (hemagglutinintag)	Covance	immunoblotting, immunofluorescence (1:1000)
anti-clathrin	mouse IgG ₁	clathrin heavy chain	Transduction laboratories	immunofluorescence (1:50)
4D1B	rat IgG _{2a}	mouse LAMP-1	T. August, Dev. Studies Hybridoma Bank, Univ. Iowa	immunofluorescence undiluted supernatant
anti Na/K ATPase	mouse IgG _{2a}	human Na/K-ATPase	H.P. Hauri, Biozentrum Basel	immunofluorescence immunoblotting (1:100)
anti-actin	mouse IgG _{1κ}	G-and F-actin	Chemicon International	immunoblotting (1:2000)
anti-GFP, (4 mg/ml)	mouse IgG _{1κ}	GFP	Roche Diagnostics	immunoblotting (1:1000)
FITC anti-CD8	rat IgG _{2a}	mouse CD8 α chain	Becton Dickinson	flow cytometry (1:100)
FITC anti-CD8	mouse IgG _{2a}	human CD8	Becton Dickinson	flow cytometry (1:50 - 1:100)
FITC anti-Vβ-TCR	mouse IgG _{1κ}	mouse Vβ 5.1, 5.2 TCR	Becton Dickinson	flow cytometry (1:100), typing OT-1 mice
R-PE anti-Vα-TCR	rat IgG _{2a}	mouse Vα 2 TCR	Becton Dickinson	flow cytometry (1:1000), typing OT-1 mice
anti-CD4	rat IgG _{2a}	mouse CD4	Becton Dickinson	coupled to dynabeads
anti-MHC class II	rat IgG _{2b}	mouse	Becton Dickinson	coupled to dynabeads
PE anti-CD11c	hamster IgG ₁	mouse CD11c α-chain	Becton Dickinson	flow cytometry (1:200)
FITC anti-CD11b (Mac1)	rat IgG _{2b}	mouse integrin α _M -chain	Becton Dickinson	flow cytometry
FITC anti F4/80	rat	mouse F4/80	Serotech	flow cytometry (1:1000)
NLDC145	rat	mouse DEC-205	Georg Kraal, University of Amsterdam	flow cytometry (1:40)
R-PE-HLA- A*0201/GILGFVFTL pentamers	-	human GILGFVFTL specific TCR	Proimmune	flow cytometry (1:50 - 1:100)
anti-rat IgG(H+L)- TXRD	goat	rat IgG (H+L)	Southern Biotechnology Association	immunofluorescence, (1:200)

Alexa Fluor™-586 goat-anti-mouse IgG (H+L), (2 mg/ml)	goat	rat IgG (H+L)	Molecular Probes	immunofluorescence (1 :200)
Alexa Fluor™-488 goat-anti-mouse IgG (H+L), (2 mg/ml)	goat	rat IgG (H+L)	Molecular Probes	immunofluorescence (1:200)
goat-anti-mouse IgG ₁ - TXRD (1 mg/ml)	goat	heavy chain of mouse IgG ₁	Southern Biotechnology Association	immunofluorescence (1:200)
goat-anti-mouse IgG _{2b} - FITC, (1 mg/ml)	goat	heavy chain of mouse IgG _{2b}	Southern Biotechnology Association	immunofluorescence (1:200)
goat-anti-mouse IgG ₁ - TXRD (1 mg/ml)	goat	heavy chain of mouse IgG ₁	Southern Biotechnology Association	immunofluorescence (1:200)
goat-anti-mouse IgG _{2b} - TXRD, (1 mg/ml)	goat	heavy chain of mouse IgG _{2b}	Southern Biotechnology Association	immunofluorescence (1:200)
anti-mouse IgG (H+L)- HRP (1mg/ml)	goat	heavy chain of mouse IgG	Southern Biotechnology Association	immunoblotting (1:10 000)
anti-rabbit IgG (H+L)- HRP (1 mg/ml)	goat	heavy chain of rabbit IgG	Southern Biotechnology Association	immunoblotting (1:10 000)
AlexaFluor®- Phalloidin 568	-	F-actin	Molecular Probes	immunofluorescence (1:100)
AlexaFluor®- Phalloidin 488	-	F-actin	Molecular Probes	immunofluorescence (1:100)
Filipin (5% in MeOH)	-	cholesterol	Fluka	immunofluorescence (1:100)
CD14 Microbeads	mouse IgG2a	human CD14	Miltenyi Biotech	isolation of CD14 ⁺ monocytes by magnetic bead separation (1:10)
CD8 Microbeads	mouse IgG2a	human CD8	Miltenyi Biotech	isolation of CD8 ⁺ T-cells by magnetic bead separation (1:10)

2.8. Bacteria, culture conditions

Name	Source	Culture Medium	Culture Conditions	Applications
<i>E. coli</i> DH10β	S. Arber, Biozentrum Basel	LB-media	37°C, 250 rpm	propagation and storage of plasmid DNA
<i>E. coli</i> BL21	J. Pieters Biozentrum Basel	LB-media	37°C, 250 rpm	protein expression

2.9. Cells and cell lines, culture conditions

Name	Cell type	Source	Culture Medium
J774A.1	mouse macrophage-like cell line (Balb/c-mouse)	ATCC	DMEM, 10% (v/v) FCS 1% (v/v) 200 mM glutamine
BMMØ	bone marrow derived macrophages	C57BL/6 mouse	DMEM, 10% (v/v) FCS 5% (v/v) horse serum 1% (v/v) penicillin/streptomycin 1% (v/v) 200 mM glutamine 1% (v/v) 100 mM sodium pyruvate 0.1% (v/v) 50 mM β -mercaptoethanol 30% (v/v) L929-conditioned medium
BMDC	bone marrow derived dendritic cells	C57BL/6 mouse	DMEM, 10% (v/v) FCS 1% (v/v) penicillin/streptomycin 1% (v/v) 200 mM glutamine 25 ng/ml GM-CSF after three days of culture 1.5 ng/ml of murine IL-4 were added
HEK293	human embryonic kidney cells	ATCC	DMEM, 10% (v/v) FCS 1% (v/v) 200 mM glutamine
OT-1 lymphocytes	lymphocytes	ova WT Rag ^{-/-} OT-1 mouse (Hogquist <i>et al.</i> , 1994), obtained from E. Palmer, ZLF, Kantonsspital Basel Switzerland	IMDM, 5% (v/v) FCS 1% (v/v) penicillin/streptomycin 1% (v/v) 200 mM glutamine 0.1% (v/v) 50 mM β -mercaptoethanol
human dendritic cells (hDC)	derived from peripheral blood monocytes	isolated from blood of a healthy donor	RPMI 1640, 10% (v/v) FCS 1% (v/v) kanamycin 1% (v/v) 200 mM glutamine 1% (v/v) 100 mM sodium pyruvate 1% (v/v) MEM 0.1% (v/v) 50 mM β -mercaptoethanol 1000 U/ml human IL-4 50 ng/ml GM-CSF
human T cells	derived from peripheral blood	isolated from blood of a healthy donor	RPMI 1640, 5% (v/v) HS 1% (v/v) kanamycin 1% (v/v) 200 mM glutamine 1% (v/v) 1 M HEPES 1% (v/v) sodium pyruvate 1% (v/v) MEM
L929	fibroblasts	(Wiltschke <i>et al.</i> , 1989) obtained from M. Kopf, ETH, Zürich, Switzerland	IMDM, 10% (v/v) FCS 0.1% (v/v) 50 mM β -mercaptoethanol 1% (v/v) 200 mM glutamine

Cells and cell lines were cultured at 37°C in a humidified atmosphere at 5 % CO₂.

2.10. Molecular biology

2.10.1. Agarose gel electrophoresis

Analytical and preparative gel electrophoretic separation of DNA was performed using low endotoxin agarose (Roche Diagnostics) gels of different concentrations in 1x TBE buffer. Ethidium bromide (10 µg/ml) was normally added to the gel before pouring and prior to loading 6x DNA loading buffer was added to each sample. Electrophoresis was performed at 50-90V using gel electrophoresis chambers (Werkstatt, Biozentrum Basel).

2.10.2. Preparation of electro-competent *E. coli* BL21

Materials

- 10% glycerol, sterile
- 2L dH₂O, sterile

1L of LB media was inoculated with 10 ml of a fresh overnight culture of *E. coli* BL21 from a single bacteria colony. The culture was grown at 37°C with vigorous shaking to an OD₆₀₀ of 0.5-0.8, and then the flask was placed on ice for 15-30 min. All of the following steps were performed at 4°C. The bacteria were washed subsequently with 1L of ice-cold dH₂O, with 0.5L of ice-cold dH₂O and with 20 ml of 10% ice-cold glycerol. Bacteria were pelleted in between the different wash steps by centrifugation at 4000 x g (15 min, 4°C). After the last wash, the bacteria were resuspended to a final volume of 2-3 ml in 10% glycerol (final cell concentration 3x 10¹⁰ bacteria /ml) and 50 µl aliquots were prepared, frozen in a mixture of ethanol and dry ice or liquid nitrogen and stored until use at -70°C.

2.10.3. Preparation of ultra-competent *E. coli* DH10β

Materials

- SOB solution: 0.5% (w/v) yeast extract, 2% (w/v) tryptone, 10 mM NaCl, 2.5 mM KCl, 10 mM MgCl₂, 10 mM MgSO₄ were dissolved in 1L dH₂O and autoclaved
- TB solution: 10 mM PIPES, 15 mM CaCl₂, 250 mM KCl were dissolved in dH₂O, the pH was adjusted to 6.7 with KOH or HCl then 55 mM MnCl₂ were added, filled up to 1L with dH₂O and filtered (0.45 µm)
- DMSO storage O/N at -20°C

Preparation of ultra-competent *E. coli* DH10β cells was performed according Inoue *et al.*, (1990). Ten to twelve large colonies of DH10β cells were picked from a LB agar plate cultured O/N at 37°C and used for inoculation of 250 ml SOB media. Culture in 1L flask was grown at 19°C under vigorous shaking till OD₆₀₀ = 0.5, then the flask was placed for 10 min on ice. All of the following steps were performed at 4°C. Bacteria were pelleted by centrifugation at 4000 rpm (Sorvall®RC5C, rotor GS3) for 10 min. The obtained pellet was gently resuspended in 80 ml ice-cold TB and stored for 10 min on ice. After a further centrifugation at 4000 rpm for 10 min (4°C), the supernatant was discarded, 20 ml ice-cold TB and 1.4 ml DMSO were added and the bacterial pellet was gently resuspended. For

transformation 50 µl to 500 µl aliquots were prepared, frozen in a mixture of ethanol and dry ice or liquid nitrogen and stored until use at -70°C.

2.10.4. Transformation

Materials

- 14 ml miniprep tubes (Falcon)
- electroporator 2510 (Eppendorf)
- electroporation cuvettes, sterile and disposable, 1 mm gap or 2 mm gap (Eppendorf)

For transformation of ultra-competent *E. coli* DH10β, a 50 µl aliquot was thawed on ice (maximal 15 min) and then 5 µl of the ligation mix was added. After 5 min incubation on ice, bacteria were transferred into a 14 ml miniprep tube containing 1ml pre-warmed LB + 0.1% glucose without antibiotics. Following shaking (250 rpm) for 60 min at 37°C, bacteria were plated onto agar plates including the appropriate antibiotics and incubated O/N at 37°C. On the next day, single colonies were picked, expanded in liquid culture and the DNA isolated and analyzed for correct ligation by restriction digest.

Electro-competent bacteria *E. coli* BL21 were transformed as follows. A 50 µl aliquot was thawed on ice (maximal 15 min), then 1 µl DNA (0.5-2 µg) was added, the mixture was transferred into pre-cooled electroporation cuvette and placed in the electroporator. After pulsing (1.8V for 1 mm gap cuvette, 2.5 V for 2 mm gap cuvette), bacteria were immediately transferred into a 14 ml miniprep tube containing 1 ml pre-warmed LB + 0.1% glucose without antibiotics, and agitate for 1 hour (250 rpm) at 37°C. Afterwards bacteria were plated onto agar plates containing the appropriate antibiotics and incubated O/N at 37°C. For inoculation of liquid culture for protein expression, *E. coli* BL21 directly scraped from the plate were used.

2.10.5. Cloning procedure

2.10.5.1. Polymerase chain reaction (PCR)

PCR reactions were used for the introduction of restriction sites and of the C-terminal hemagglutinin (HA)-tag into fragments of the coronin 1 sequence, for introduction of restriction sites into matrilin 4 coiled coil sequence and for the generation of coronin 1 deletion mutants (see also site-directed mutagenesis).

Amplification was performed using Expand Long Template PCR System Kit (Roche Diagnostics).

To that end,

- x µl template DNA (10 ng)
- 1.5 µl forward primer (300 nM)
- 1.5 µl reverse primer (300 nM)
- 1.75 µl 10 mM dNTP (PCR Nucleotide Mix Cat. No. 1581295, Roche Diagnostics)
- 5 µl 10x PCR reaction buffer (containing 17.5 mM MgCl₂)
- 0.75 µl Expand Long Template Enzyme mix
- filled up with dH₂O to 50 µl

were mixed on ice, placed into the T3 thermocycler (Biometra) and PCR was performed using the following standard program:

1. initial denaturation	95°C	2 min
2. denaturation	95°C	10 sec
3. annealing	58°C	30 sec (or as calculated)
4. elongation	68°C	60 sec
		10 cycles
5. denaturation	95°C	10 sec
6. annealing	58°C	30 sec
7. elongation	68°C	60 sec + 20 sec for each successive cycle
		15 cycles
8. final elongation	68°C	7 min
9. cooling	4°C	until analysis

The PCR fragments were analyzed by agarose gel electrophoresis and purified using the PCR QIAquick Nucleotide Removal Kit (QIAGEN). Subsequently, PCR products were digested with the appropriate restriction enzymes for further cloning or directly subcloned into the pGEM-T-easy vector.

2.10.5.2. Restriction digest of plasmid DNA/PCR fragments

For restriction digest 0.25-5 µg DNA, the appropriate reaction buffer and the restriction enzyme (ratio 1U/100 ng DNA) were mixed and incubated at 37°C. For analysis of plasmid DNA, digestion was performed for 1-2 hours. To prepare DNA fragments or vectors for ligation, digest was carried out overnight. All restriction enzymes were obtained from New England Biolabs (NEB).

2.10.5.3. Dephosphorylation of DNA

To prevent self-ligation of vectors after restriction digest, the vectors were treated with shrimp alkaline phosphatase (SAP) (Roche Diagnostic) to remove the 5' phosphate groups. To that end, SAP (1U/250 ng DNA) and SAP reaction buffer were added directly to the digest mixture, and incubated for 10 min at 37°C. After heat inactivation (15 min, 65°C), agarose gel electrophoresis was performed to purify the linearized vector.

2.10.5.4. Purification of DNA from agarose gel

DNA bands of interest, visualized under UV light were excised from the agarose gel and purified with the gel extraction kit (QIAGEN) following the manufacturer's protocol.

2.10.5.5. Ligation with T4 DNA ligase

Ligation of DNA fragments into linearized vectors was performed using T4 DNA ligase (NEB, Cat. No. M0202S). To that end, the ratio between vector and insert was determined according the following formula using a vector to insert ratio of 1 to 5:

$$50 \text{ ng} \times \text{kb vector} / \text{kb vector} = \text{insert (ng)} \times 5$$

Subsequently,

- 50 ng vector DNA
- x μ l insert DNA (calculated)
- 2 μ l 5x ligation buffer
- 1 μ l T4 DNA ligase (6 Weiss U)

were mixed, filled up with dH₂O to 20 μ l, incubated overnight at 16°C and then 8 μ l of ligation mix were transformed into ultra-competent *E. coli*. As ligation control, reaction was performed without insert and without T4 DNA ligase.

2.10.5.6. Ligation of PCR products into pGEM[®]-T Easy Vector (Subcloning)

Materials

pGEM[®]-T-Easy Vector kit (Promega, Cat. No. A1360)
LB/amp/IPTG (0.5 mM) /X-Gal (80 μ g/ml) agar plates

In cases, where the restriction digest of the PCR fragments was incomplete, PCR fragments were subcloned into the pGEM[®]-T-easy vector according the manufacturer's instruction. The amount of insert was calculated using a vector to insert ratio of 1 to 8:

$$\text{ng x kb vector} / \text{kb vector} = \text{insert (ng)} \times 8$$

For ligation,

- x μ l of purified PCR product (calculated)
- 1 μ l pGEM[®]-T-Easy Vector (= 50ng)
- 5 μ l 2x reaction buffer supplied
- 1 μ l T4 DNA ligase

were mixed, filled up with dH₂O to 10 μ l and incubated for 60 min at RT. Afterwards, 5 μ l of the ligation mix was transformed into ultra-competent *E. coli*. Cells were plated onto LB/amp/X-Gal/IPTG agar plates and, after incubation O/N at 37°C, white colonies (contain inserts) were picked, expanded in liquid culture and the DNA isolated and digested with the appropriate restriction enzymes to obtain fragments for further ligation into the actual expression vector.

2.10.5.7. Preparation of plasmid DNA from *E. coli* cultures

All plasmid DNA was prepared with QIAGEN Maxi- and Mini-prep Kits according to the manufacturer's protocol. For plasmid DNA used for transfection of eukaryotic cells, purification was performed under endotoxin-free conditions.

2.10.5.8. Ethanol precipitation of DNA

To precipitate DNA, 1/10 volume of 3 M Na-acetate, pH 5.3 and 2 volumes of 100% ethanol were added to the DNA solution, mixed and incubated for at least 15 min at -20°C. Precipitated DNA was pelleted subsequently by centrifugation (20 000 x g, 15 min, 4°C), washed twice with 70% ethanol and air-dried. DNA was dissolved in dH₂O or TE-buffer (10 mM Tris/HCl, 1mM EDTA, pH 8.0). To obtain a sterile DNA solution for transfection, DNA was resuspended in sterile water or buffer.

2.10.6. Site directed mutagenesis

For generation of coronin deletion mutant Cor1- Δ 400-416-HA a two-step PCR approach was used. In a first PCR the coding sequence for the N-terminal region including the deletion 400-416 was generated using the primer pair DomI-start/Cor1M1198-1249-F resulting in the *EcoRI*-Cor1_{nt1-1197//1249-1270} fragment. The coding sequence for the C-terminal region including the deletion 400-416 was generated using the primer pair Cor1M1198-1249-R/DomIII-HAstop resulting in the Cor1_{nt1176-1197/1249-1383}-HA-*BamHI* DNA fragment. In a subsequent PCR, *EcoRI*-Cor1_{nt1-1197//1249-1270} together with Cor1_{nt1176-1197/1249-1383}-HA-*BamHI* were used as templates and with primers DomI-start/DomIII-HAstop the *EcoRI*-Cor1_{nt1-1197//1249-1383}-HA-*BamHI* fragment was amplified and subcloned into the pGEM®-T-easy Vector. For expression in mammalian cells, the pGEM-Cor1- Δ 400-416-HA construct was digested with HindIII and BamHI and the HindIII-BamHI fragment containing the deletion was used for exchanging the corresponding wildtype fragment in the pCB6-Cor1-HA construct.

Generation of the Cor1- Δ 361-422 deletion construct was performed following the same protocol using the primers Cor1M1081-1266-F/R instead of Cor1M1198-1249-F/R.

2.10.7. Sequencing

Materials

- Big Dye 1.1[®] Terminator v 1.1 Cycle Sequencing Kit (Applied Biosystems, Cat. No. 4337452)
- 500 μ l PCR-tubes (Treff) or 96-well optical reaction plate (Applied Biosystems)
- T3 thermocycler (Biometra) or Primus 96 plus (MWG Biotec) for 96 well plate
- Hi-Di[™] Formamide (Applied Biosystems, Cat. No. 4311320)

Sequencing of plasmid DNA was performed using the Big Dye Terminator chemistry following the manufacturer's protocol.

To that end,	2 μ l plasmid DNA (300-500 ng)
	4 μ l Big Dye (containing DNA polymerase, reaction buffer, fluorescent dideoxynucleotide)
	0.5 μ l primer (stock 10 pmol/ μ l)
	3.5 μ l dH ₂ O

were mixed in a 0.5 ml tube or in one well of a 96 well plate. For the subsequent amplification of the plasmid template DNA the following program was used:

1. preheating	98°C	
2. denaturation	96°C	30 sec
3. annealing	50°C	15 sec
4. elongation	60°C	4 min
		25 cycles
5. cooling	4°C	until analysis of sample

The extension products were purified afterwards by ethanol precipitation. 26 μ l dH₂O and 64 μ l ethanol (100%) were added to each sample, mixed by pipetting, and incubated for 15

min at RT away from exposure to bright light. DNA was pelleted by centrifugation at 3000 x g (RT) for 30 min, then the supernatant was carefully removed and the pellet was washed with 150 μ l ethanol (70%). After centrifugation at 2000 x g (RT) for 10 min, supernatant was removed completely, the pellet was air-dried and then stored at 4°C in the dark until use, or, for direct use immediately resuspended in 30 μ l of 67% formamide.

Sequencing was performed by capillary electrophoresis on an ABI PRISM Genetic Analyzer 3700 and sequences were analyzed using MacVector™ software (version 7.2.2).

2.11. Cell culture

2.11.1. Determination of cell numbers

The cell number was determined in a Neubauer counting chamber (0.1 mm depth). An aliquot of the cell suspension was diluted 1:10 with trypan blue solution [0.05% (w/v)] and the cells in 16 small squares were counted. The cell number per ml was calculated from the counted cell number multiplied by 2×10^4 .

2.11.2. Freezing and thawing of cells

For freezing, cells were suspended in freezing medium (FCS / 10% (v/v) DMSO), at a minimal cell density of 5×10^6 cells /ml. Then 1 ml aliquots were transferred to 2 ml cryotubes (Nunc), placed in pre-cooled freezing containers (Nalgene) and put O/N at -80°C prior to the final storage in the liquid nitrogen.

Cell were thawed in a water bath at 37°C and immediately transferred into 10 ml of pre-warmed appropriate medium and pelleted (5 min, 1200 rpm, RT; Sorvall®T6000D, rotor: H-1000B). The pellet was gently resuspended in medium and transferred into a culture dish.

2.11.3. Subculture and freezing of J774A.1 cells

J774A.1 cells were washed once with PBS and then detached from the culture plate using a cell scraper. The cell suspension was transferred into a 15 ml Falcon tube, centrifuged (5 min, 1200 rpm, RT; Sorvall®T6000D, rotor: H-1000B), and cell pellet resuspended in culture media or freezing media.

2.11.4. Subculture and freezing of adherent cells

Adherent cells such as the human embryonic kidney cell line HEK293 or the fibroblast cell line L929 have to be trypsinized prior to subculture or freezing. Therefore cells were washed once with PBS and then incubated for 5 min at 37°C with trypsin/EDTA. Trypsinization was stopped by addition of two volumes of cell culture media containing FCS. Detached cells were pelleted by centrifugation (5 min, 1200 rpm, RT; Sorvall®T6000D, rotor: H-1000B) and resuspended either in cell culture or freezing medium.

2.11.5. Preparation of L929-conditioned medium

10^7 L929 cells were plated out in 100 ml L929-medium onto a 15 cm tissue culture dish. After 7 days, the medium was removed, filtered (0.2 μ m) and stored at 4°C before use. This procedure was repeated 3-4 times before the cells were discarded.

2.11.6. Generation of murine bone marrow derived macrophages and dendritic cells

For the generation of bone marrow derived macrophages and dendritic cells, bone marrow cells were isolated from C57BL/6 mice and cultured in the presence of different growth factors/cytokines, which induce the differentiation of monocytes present in the bone marrow into macrophages or dendritic cells.

Isolation of bone marrow was performed as follows. Mice were killed by CO₂ and afterwards their hind legs isolated and freed from all muscle tissue. Subsequently, the femur bone was cut above the knee, the lower leg bone above the foot. Then the bones were transferred into a yellow pipette tip with the cut surface pointing downwards. The loaded tip was placed in a 5 ml centrifugation tube containing 200 μ l DMEM and centrifuged 12 min by 2000 rpm (Eppendorf 5810R, rotor: A-4-62) at RT to isolate the bone marrow cells. Afterwards the tips with the empty bones were discarded, the pelleted bone marrow cells resuspended in culture media, counted and transferred to culture dishes.

Generation of macrophages from bone marrow monocytes was performed as described before (Wiltshcke *et al.*, 1989). In brief, 1×10^7 isolated bone marrow cells were plated in a 10 cm teflon dish (Rowatec) and cultured for 6-10 days in BMM \emptyset -medium, at 37°C and 5% CO₂. The cultured cells had typical macrophage morphology, expressed macrophage markers (such as Mac-1) and were phagocytic (uptake of *E. coli*).

Generation of dendritic cells was performed according to previous reports (Schreurs *et al.*, 1999). To that end, 5×10^6 bone marrow cells were plated in 5 cm culture dishes (Corning) and cultured in DMEM containing 10% (v/v) FCS, 1% (v/v) penicillin/streptomycin, 2 mM glutamine and 25 ng/ml GM-CSF for 2 days. On the third day, non-adherent cells (predominately granulocytes) were carefully removed by aspiration and medium with fresh GM-CSF and IL-4 (1.5 ng/ml) was added. Maximal yield of DCs was obtained between day 6 and 8 of culture. The cells displayed typical dendritic cell morphology and expressed dendritic cell markers (CD11c, NLDC145).

2.11.7. Isolation of total and CD8⁺ lymphocytes from OT-1 mice

Materials

- Dynabeads M-450 Sheep anti-Rat IgG (Dynal Biotech) coupled to anti-murine CD4 and anti-murine MHC class II
- Magnet (Dynal MPC)

Total lymphocytes were isolated from OT-1 mice, which are transgenic for the T-cell receptor for the H-2K^b-MHC I-SIINFEKL complex (Hogquist *et al.*, 1994). The animals were killed by CO₂, the thymus and lymph nodes (inguinal, mesenteric, axillary, brachial) were removed, transferred to culture dish and mashed between 2 nylon nets to obtain a single cell suspension. Cells were pelleted by centrifugation, washed once with media, counted and added to antigen-presenting cells.

Isolation of CD8⁺ T-cells from total lymphocytes was performed by immunomagnetic cell separation using the Dynabeads system. To that end, lymphocytes were counted and transferred into a 15 ml polypropylene falcon tube such that the final volume of the cell suspension would be at least 2 ml to allow effective separation. Then dynabeads coated with an anti-CD4 and anti-MHC class II antibodies were added (1 bead of each antibody/cell) and the cell suspension was incubated for 20-30 min at 4°C under rotation to allow cell selection to take place.

A magnet was then applied to the tube for two minutes and the supernatant was carefully removed, leaving CD4⁺ T-cells and APCs bound to the dynabeads behind. Cells of the supernatant (= CD8⁺ T-cells) were washed once with PBS, then pelleted by centrifugation at 1200 rpm (5 min, 4°C; Eppendorf 5810R, rotor: A-4-62), counted and used in a further proliferation assay.

2.11.8. Isolation of CD14⁺ monocytes and CD8⁺ T-cells from human peripheral blood

Materials

- Ficoll-Paque™ (Pharmacia)
- MACS buffer: PBS/0.5% FCS/2 mM EDTA, pH 8.0, filtered (0.22 µm)
- anti-human CD14 microbeads/anti-human CD8 microbeads Miltenyi Biotech
- LS MACS column and MACS separator Miltenyi Biotech

Peripheral blood monocytes (PBMC) were isolated from heparinized venous peripheral blood of a healthy HLA-A*0201 donor. 10 ml of blood was diluted with 20 ml PBS, layered onto 10 ml of Ficoll and centrifuged at 315x g for 15 min (no brake). PBMCs localized in the interphase between the blood plasma and Ficoll were collected and washed once with PBS. Isolation of CD14⁺ monocytes and CD8⁺ T-cells was performed afterwards by using the Midi-Macs magnetic bead system (Miltenyi Biotech). To that end, PBMCs washed once with MACS buffer were resuspended in 1:10 with MACS buffer diluted solution of anti-CD14 or anti-CD8 microbeads (1x10⁸ cells/ml), vortexed and incubated for 30 min on ice. For the subsequent cell separation, a LS MACS column was placed onto the MACS separator (strong magnet) and equilibrated with 3 ml of MACS buffer. In the meantime, cells were washed once again with MACS buffer, resuspended in 3 ml MACS buffer, filtered (30 µm nylon mesh) and loaded onto the equilibrated LS MACS column. Cells coupled to microbeads are retained due to magnetic forces in the column and therefore separated from the other cells. After washing the column three times with 3 ml MACS buffer, the MACS separator was removed. Next the column was placed onto a 15ml falcon tube and cells were eluted with 2x 2ml MACS buffer by firmly applying force using a plunger supplied with the column. Eluted cells were washed once with PBS and then resuspended in the appropriate media.

2.11.9. Generation of immature dendritic cells from CD14⁺ monocytes

Culturing CD14⁺ monocytes in the presence of GM-CSF and IL-4 induces these cells to differentiate into immature dendritic cells. This was done by resuspending CD14⁺ monocytes in DC media and seeding them into a 6-well plate (1x10⁶ cells/well). The maximal yield of DCs was obtained between day 5 and 8 of culture.

2.11.10. Transient transfection of HEK293

Transient transfection of HEK293 cells was performed using PolyFect® Transfection Reagent (QIAGEN, Cat. No. 301105) following the manufacturer's protocol. HEK293 cells were seeded in a 6 well culture dish (1×10^6 cells /plate) or on glass slides (1×10^5 cells /well) and allowed to adhere O/N. For transfection of one 10 well slide and one well of a 6 well culture dish, 2 μ g plasmid DNA and 20 μ l PolyFect reagent were mixed with 100 μ l DMEM (without FCS) and incubated for 10 min at RT to allow the formation of a PolyFect-DNA complex. After addition of 2.1 ml DMEM containing FCS and glutamine, the solution was layered onto the washed (PBS) cells (50 μ l/slide well; 1.7 ml /well of 6 well culture dish). Gene expression was analyzed twenty-four hours after transfection.

2.11.11. Cholesterol depletion and replenishment

Materials

- 10 mM lovastatin stock solution: To 25 mg lovastatin 100% ethanol and 938 μ l NaOH were added and the suspension was heated for 2 hours at 50°C in the dark. After complete dissolving, pH was adjusted to 7.0-7.5 by addition of 2-3 drops of 1N HCl and then solution was filled up to 6.25 ml with dH₂O, filtered (0.2 μ m) and stored at -20°C in 50 μ l aliquots.
- 250 mM mevalonic acid stock solution: 0.25 mg of mevalonate was dissolved in 7.7 ml dH₂O, filtered (0.2 μ m), and stored at -20°C in 50 μ l aliquots.
- 200 mM methyl- β -cyclodextrin (MCD): The average molecular weight was estimated at 1303 g/mol. For preparation of a 200 mM stock solution, made freshly before every experiment, 260 mg of MCD were dissolved in DMEM to give a volume of 1 ml.
- 6 mg/ml cholesterol- β -methyl-cyclodextrin inclusion complex in DMEM

Cholesterol depletion was performed as described previously (Gatfield *et al.*, 2000). In brief, cells were grown in the presence of 4 μ M lovastatin and 250 μ M mevalonate (J774A.1 for 60 hours, bone marrow derived macrophages and dendritic cells for 108 hours) after which the residual plasma membrane cholesterol was extracted with methyl- β -cyclodextrin (J774A.1: 10 mM MCD for 45 min, bone marrow derived macrophages: 20 mM MCD for 108 hours, bone marrow derived dendritic cells: 15 mM MCD for 45 min). All subsequent experiments were done in serum-free media. For the replenishment of cholesterol, depleted cells were incubated for one hour in DMEM containing 6 mg/ml cholesterol- β -methyl-cyclodextrin complex.

2.11.12. Cross-presentation

2.11.12.1. Proliferation assay

Irradiated (3000 rad) bone marrow derived macrophages were seeded in 96 well plates (2×10^4 cells/well). After PMA stimulation and cholesterol extraction, cells were incubated with ovalbumin / palmitoylated ovalbumin or SIINFEKL /palmitoylated SIINFEKL peptide for 3 hours. The non-internalized and non-bound antigens were removed by extensive washing. Lymphocytes (total or CD8⁺ T-cells) isolated from OT-1 mice (Hogquist *et al.*, 1994) were then added to the bone marrow derived macrophages (ratio 5:1). T-cell proliferation was measured after three days by labeling the cells with [methyl-³H]-thymidine (Amersham

Pharmacia Biotech). Lactacystin treatment was performed by incubating the cells with 10 μ M lactacystin one hour before and during the three hour antigen pulse. In case of fixing the APCs, fixation with 1% paraformaldehyde (30 min, 37°C) was done prior to incubation with the antigen.

2.11.12.2. CTL induction

Cross-presentation of the influenza matrix protein (IM) (1-164) was measured by induction of HLA class I restricted CTLs specific for the IM derived GILGFVFTL peptide (IM 58-66). To that end, immature dendritic cells generated from peripheral blood monocytes (PBMC) of a healthy HLA-A*0201 donor were seeded in a 24 well culture dish (5×10^5 cells/well) and treated with LPS or LPS + 50 μ g/ml IM (1-164) or LPS + 125 μ g/ml ovalbumin for twenty-four hours. Subsequently cells were washed three times with PBS to remove LPS and non-internalized antigen. Cells were then resuspended in T-cell media, counted and seeded into a 24-well culture dish (1×10^5 cells/well). CD8⁺ T-cells isolated from PB of the same donor were added to each well (ratio dendritic cells:T-cell=1:15). To dendritic cells only treated with LPS 2.5 μ g/ml ras (4-12) peptide or 2.5 μ g/ml IM (58-66) were added. Dendritic cells and T-cells were co-cultured for seven days. At day 4, 5, and 6 the media was supplemented with 10 U/ml of interleukin 2.

To determine the percentages of IM (58-66) specific CD8⁺ T-cells within the cultured cells after seven days of co-culturing, tetramer staining was performed.

2.12. Flow cytometry

2.12.1. Testing of transgenic OT-1 mice

Mice carrying the transgene were identified by staining peripheral T-cells for expression of the transgenic TCR ($V\alpha_2 / V\beta_{5.1/5.2}$). To that end, 20 μ l of heparinized peripheral tail blood was transferred into a 96 well V bottom plate and mixed with 100 μ l of antibody solution (final concentration in PBS/2% BSA: FITC-anti-V β -TCR 1:100, R-PE-anti-V α -TCR: 1:1000). After a one hour incubation on ice in the dark, cells were pelleted by centrifugation (1200 rpm, 5 min, 4°C, Eppendorf 5810R, rotor: A-4-62), the supernatant was flicked out, then cells were washed once with PBS / 2% BSA, resuspended in 100 μ l 1x lysis buffer (FacsTMLysing Solution, BD) and incubated for 5-10 min at RT. After complete lysis of red blood cells, the solution is clear. The remaining lymphocytes were washed once with PBS / 2% BSA, then transferred into FACS tubes and analyzed onto a FACS calibur (Becton Dickinson).

2.12.2. Quantification of IM (58-66) specific CD8⁺ T-cells by tetramer staining

Co-cultured DCs and CD8⁺ T-cells were washed once with PBS and resuspended after pelleting in 100 μ l of R-PE-HLA-A*0201/GILGFVFTL pentamers (Proimmune) diluted 1:100 in PBS. After a 15 min incubation at RT in the dark, cells were washed with PBS and 100 μ l of FITC anti-CD8 antibody diluted 1:100 with PBS were added. Following an incubation of 30 min on ice, cells were washed twice with PBS, resuspended in 200 μ l of PBS and analyzed by flow cytometry.

2.12.3. Flow cytometry phagocytosis assay

J774A.1 cells grown in a 24 well culture dish (5×10^5 cells /well) were left untreated or depleted for cholesterol and then incubated for 1 hour at 37°C or 4°C with FITC-labeled latex beads (FITC-microspheres, \varnothing 1 μ m, Molecular Probes), diluted in DMEM 1:100. Following a 30 min chase, cells were placed on ice and washed three times with ice-cold PBS/2% BSA to remove adherent, non-internalized beads before 200 μ l of PD-buffer was added. After a 10 min incubation on ice, cells were scraped from the culture dish and the cell suspension was transferred into a FACS tube containing 200 μ l 3% PFA and fixed on ice for 30 min. Uptake of beads was quantified by flow cytometry by measuring an increase in fluorescence.

2.12.4. Quantification of internalization of FITC labelled ovalbumin and palmitoylated ovalbumin

Bone marrow derived macrophages were incubated with 0.1 mg/ml FITC labeled ovalbumin or palmitoylated ovalbumin for 20 min at 37°C and at 4°C. Cells were then washed, fixed with 3% PFA for 30 min on ice and analyzed by flow cytometry. Internalization of ovalbumin measured as increase in fluorescence was corrected for background adherence at 4°C.

2.13. Microscopy

2.13.1. Indirect immunofluorescence and filipin staining of cells

Materials

- teflon-coated ten well slides (Polysciences, Inc., Cat. No. 18357)
- FluoroGuard Antifade Reagent (Bio-Rad)
- Q-tips
- wet chamber for staining (Kartell®, Italy)
- slide jar (Glaswerk, Germany)
- 3% paraformaldehyde (PFA) in PBS:

For preparation of 100 ml 3% PFA, 90 ml dH₂O and 300 μ l 0.1 N NaOH were added to 3 g PFA, heated with stirring to 60°C until completely dissolving. The solution was then cooled down to 37°C, 10 ml of 10x PBS was added and the pH was adjusted to 7.2.

Microscopes and software:

- confocal scanning laser microscope system: Axiovert 200M + laser scanning module (LSM 510 Meta) (Zeiss), LSM 510 software (version 3.2 SP2)
- fluorescence microscope: Axiovert 100 TV (Zeiss), OpenLab software (version 2)

For staining, the cells were grown on teflon-coated ten well slides at a density of 1×10^5 cells per well. After aspiration of the media, cells were washed once with PBS, fixed in a slide jar with pre-warmed 3% (w/v) paraformaldehyde, pH 7.2 for 10 min at 37°C. Afterwards,

slides were transferred into a new slide jar and washed 5 min with PBS, 5 min with PBS + 5 mM glycine, and 5 min with PBS.

For intracellular staining cellular membranes were permeabilized by treatment with saponin, a mild detergent which does not solubilize membranes and thus allows staining of cytosolic proteins as well as intracellular membrane components. To that end, slides were incubated for 20 min at RT with 0.1 % (w/v) saponin dissolved in PBS (SAP). After blocking with 2% (w/v) BSA/0.1% saponin/PBS (SAP+) for 20 min at RT, the slides were dried carefully around each well with a Q-tip, placed in a wet chamber and the primary antibody (diluted in SAP+ or undiluted hybridoma supernatant) was added. After 30-45 min (depending on the antibody used) incubation at RT the slides were transferred into a slide-jar and washed three times each for 5 min with SAP+. Then the slides were placed back in the wet chamber, the liquid around each well was removed with a Q-tip and the secondary antibody coupled to a fluorescent dye and diluted in SAP+ was added. After 30 min incubation in the dark, the slides were transferred again into a slide-jar and washed 3x 5 min with SAP+ and 3x 5 min with PBS. For mounting, the slides were dried carefully around each well, a drop of FluoroGuard-Anti-Fade reagent was added onto each well and subsequently covered with a cover slip. Slides were stored at 4°C in the dark to prevent bleaching of the fluorescent dyes.

To stain for cholesterol, cells were fixed, washed and then incubated for 45 min with 0.05% filipin complex III (stock solution: 50 mg/ml, freshly made), washed three times with PBS and mounted. When filipin was used together with antibody staining, the normal saponin-based staining protocol was performed, whereby filipin was included with the primary and secondary antibodies.

2.13.2. Internalization of FITC-Dextran

To study internalization of the fluid-phase marker Dextran, a FITC labeled form of this glucose polymer with a molecular weight of 2000000 K was used. The assay was performed as follows. Cells grown on glass slides were washed once with PBS and then incubated in FITC-Dextran solution (1 mg/ml in DMEM / 1% (v/v) glutamine) for 7 or 12 min. The diluted FITC-Dextran solution was always centrifuged (50 000 rpm, 20 min, RT; Optima™ TLX-UZ, rotor: TLA 120.1) prior to use to remove aggregates that may cause background fluorescence. After incubation, the FITC-Dextran solution was aspirated and the cells were washed twice with PBS prior to fixation. When indicated, the cells were stained subsequently using Texas-Red coupled antibodies against cellular markers.

2.13.3. Internalization and detection of horseradish peroxidase

For visualization of internalized fluid-phase marker horseradish peroxidase a colourimetric reaction based on a redox reaction catalysed by HRP was used. The intensity of the cell staining (brown) was dependent on the amount of internalized HRP.

Internalization of horseradish peroxidase (5 mg/ml) was performed for one hour at 37°C followed by a chase of four hours. Afterwards the cells were washed five times with PBS, fixed in glutaraldehyde (0.5% w/v) at RT and internalized horseradish peroxidase was visualized by incubation with 0.5 mg/ml diaminobenzidine (Sigma), 0.05% (v/v) H₂O₂ in PBS for 10 min (Sallusto *et al.*, 1995).

For palmitoylated horseradish peroxidase, internalization was performed for one hour with 0.5 mg/ml of control or palmitoylated protein. Afterwards the cells were washed, fixed, permeabilized with 0.1% saponin for 20 min and internalized horseradish peroxidase was

visualized as described above. Slides were viewed under a Leica DMIL microscope (Leica) and pictures were taken using Coolpix 995 digital camera (Nikon).

2.13.4. Time-lapse video microscopy

Time-lapse video microscopy was used to investigate the effect of cholesterol on macropinosome formation. Control and cholesterol-depleted J774A.1 cells, bone marrow derived macrophages and dendritic cells were plated out at 10-20% confluence in 5 cm dishes with a gas-permeable lumoxTM fluorocarbon film base (Greiner Bio-one, Cat. No. 96077303). These plates were placed under a microscope (Axiovert 100 TV, Zeiss) equipped with a thermoequilibrated chamber (37°C, 5% CO₂). After addition of 10⁻⁷ M PMA (in the case when macrophages were observed) 30 min video sequences were recorded at 10 seconds intervals using a digital camera controlled by OpenLab software (version 2.0).

2.14. Biochemical methods

2.14.1 Determination of protein concentration

Materials

- BCA reagents (Pierce)
- Bradford reagent: 100 mg Coomassie G-250 (Bio-Rad), 50 ml 95% ethanol, 100 ml of 85% phosphoric acid, filled up to 200 ml with dH₂O, filtered
- Standard: 1 mg/ml protein standard (Bio-Rad, Cat. No. 500-0005) in dH₂O
- microplate reader (Paul Bucher), software: SoftMax[®] Pro (version 1.2.0)

Protein concentration was determined according the Bradford method (Bradford, 1976). In cases where the sample contained detergents such as TritonX-100 or NP40 protein concentration was then measured with the BCA method (Smith *et al.*, 1985).

Measurements were performed as follows. Different volumes of the sample (1-20 µl) and the standard solution (1, 3, 5, 7 and 9 µl) were placed in a 96-well plate, flat bottom and 200 µl of BCA-solution (prepared according manufacturer's protocol) or 200 µl Bradford reagents respectively were added. Samples were measured using an ELISA reader immediately (Bradford, OD₅₉₅) or after 15 min incubation at RT (BCA, OD₅₆₀). The protein concentration was calculated from the measured values using a standard curve under consideration of sample volume and dilution factors.

2.14.2. Protein precipitation with trichloroacetic acid (TCA)

TCA (50% in acetone) was added to protein samples given a final concentration of 10%. Samples were mixed and incubated on ice for 30 min. Precipitated proteins were pelleted by centrifugation (20 000 x g, 30 min, 4°C), and washed two times with acetone (-20°C). The pellet was air-dried and then resuspended in 1x SDS-PAGE sample buffer.

For analysis of total protein synthesis, an aliquot of the lysate of metabolically labeled cells was spotted onto 3MM Whatman paper. The filter was dried, then soaked in ice-cold TCA (10% in acetone) and incubated for 30 min on ice. After washing 1x 5 min with ice-cold

TCA (5% in acetone) and 1x 5 min in acetone (-20°C), the filters were dried and amount of radioactivity determined by liquid scintillation counting (Ultima Gold, Becton Dickinson, LS-analyzer TRI-CARB 2000CA, Packard).

2.14.3. Discontinuous SDS polyacrylamide gel electrophoresis (SDS-PAGE)

Materials

- Protean II minigel system (Biorad)
- 5x reducing sample buffer
- 10x SDS-PAGE electrophoresis running buffer
- 30% (w/v) acrylamide/ 0.8% (w/v) bisacrylamide in water (0.2 µm filtered)
- 20% (w/v) SDS
- 2 M Tris/HCl, pH 8.8
- 0.5 M Tris/HCl, pH 6.8
- 10% (w/v) ammonium persulfate (APS)
- TEMED (Biorad)
- Biorad SDS-PAGE standard (broad range)

Preparation of minigels (7 cm x 10 cm x 0,75 mm)

Components of the running gel were mixed together according table 2.1, poured into the glass plate assembly and overlaid during the polymerization with water-saturated isobutanol. The stacking gel was poured onto the top of the polymerized running gel and the comb was inserted immediately. Before sample loading, the gel slots were washed with running buffer. Samples were mixed with 5x reducing sample buffer, boiled for 5 min at 95°C, centrifuged and loaded.

Running conditions: constant voltage (80V for stacking, 120-150 V for running gel).

Table 2.1. Preparation of Minigels

	Running gel 15% (ml)	Running gel 10% (ml)	Stacking gel (4%) (ml)
30% acrylamide/bisacrylamide	5	3.3	0.65
2 M Tris/HCl, pH 8.8	2	2	-
0.5 M Tris/HCl, pH 6.8	-	-	1.25
20 % SDS	0.05	0.05	0.025
dH ₂ O	2.9	4.6	3.05
10% APS	0.05	0.05	0.025
TEMED	0.01	0.01	0.005

(Shown quantities are for two minigels)

2.14.4. Coomassie staining after SDS-PAGE

Materials

- staining solution: 0.25% Coomassie brilliant blue R-250 (Biorad), 10% acetic acid, 45% methanol in dH₂O
- fixation solution: 10% acetic acid, 45% methanol in dH₂O

Gels were agitated in the staining solution for 30-60 min and then destained with fixation solution. Afterwards the gels were placed onto a filter paper and dried under vacuum at 60°C.

2.14.5. Semi-dry protein transfer onto nitrocellulose membranes and immunodetection

2.14.5.1. Transfer

Materials

- semi-dry transfer cell (Biorad)
- semi-dry transfer buffer
- Ponceau S solution [0.1% in 5% acetic acid (Sigma)]
- Hybond C super nitrocellulose membrane (Amersham Bioscience)
- filter paper (FP) [7 cm x10 cm, Whatmann 3MM (thin) and Macherey&Nagel MN440 (thick)]
- ECL™ Western Blotting Detection Reagents (Amersham Bioscience)
- Hyperfilm™ ECL (Amersham Bioscience)

The gel, membrane and filter papers were soaked in transfer buffer and assembled in a sandwich formation [lower electrode (anode)/FP thick/ FP thin/ membrane/gel/FP thin/FP thick]. Then all air bubbles between the single layers were removed and the upper electrode fitted (cathode) and the transfer started (time: 0.6 h, voltage: 25 V and ampere: $2.5 \text{ mA/cm}^2 = 0.17 \text{ A/minigel}$). After the transfer the membrane was stained with Ponceau S solution, photocopied and the molecular weight standards were marked with a pen.

2.14.5.2. Immunodetection

After transfer and Ponceau S staining, membranes were incubated for 2 hours at RT under agitation in 5% (w/v) low fat milk powder in PBST. Incubation with the primary antibody diluted in PBST/milk for 45 min at RT was performed on parafilm, afterwards the membranes were washed three times with PBST/milk and incubated for further 30 min with the secondary HRP-labeled antibody diluted in PBST/milk. Finally the membranes were washed 3x 5min with PBST/milk and 3x 5min PBST and subsequently incubated in the ECL solution for 1 min at RT. Subsequently the membranes were dried with a paper towel, transferred to a transparent plastic bag and exposed for different times to films.

2.14.5.3. Stripping of antibody stained membranes for reprobing

Materials

- stripping buffer: 67 mM Tris/HCl, pH 6.7, 2% SDS, 100 mM β -mercaptoethanol

Antibody stained membranes were incubated in stripping buffer for 30 min at 50°C under agitation, washed two times 10 min with PBST and then blocked for 2 hours in 5% (w/v) low fat milk powder in PBST at RT. Subsequently staining was performed as described above (2.14.5.2.).

2.14.6. Purification of the nuclear localization sequence (NLS)-mutant of the influenza matrix protein IM (1-164)

Materials

- buffer A: 20 mM MES/KOH, pH 5.7, 10 mM NaCl, 10 mM β -mercaptoethanol
- buffer B: 20 mM MES/KOH, pH 5.7, 500 mM NaCl, 10 mM β -mercaptoethanol
- buffer C: 20 mM MES/KOH, pH 5.7, 250 mM NaCl, 10 mM β -mercaptoethanol, 10 mM MnCl_2
- buffer D: 10 mM Tris/HCl, pH 7.5, 200 mM NaCl, 10 mM β -mercaptoethanol
- Elastase from porcine pancreas (Roche Diagnostics, Cat. No. 1027891)
- SP Sepharose FF (Amersham Bioscience)
- Superdex 75 HP 10/30 (Pharmacia Biotech)
- Amicon[®] Ultra-4 /15 Centrifugal Filter Units, NMWL membrane, cut-off 5 000 kDa, 10 000 kDa (Millipore)

For inoculation of the liquid culture, *E. coli* BL21 transformed via electroporation (2.10.4.) with plasmid DNA encoding for NLS-mutant IM (1-252) (pET16-NLS-IM-1-252) were directly scraped from LB-amp agar plates. For 1L of LB-amp media, two agar plates with a confluent bacteria lawn were used. After inoculation, the culture was grown at 30°C under agitation. Protein expression was induced at $\text{OD}_{600} = 0.5$ with 0.5 mM IPTG and after 4 hours growth, bacteria were harvested by centrifugation (5000 rpm, 10 min, 4°C; Sorvall[®]RC3C, rotor: H-6000A). The bacteria pellet was washed once with 50 ml PBS, resuspended in 5 ml buffer A, and bacteria were lysed by sonication.

Purification of the NLS-mutant IM (1-252) protein from the bacteria lysate was performed as described before (Baudin *et al.*, 2001; Arzt *et al.*, 2004) using a two-step FPLC protocol. The bacteria lysate was centrifuged (14 000 rpm, 20 min, 4°C; Eppendorf centrifuge 5417R, rotor type F4530-11) to remove insoluble material, the obtained supernatant was filtered (0.2 μm filter) and then loaded onto an ion exchange column (SP Sepharose FF). By applying a linear FPLC gradient (10-500 mM NaCl), proteins were eluted and collected in 1 ml fractions.

The fractions containing the NLS-mutant IM (1-252) determined by Coomassie Blue-stained SDS-PAGE were pooled, concentrated to 1/10 of the starting volume by centrifugation (cut-off 10 000 kDa, 4000 rpm; Eppendorf centrifuge 5810R, rotor type: A-4-62) and dialysed against buffer C.

Subsequently size exclusion chromatography was performed. To that end, the 200 μl of the concentrated protein solution was loaded onto a Superdex 75 column. Separation was performed at a flow-rate of 0.5 ml/min using buffer C as running solvent. 0.5 ml fractions were collected and analyzed for the presence of NLS-mutant IM (1-252) by Coomassie Blue-stained SDS-PAGE. The NLS-mutant IM (1-252) containing fractions were pooled and dialysed against buffer D. To obtain the NLS-mutant IM (1-164) protein, the full-length protein (1-252) was then digested with elastase in a 50:1 molar ratio at 37°C for 2.5 hours. The reaction was stopped by addition of 1 mM PMSF and the protein solution was concentrated by centrifugation (cut-off 5 000 kDa, 4000 rpm; Eppendorf centrifuge 5810R, rotor type: A-4-62) to 1/10 of starting volume. To further purify the N-terminal domain, size exclusion chromatography was performed again, as described above.

2.14.7. Expression of recombinant Cor1^{L+C} in *E. coli* and purification

Materials

- buffer A: 20 mM Tris/HCl, pH 8.0, 10 mM NaCl, 1 mM β -mercaptoethanol
- buffer B: 20 mM Tris/HCl, pH 8.0, 1M NaCl, 1 mM β -mercaptoethanol
- lysozyme (Sigma)
- protease inhibitors (1x CLAAP, 1x PMSF)
- Mono Q (10/10, Pharmacia Biotech)
- Superdex 200 High load (16/60, Pharmacia Biotech)

1L LB/Amp were inoculated with *E.coli* BL21 transformed with pET22-Cor1^{L+C} plasmid by electroporation (2.10.4.), scraped from two agar-plates. Expression of Cor1^{L+C} protein was induced at OD₆₀₀= 0.5 by addition of 0.5 mM IPTG and after 3 hours growth at 37°C under agitation (250 rpm), bacteria were harvested by centrifugation (5000 rpm, 10 min, 4°C; Sorvall®RC3C, rotor: H-6000A). The bacteria pellet was washed once with 50 ml PBS, resuspended in 5 ml buffer A and incubated for 20 min on ice with 1 mg/ml lysozyme. After addition of 1x CLAAP and 1x PMSF, cells were lysed by sonication.

Insoluble material and intact cells were removed by centrifugation (14 000 rpm, 20 min, 4°C; Eppendorf centrifuge 5417R, rotor type F4530-11), then the supernatant was transferred into 1.5 ml Eppendorf tubes and heated for 5 min at 95°C in order to denature the proteins. Subsequently the protein solution was slowly cooled down at RT to allow the refolding of Cor1^{L+C}. Precipitated proteins were removed by centrifugation (14 000 rpm, 20 min, 4°C; Eppendorf centrifuge 5417R, rotor type F4530-11), the supernatant was filtered (45 μ m) and then loaded onto an anion exchange column (Mono Q). By applying a linear FPLC gradient (10-1000 mM NaCl), proteins were eluted and collected in 1 ml fractions. The fractions containing the Cor1^{L+C} proteins as determined by Coomassie Blue-stained SDS-PAGE analysis were pooled, concentrated to 1/10 of the starting volume by centrifugation and loaded onto a size exclusion column. Proteins were eluted in 1 ml fractions, pooled, dialysed against PBS, and stored until use at -80°C.

2.14.8. Preparation of total cell lysate

Materials

- 1x lysis buffer
- protease inhibitors (1x CLAAP, 1x PMSF)

Cells were washed three times with ice cold PBS, scraped from the culture dish and transferred into a 15 ml tube. After centrifugation (1200 rpm, 5 min, 4°C; Eppendorf 5810R, rotor: A-4-62), the supernatant was removed and cell pellet was resuspended in 1x lysis buffer containing protease inhibitors. To clear the lysate, a further centrifugation (10 min, 14 000 rpm, 4°C; Eppendorf centrifuge 5417R, rotor type F4530-11) was performed and the supernatant was transferred into a new tube. The lysate can be stored at -80°C until use.

2.14.9. Homogenization of cells and preparation of membrane and cytosol

Materials

- homogenization buffer (HB): 10 mM Triethanolamine, 10 mM acetic acid, 1 mM EDTA, 250 mM sucrose, pH 7.4
- protease inhibitors (1x CLAAP, 1x PMSF)

Subcellular fractionation was performed according to standard protocols (Tulp *et al.*, 1994; Ferrari *et al.*, 1997). Cell monolayers were washed three times with ice-cold homogenization buffer on ice and subsequently cells were scraped from the culture dish in a minimal volume of HB (cell density 1×10^7 cells /ml) and transferred into a tube of suitable size. Homogenization of the cells was performed by mechanical disruption using a syringe and a 22G 1¼ needle (0.7 x 30 mm, Becton Dickinson). To that end, the cell suspension was kept on ice, mixed with protease inhibitors and was pushed several times through the needle. Homogenization was continued until the ratio of intact cells and nuclei was 1:10 as determined by transmission microscopy. The number of strokes needed for 90% homogenization is dependent on the cell type. To clear the homogenate from unbroken cells and cell nuclei, a low speed centrifugation at 240 x g for 15 min was performed. The obtained postnuclear supernatant (PNS) was further subjected to ultracentrifugation (100 000 x g, 30 min, 4°C) to isolate cytosol and membranes.

2.14.10. Isolation of cytoskeleton

Materials

- resuspension buffer: 80 mM PIPES, pH 6.8, 5 mM EGTA, 1mM MgCl₂
- cytoskeletal isolation buffer: resuspension buffer + 1% Triton X-100

Isolation of the cytoskeleton-containing detergent insoluble fraction was performed as follows. Cells were washed once with PBS, scraped from the culture dish and the cell number was determined. Subsequently, 1×10^5 cells were pelleted (1200 rpm, 5 min, 4°C; Eppendorf centrifuge 5417R, rotor type F4530-11), the cell pellet was resuspended in 10 µl of resuspension buffer and 190 µl of ice cold cytoskeletal isolation buffer was added. The tube was flicked five times and immediately centrifuged (3000 x g, 2 min). The supernatant was carefully removed and the TX-100 insoluble pellet was resuspended in 200 µl cytoskeletal isolation buffer prior to the addition of 5x sample buffer. For analysis, the same volume of the supernatant and the pellet fraction was loaded on SDS-PAGE.

2.14.11. Gel filtration of HEK293 cytosol

Materials

- SMART system (Amersham Bioscience)
- Superdex 200 (3.2 mm x 300 mm, Pharmacia Biotech)
- gel filtration standard (Bio-Rad, Cat. No. 151-1901)

For size exclusion chromatography, HEK293 cells transfected with different Cor-1 constructs were homogenized in homogenization buffer, and the cytosolic fractions were prepared as described earlier (2.14.9.). To completely solubilize residual membranes in the cytosolic

fractions, the cytosol was incubated for 30 min on ice in the presence of 2% (w/v final concentration) octylglucopyranoside. Next the samples were filtered (0.2 μm) and the protein concentrations were adjusted to 1 mg/ml. 50 μl of each sample was loaded on a Superdex 200 gel filtration column. Separation was performed at a flow-rate of 50 $\mu\text{l}/\text{min}$ using PBS as a running solvent. 75 μl fractions were collected and the presence of Cor1 in these fractions was determined by subsequent SDS-PAGE and immunoblotting. Molecular weight was calibrated using 180 μg of gel filtration standard.

2.14.12. Metabolic labeling of cells using ^{35}S -methionine / cysteine

Materials

- starvation medium: RPMI 1640, lacking methionine/cysteine (Gibco BRL, Cat. No. 51871-010)
- ^{35}S -methionine/cysteine: Promix, 14.3 mCi/ml (Amersham Pharmacia, Cat. No. SJQ0078)
- 1x lysis buffer

Cells were washed twice with PBS, then starvation medium was added and cells were starved for 45 min at 37°C. Subsequently ^{35}S -methionine/cysteine (Promix) was added to a final concentration of 0.2 mCi/ml. After one hour incubation at 37°C, cells were washed three times with PBS, then lysed in TX-100 lysis buffer and the proteins were precipitated with TCA (2.14.2.).

2.14.13. Quantitation of horseradish peroxidase internalization

Materials

- 1x lysis buffer
- reaction buffer: 0.342 mM o-dianisidine, 0.003% (v/v) H_2O_2 , 50 mM Na-phosphate pH 5.0, 0.3% (v/v) Triton-X100

Cells seeded in a 48 well plate (3×10^5 cells/well) were incubated with 2 mg/ml horseradish peroxidase for one hour at 37°C or 0°C, washed and subsequently lysed in TX-100 lysis buffer. The enzymatic activity of horseradish peroxidase in the lysates was determined by mixing 10 μl of cell lysate with 200 μl reaction buffer and after a five minute incubation at RT the absorbance was measured at 455 nm. The obtained values, which correlate with the amount of horseradish peroxidase in the lysate were related to the total protein amount in the lysates.

2.14.15. F-actin co-sedimentation assay

Materials

- G-actin purified from rabbit skeletal muscle
- 2.5 M KCl
- G-actin-buffer: 2 mM imidazole, pH 7.2, 0.2 mM MgCl_2 , 0.2 mM ATP
- Protein-buffer: 40 mM Tris/HCl, pH 7.4, 20 mM KCl, 4 mM MgCl_2
- Polycarbonate Centrifuge Tubes 8 x 34 mm (Beckman)

Protein association with F-actin was investigated by *in vitro* co-sedimentation of the protein with F-actin during high-speed centrifugation. G-actin purified as described previously (Steinmetz *et al.*, 2000) was obtained from Dr. C.A. Schoenenberger, Biozentrum, Basel, Switzerland.

These assays were performed in centrifugation tubes using a batch volume of 100 μ l. First, F-actin was pre-assembled from purified rabbit skeletal muscle actin (50 μ l, 10 μ M) in G-buffer by addition of KCl to a final concentration of 100 mM and incubated for 45 min at RT. Then 50 μ l of purified Cor1^{L+C} (final concentration: 5 μ M) in P-buffer was added and the mixture was incubated for further 45 min at RT. The mixture was then centrifuged (100 000 x g, 30 min, RT) and the obtained supernatant and pellet were analyzed by Coomassie Blue-stained SDS-PAGE. To control for sedimentation, G-actin, F-actin and Cor^{L+C} samples were also subjected to ultracentrifugation at the same time.

2.15. Synthesis of activated lipid substrates and protein modification

2.15.1. Preparation of the cholesterol-methyl- β -cyclodextrin inclusion complex

Materials

- cholesterol, 98% pure (Avanti Polar-Lipids, Inc.)
- methyl- β -cyclodextrin (Sigma)

The synthesis of the cholesterol-methyl- β -cyclodextrin complex was performed as described before (Klein *et al.*, 1995). In brief, 30 mg cholesterol was dissolved in 2-propanol and added in small aliquots to a stirred solution of 1 mg methyl- β -cyclodextrin (5 % w/v) on a water bath (80°C). Stirring was continued until everything was dissolved. After removal of solvents by freeze-drying, the cholesterol-methyl- β -cyclodextrin complexes were stored at room temperature.

2.15.2. Synthesis of succinimidyl carbonate (SC)-farnesol

Materials

- *trans, trans*-farnesol, 96% (Sigma)
- N,N'-disuccinimidyl carbonate (DSC) (Sigma)
- 4-(dimethylamino)-pyridine (DMAP) (Sigma)
- dioxane and acetone were dried by filtration over Al₂O₃ (Fluka, type 5016A, basic)
- silica gel (Uetikon, 40-60 mesh)

Activation of farnesol with N,N'-disuccinimidyl carbonate (DSC) was performed as previously described (Zalipsky *et al.* 1992; Miron and Wilchek, 1993). The reaction was performed under water-free conditions using dry reaction vessels and dry solvents.

Following solutions were prepared:

- 500 μ l of farnesol (=1 mmol) were added to 5 ml dry dioxane
- 2.5 g DSC (= 8 mmol) were dissolved in 15 ml dry acetone
- 0.97 g DMAP (= 8 mmol) were dissolved in 10 ml dry acetone

With stirring, first the dissolved DSC was added to the farnesol / dioxane solution, and then DMAP solution was added drop by drop. The reaction was allowed to proceed under argon overnight at RT with continuous stirring. Completion of reaction was determined by thin layer chromatography. Material precipitated during the reaction was filtered out using a glass-fiber filter pad, and solvent was evaporated. To the remaining yellowish solution 10 volumes of dichloromethane were added, and subsequently loaded onto a silica gel column and then eluted with dichloromethane/petrol ether starting with a 8:2 mixture, then 9:1, 9.5:0.5 and 10:0. Flow-through was collected in 5 ml glass tubes and fractions were analyzed by thin-layer chromatography for the presence of SC-farnesol. Fractions containing SC-farnesol were pooled, the solvent was evaporated and product was analyzed by nuclear magnetic resonance (NMR).

2.15.3. Synthesis of NHS esters of fatty acids

Materials

- fatty acids were obtained from Sigma
- N-hydroxysuccinimide (NHS) (Perbio)
- dicyclohexyl carbodiimide (DCC) (Sigma)
- ethyl acetate was dried by filtration over Al_2O_3 (Fluka, type 5016A, basic)

Synthesis of the NHS ester of fatty acids was performed according to Huang *et al.*, (1980) with some modifications. Reaction was performed under water-free conditions using dry reaction vessels and dry solvents.

3 mmol NHS were dissolved in 30 ml ethyl acetate and then mixed with 3 mmol of fatty acid. After addition of 3 mmol DCC dissolved in 10 ml ethyl acetate to the NHS/fatty acid solution, the mixture was incubated overnight at RT under a argon blanket and if needed under light exclusion. After completion of the reaction, checked by TLC, the formed insoluble dicyclohexyl urea was removed by filtration using a glass fiber filter pad and the solvent was evaporated. The products were further purified by re-crystallization. This was done by dissolving the activated fatty acids in a minimal volume of hot ethanol and immediately filtering the solution through a filter funnel containing a fluted glass fiber pad, both of which have been warmed to the same temperature as the ethanol solution. The filtrate was incubated overnight at RT to allow re-crystallization. Excess solvent was removed afterwards from the re-crystallized solid by filtration, the product was dried under vacuum and analyzed by TLC. The NHS esters of the unsaturated fatty acids were not re-crystallized to avoid decomposition, as they are not stable.

2.15.4. Palmitoylation of ovalbumin and horseradish peroxidase

Materials

- palmitic acid-N-hydroxy succinimidester (NHS-palmitic acid) (Sigma)
- palmitoylation buffer: 20 mM sodium phosphate, 150 mM NaCl, 2% deoxycholate pH 8.5
- PD 10 column (Amersham, Bioscience)
- phenyl superose column (HR 10/10, Pharmacia Biotech)
- buffer A: 1.7 M $(\text{NH}_4)_2\text{SO}_4$ 50 mM sodium phosphate pH 7.0
- buffer B: 50 mM sodium phosphate

Palmitoylation was performed following the method previously described (Huang *et al.*, 1980). In brief, 5-30 mg proteins were dissolved in 1 ml palmitoylation buffer. A 20 molar excess of NHS-palmitic acid was dissolved in 100 μ l dioxane and together with 300 μ l DMSO slowly added to the protein solution. After an overnight incubation, the reaction was stopped by addition of 1/100 volume of 1 M lysine and free NHS-palmitic acid was removed by gel filtration (PD 10 column). To separate palmitoylated from non-palmitoylated protein, hydrophobic interaction chromatography (HIC) was performed following the palmitoylation reaction. Proteins were loaded onto a phenyl superose column under high salt condition (20% buffer B) allowing exclusively the binding of palmitoylated protein. To elute column bound palmitoylated protein the salt concentration was gradually reduced (100% buffer B in 20 min). Palmitoylated proteins were analyzed by mass spectrometry.

2.15.5. Coupling of NHS-activated lipids to peptides

To modify the model peptide NH₂-GSGSGSK(Acetyl) with the synthesized NHS activated lipids, a 1 mg/ml peptide solution in DMF was prepared and mixed to an equal volume of DMF containing a twenty molar excess of NHS activated lipid. After addition of one equimol of triethylamine, which served as base, the mixture was incubated overnight at 4°C. Subsequently the solvent was evaporated and peptides resuspended in 80% acetonitril/0.1% TFA for further analysis by mass spectrometry.

2.15.6. FITC labeling of ovalbumin and palmitoylated ovalbumin

Materials

- Oregon Green-NHS (Molecular Probes)
- PD 10 column (Amersham, Bioscience)

Ovalbumin or palmitoylated ovalbumin was dissolved in PBS and a five molar excess of Oregon Green-NHS in DMSO was added to the protein solution. The reaction was performed at RT for 2 hours under rotation. Finally the free Oregon Green-NHS was removed by gel filtration (PD10 column).

2.16. Analytical methods

2.16.1. Nuclear magnetic resonance analysis (NMR)

NMR spectra were recorded on a Bruker Avance DMX-500 (500MHz) spectrometer. Assignment of ¹H and ¹³C spectra was performed using 2D methods (COSY and HSQC). As a solvent, CDCl₃ was used.

2.16.2. Mass spectrometry – sample preparation

Covalent attachment of lipid tails to proteins and peptides was confirmed in mass spectrometry by detection of an appropriate shift in molecular mass of the peptide /protein after modification. To that end, control and modified peptides or proteins were analyzed by MALDI-TOEF or by ESI LC-MS.

Furthermore, mass spectrometry analysis was performed to confirm the identity of recombinantly expressed proteins. To that end, SDS-PAGE of protein samples were stained by 30-40 min incubation in 50% methanol, 7.5 % acetic acid, 0.1 (w/v) Coomassie Blue G250. After destaining of the gel with 20% methanol, 7.5 % acetic acid, the protein band of interest was excised and an in-gel tryptic digest was performed. Generated peptides were analyzed by ESI LC-MS and obtained peptide fragments compared with entries in databases to identify the protein.

Mass spectra were recorded on a Bruker Reflex III instrument (Bruker Daltonik) (MALDI-TOF) or on a Finnigan TSQ7000 (ESI LC-MS).

2.16.3. Static light scattering (SLS)

Static light scattering (SLS) experiments were performed at the Paul Scherrer Institut, Villingen, Switzerland using a miniDAWN TriStar with Optilab rex refractometer (Wyatt) coupled to a Superdex 200 10/30 gel filtration column on an Agilent 1100 Series HPLC. 100 μ l of 1 mg/ml protein solutions were injected on the column equilibrated in 20 mM Tris pH 7.4, 150 mM NaCl. Molecular weights were calculated using the Wyatt Astra version 4.90.08 software package.

2.16.4. Thin layer chromatography (TLC)

Materials

- 5 x 10 cm TLC pre-coated plates silica gel (Merck, Ca.No. 105719)
- solvent A: chloroform : petrol ether (40-60°C): 8:2
- solvent B: dichloromethane : petrol ether (40-60°C): 8:2
- Iodine chamber: TLC chamber with few iodine crystals
- Mostain: 800 ml 10% H₂SO₄, 40 g (NH₄)₆Mo₇O₂₄ x 4H₂O, 0.8 g Ce(SO₄) x 4H₂O
- NHS- stain, solution A: 10% (w/v) hydroxylamine in 0.1 N NaOH
- solution B: 5% (w/v) FeCl₃ in 1.2 N HCl

Synthesis of NHS activated lipids was followed by thin layer chromatography. To that end 5-10 μ l of the reaction mixture or the eluted chromatography fractions were spotted onto a TLC plate, dried and placed into a pre-equilibrated TLC-chamber containing solvent A (NHS esters of fatty acids) or solvent B (SC-farnesol). After the solvent front had reached the top of the plate, the plate was taken out and dried.

For staining of the plate with iodine, the plate was placed into a chamber saturated with iodine vapour, which has a high affinity for unsaturated and organic compounds. As iodine staining is reversible, plate was immediately photocopied afterwards.

Staining with Mostain (cerium molybdate stain) was performed as follows. The TLC plate was dipped once in Mostain solution, immediately placed in a 120°C oven and baked for 5-10 until samples turned dark-blue.

Visualization of the NHS group after TLC was performed as previously described (Huang *et al.*, 1980). To that end, the TLC plate was incubated first in NHS staining solution A and after 2 min in solution B, whereby the NHS-groups stain red.

2.17. References

- Arzt, S., Petit, I., Burmeister, W.P., Ruigrok, R.W., Baudin, F. Structure of a knockout mutant of influenza virus M1 protein that has altered activities in membrane binding, oligomerisation and binding to NEP (NS2). *Virus Res.* 2004, **99**: 115-9.
- Baudin, F., Petit, I., Weissenhorn, W., Ruigrok, R.W. In vitro dissection of the membrane and RNP binding activities of influenza virus M1 protein. *Virology.* 2001, **281**: 102-8.
- Bradford, M.M. A rapid and sensitive method for the quantitation of microgram quantities of protein utilizing the principle of protein-dye binding. *Anal Biochem.* 1976, **72**: 248-54.
- Ferrari, G., Knight, A.M., Watts, C., Pieters, J. Distinct intracellular compartments involved in invariant chain degradation and antigenic peptide loading of major histocompatibility complex (MHC) class II molecules. *J Cell Biol.* 1997, **139**: 1433-1446.
- Gatfield, J., Pieters, J. Essential role for cholesterol in entry of mycobacteria into macrophages. *Science.* 2000, **288**: 1647-50.
- Hogquist, K.A., Jameson, S.C., Heath, W.R., Howard, J.L., Bevan, M.J., Carbone, F.R. T cell receptor antagonist peptides induce positive selection. *Cell.* 1994, **6**: 17-27.
- Huang, A., Huang, L., Kennel, S.J. Monoclonal antibody covalently coupled with fatty acid. A reagent for in vitro liposome targeting. *J Biol Chem.* 1980, **255**: 8015-8.
- Inoue, H., Nojima, H., Okayama, H. High efficiency transformation of *Escherichia coli* with plasmids. *Gene.* 1990, **96**: 23-8.
- Klein, U., Gimpl, G., Fahrenholz, F. Alteration of the myometrial plasma membrane cholesterol content with beta-cyclodextrin modulates the binding affinity of the oxytocin receptor. *Biochemistry.* 1995, **34**: 13784-93.
- Miron, T., Wilchek, M. A simplified method for the preparation of succinimidyl carbonate polyethylene glycol for coupling to proteins. *Bioconjug Chem.* 1993, **4**: 568-9.
- Sallusto, F., Cella, M., Danieli, C., Lanzavecchia, A. Dendritic cells use macropinocytosis and the mannose receptor to concentrate macromolecules in the major histocompatibility complex class II compartment: downregulation by cytokines and bacterial products. *J Exp Med.* 1995, **182**: 389-400.
- Schreurs, M.W., Eggert, A.A., de Boer, A.J., Figdor, C.G., Adema, G.J. Generation and functional characterization of mouse monocyte-derived dendritic cells. *Eur J Immunol.* 1999, **29**: 2835-41.
- Smith, P.K., Krohn, R.I., Hermanson, G.T., Mallia, A.K., Gartner, F.H., Provenzano, M.D., Fujimoto, E.K., Goeke, N.M., Olson, B.J., Klenk, D.C. Measurement of protein using bicinchoninic acid. *Anal Biochem.* 1985, **150**: 76-85.
- Steinmetz, M.O., Hoenger, A., Stoffler, D., Noegel, A.A., Aebi, U., Schoenenberger, C-A. Polymerization, 3-D structure and mechanical properties of *Dictyostelium* versus Rabbit Muscle Actin Filaments. *J. Mol. Biol.* 2000, **303**: 171-184.
- Tulp, A., Verwoerd, D., Dobberstein, B., Ploegh, H.L., Pieters, J. Isolation and characterization of the intracellular MHC class II compartment. *Nature.* 1994, **369**: 120-126.
- Wiltshcke, C., Nemet, H., Holzinger, C., Gessl, A., Pernerstorfer, T., Forster, O., Boltz-Nitulescu, G. Murine recombinant GM-CSF-driven rat bone marrow cell differentiation and factors suppressing cell proliferation. *Immunobiology.* 1989, **179**: 145-58.
- Zalipsky, S., Seltzer, R., Menon-Rudolph, S. Evaluation of a new reagent for covalent attachment of polyethylene glycol to proteins. *Biotechnol Appl Biochem.* 1992, **15**: 100-14.

- Chapter 3 -

Essential Role for Cholesterol in the Delivery of Exogenous Antigens to the MHC Class I Presentation Pathway

Imke Albrecht, John Gatfield, Thierry Mini, Paul Jenoe
and Jean Pieters

Biozentrum, University of Basel, Klingelbergstrasse 50,
CH-4056 Basel, Switzerland

Submitted

3.1. Abstract

Cross-presentation, which is crucial for the generation of immunity against virus-infected and tumour cells requires exogenous antigens to be internalized into antigen-presenting cells followed by translocation to the cytosol by unknown mechanisms. One important entry route for such antigens is macropinocytosis. We describe here that cholesterol is essential for cross-presentation of antigens loaded via macropinocytosis into antigen presenting cells. Modification of antigens by palmitoylation to target antigens to cholesterol-enriched plasma membrane domains resulted in a dramatically increased T-cell activation. These results define cholesterol as an essential factor for cross-presentation and suggest that specific modification of antigens to increase their affinity for cholesterol may be utilized to enhance immunity.

3.2. Introduction

Generation of an immune response occurs through the activity of the molecules encoded in the major histocompatibility complex (MHC). These molecules come in two forms, the MHC Class I and MHC Class II molecules, whose function is to present foreign peptides to CD8⁺ and CD4⁺ T-cells, respectively. MHC class II molecules are synthesized in the endoplasmic reticulum and form a complex with an invariant chain which targets the MHC class II complex to post-Golgi endosomal/lysosomal organelles, the so-called MHC class II compartments (Amigorena *et al.*, 1994; Tulp, *et al.*, 1994; West *et al.*, 1994). Within these organelles, they assemble with peptides derived from exogenous antigens (Cresswell *et al.*, 1996; Pieters, 1997; Trombetta and Mellman, 2005). Such antigens are internalized via endocytosis and degraded in endosomal/lysosomal organelles (Watts, 1997). These intracellularly formed MHC class II-peptide complexes are then transported to the cell surface for presentation to CD4⁺ (helper) T-cells (Germain, 1994).

MHC class I molecules, in contrast, are synthesized in the endoplasmic reticulum, assemble with beta 2-microglobulin and remain in the endoplasmic reticulum until they become loaded with antigenic peptides (Townsend *et al.*, 1989). Antigenic peptides loaded onto MHC class I molecules are derived from antigens residing in the cytosol, such as viral proteins as well as tumor derived antigens (Koopmann *et al.*, 1997). These cytosolic antigens are degraded by the

proteasome, a cytosolic multiprotease complex, into peptides (Monaco 1995; Baumeister *et al.*, 1998), which are subsequently translocated into the endoplasmic reticulum in an ATP-dependent manner by the TAP transporter (Spies *et al.*, 1990; Androlewicz *et al.*, 1993). Assembly of antigenic peptides with the MHC class I/beta 2-microglobulin complex in the ER triggers their transport to the cell surface where they can activate CD8⁺ (killer) T-cells (Townsend *et al.*, 1989). This dichotomy between the MHC class I and class II pathways ensures the efficient and selective killing of virally infected or tumour cells, while generating a help response in the case of bacterial infections (Pieters, 1997; Watts and Powis, 1999). In addition, restricting MHC class I presentation to endogenous antigens prevents healthy cells from becoming targets for killing by CD8⁺ T-cells (Ackerman, 2004).

An important step in the generation of an immune response is the activation of naïve T-cells, which occurs through their stimulation by dendritic cells (Cella *et al.*, 1997; Banchereau and Steinman, 1998; Heath and Carbone, 2001). Dendritic cells sample peripheral tissue for the presence of antigens, and migrate to lymphoid organs where antigenic peptides captured in the periphery can be presented to naïve T-cells (Banchereau and Steinman, 1998). For the generation of CD4⁺ T-cells, antigens are captured within the endocytic pathway, and during migration to the secondary lymphoid organs the dendritic cells mature and increase the expression of MHC class II-peptide complexes at the cell surface in order to efficiently induce T-cell activation (Cella *et al.*, 1997; Pierre *et al.*, 1997; Boes *et al.*, 2002). How CD8⁺ T-cells can be activated against antigens present in the periphery has been less well defined. For generation of CD8⁺ T-cells, antigens captured in the periphery by professional antigen-presenting cells have to acquire access to the MHC class I pathway. It is now becoming clear that a pathway does exist both in dendritic cells and macrophages to deliver exogenously captured antigens to the MHC class I processing compartments referred to as cross-presentation (Bevan, 1976; Heath and Carbone, 2001; Rock *et al.*, 1990; Reis e Sousa and Germain, 1995). Cross-presentation is crucial for the establishment of immunity against virus-infected and tumour-transformed cells as well as for the induction of tolerance (den Haan and Bevan, 2001; Heath and Carbone, 2001). The precise mechanisms involved in transfer of exogenous antigens to the MHC class I processing and presentation machinery are still unclear (Guermónprez and Amigorena, 2005; Ackerman and Cresswell, 2004).

One internalization route used by macrophages and dendritic cells in particular to sample exogenous antigens to be cross-presented is macropinocytosis (Ackerman *et al.*, 2005;

Ackerman *et al.*, 2003; Watts and Powis, 1999; Norbury *et al.*, 1997; Norbury *et al.*, 1995; Brossart and Bevan, 1997; Sallusto *et al.*, 1995). Macropinocytosis refers to the uptake of non-particulate material through the formation of 0.5-2 μm diameter vesicles in an actin-dependent process (Steinman and Swanson, 1995). Macropinosome formation starts at the cell periphery by extension of a large planar membrane ruffle (lamellipodium) that folds back to form the macropinosome (Cardelli, 2001; Amyere *et al.*, 2000; Araki *et al.*, 1996; Rupper *et al.*, 2001). In macrophages and dendritic cells, formation of macropinosomes is a constitutive activity, which can be further enhanced by treatment with growth factors and activators of protein kinase C such as phorbol esters. Also in other cell types, macropinocytosis can be induced, although the significance of such macropinocytic events for internalization processes in these cells is unclear (Steinman and Swanson, 1995; West *et al.*, 1989; Grimmer *et al.*, 2002). Both induced and constitutive macropinosome formation is dependent on the activity of phosphatidylinositol (PI)-3-kinase (Araki *et al.*, 1996; Amyere *et al.*, 2002) and the activity of Rho family member Rac 1 (Ridley *et al.*, 1992; West *et al.*, 2000). Whereas activation of GTPase Rac 1 and its subsequent signaling to downstream effectors such as WAVE 2, an activator of the Arp2/3 complex (Miki *et al.*, 1998; Miki *et al.*, 2000) or p21 activated kinases (PAK) (Dharmawardhane *et al.*, 2000) is required for the rearrangement of the actin cytoskeleton, activated phosphatidylinositol (PI)-3-kinase seems to be necessary for the completion of macropinosome formation (Araki *et al.*, 1996). Macropinosomes remain separate from conventional endosomes (Hewlett *et al.*, 1994) although fluid phase markers internalized via macropinocytosis may eventually reach lysosomes (Racoosin and Swanson, 1993).

Antigens internalized into antigen-presenting cell via macropinocytosis gain access to the MHC class I processing pathway (Norbury *et al.*, 1995; den Haan and Bevan, 2001; Ackerman *et al.*, 2005) but the mechanisms involved in transfer of macropinocytosed antigens to the cytosol remain unknown. As a first step towards defining the molecular events involved in the transfer of exogenous antigens to the MHC class I processing and presentation pathway, the delivery of a model antigen, ovalbumin, to the class I presentation pathway was analyzed in here.

3.3. Results

3.3.1. Contribution of cholesterol to macropinosome formation

To gain insight into the delivery process of exogenous antigens to the MHC class I presentation pathway, different professional antigen-presenting cells were incubated with FITC labeled Dextran, a marker for macropinosomes (Sallusto *et al.*, 1995; Swanson, 1989; Norbury *et al.*, 1995). Both J774 cells and bone marrow derived macrophages as well as bone marrow derived dendritic cells contained large numbers of macropinosomes (*figure 3.1.A,B*). As macropinosomes provide a port of entry to deliver components into the cell, similar to endosomes, the relationship of these organelles with other endocytic compartments was examined.

To that end, macrophages that had internalized FITC-Dextran via macropinocytosis were analyzed for the presence of different markers of the endosomal/lysosomal pathway, including clathrin and lysosomal associated membrane glycoprotein-1 (LAMP-1), none of which co-localized with macropinosomes. However, when cells were incubated with the cholesterol-binding compound filipin (Bornig and Geyer, 1974; Drabikowski *et al.*, 1973; Gatfield and Pieters, 2000), all macropinosomes strongly labeled with filipin (*figure 3.1.B*). This suggests that cholesterol is an important component of macropinosomes in macrophages and dendritic cells.

To analyze the contribution of cholesterol to macropinosome formation, the plasma membrane of macrophages and dendritic cells was depleted for cholesterol by pharmacological treatment with lovastatin and methyl- β -cyclodextrin (Klein *et al.*, 1995; Simons *et al.*, 1998; Gatfield and Pieters, 2000). Living cells were observed under the microscope and macropinosome formation was monitored using time lapse video microscopy and thirty minute video sequences of control and cholesterol depleted cells were recorded. As shown in *figure 3.2.*, whereas membrane ruffling (marked by white arrowheads) occurred both in control as well as in cholesterol-depleted cells, macropinosome formation (marked by black arrowheads) was abolished in cells depleted for cholesterol.

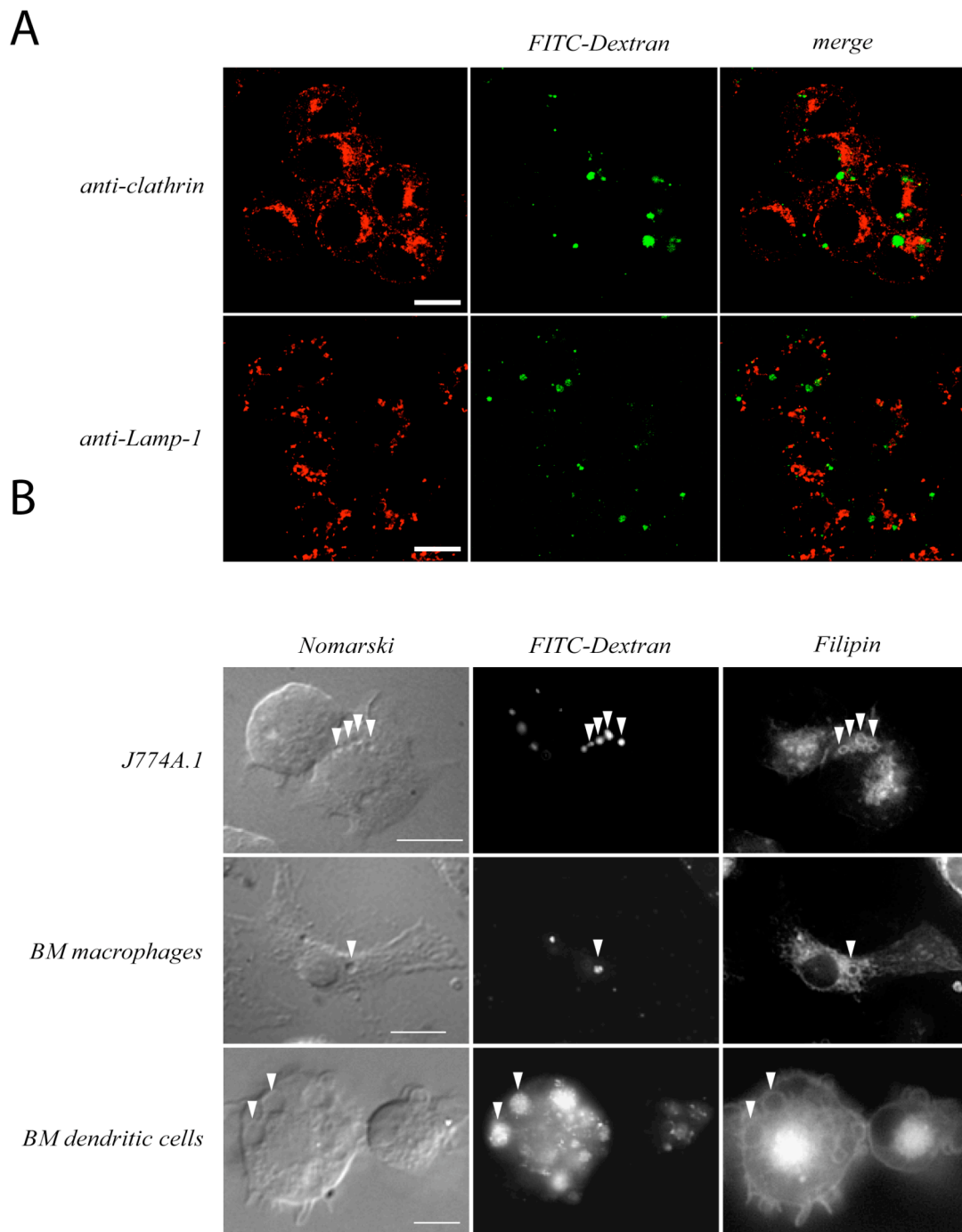


Figure 3.1. Distribution of macropinocytosed FITC-Dextran in macrophages and dendritic cells.

A. Macrophages (J774A.1 cells) were incubated with FITC-Dextran for 7 min, fixed and stained for clathrin (*upper panels*) and LAMP-1 (*lower panels*) using anti-clathrin (secondary reagent: anti-mouse IgG1-TXR) and anti-LAMP-1 (secondary reagent: anti-rat IgG-568) antibodies.

B. J774A.1 macrophages (*upper panels*), bone marrow derived macrophages (*middle panels*) and bone marrow derived dendritic cells (*lower panels*) were incubated for 12 min with FITC-Dextran, fixed and labeled for cholesterol with filipin. Arrowheads point at macropinosomes. Bar: 10 μ m.

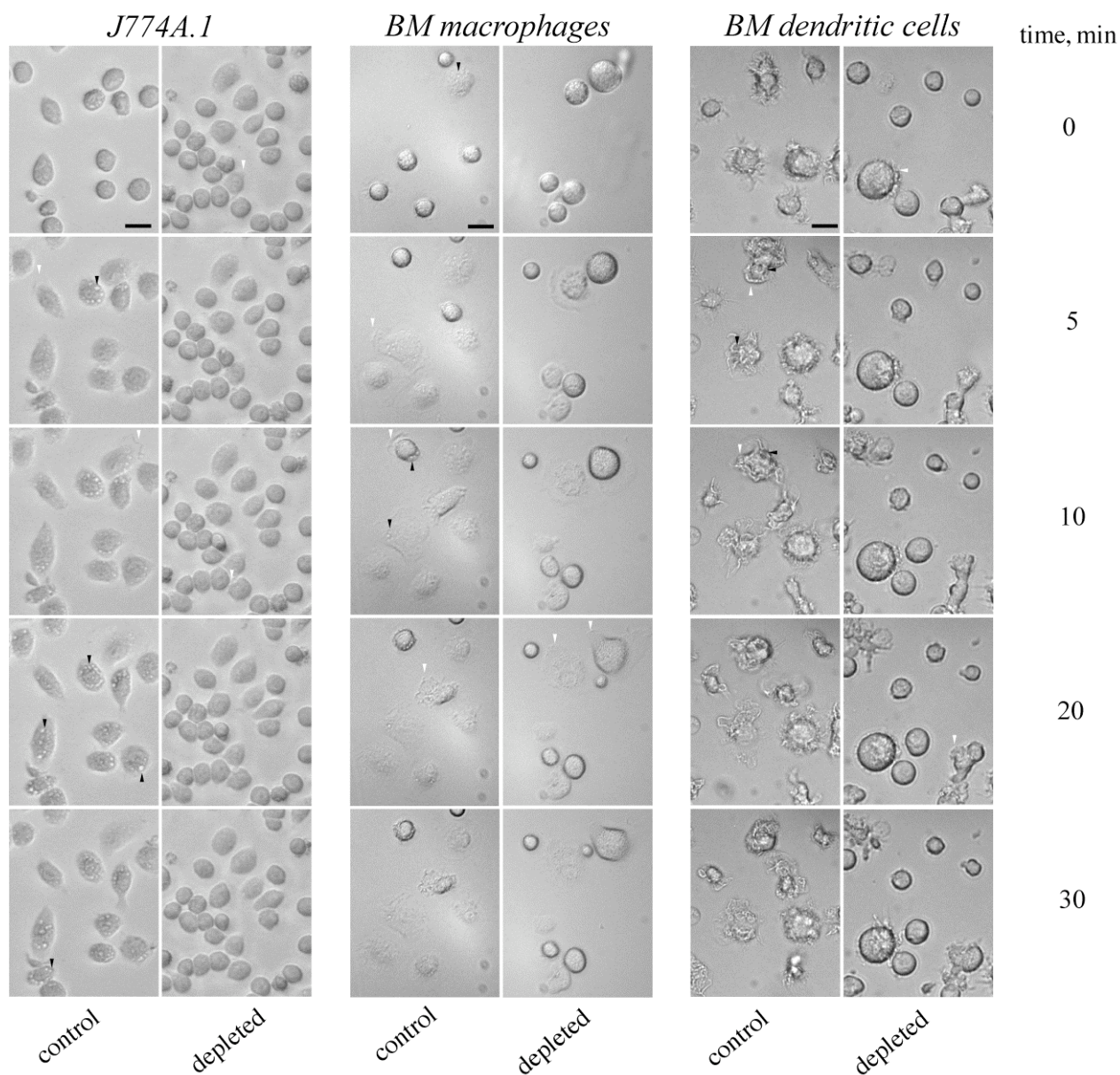


Figure 3.2. Effect of cholesterol-depletion on macropinocytosis analyzed by time-lapse video microscopy.

J774A.1 cells (*right panels*), bone marrow (BM) derived macrophages (*middle panels*), or bone marrow (BM) derived dendritic cells (*left panels*) were cholesterol-depleted (*depleted*) or left untreated (*control*) and placed under a 37°C thermoregulated and CO₂ equilibrated microscope and subsequently 30 min video sequences were recorded. Shown are images at the times indicated. Examples of membrane ruffles are marked by white arrowheads, macropinosomes are marked by black arrowheads. Bar: 10 μm.

To directly analyze internalization of the fluid-phase marker FITC-Dextran, control or cholesterol-depleted cells were incubated with FITC-Dextran for 12 min, fixed and observed under the fluorescence microscope. After cholesterol-depletion, internalization of FITC-Dextran in macrophages and dendritic cells was strongly reduced, in contrast to control cells (figure 3.3.).

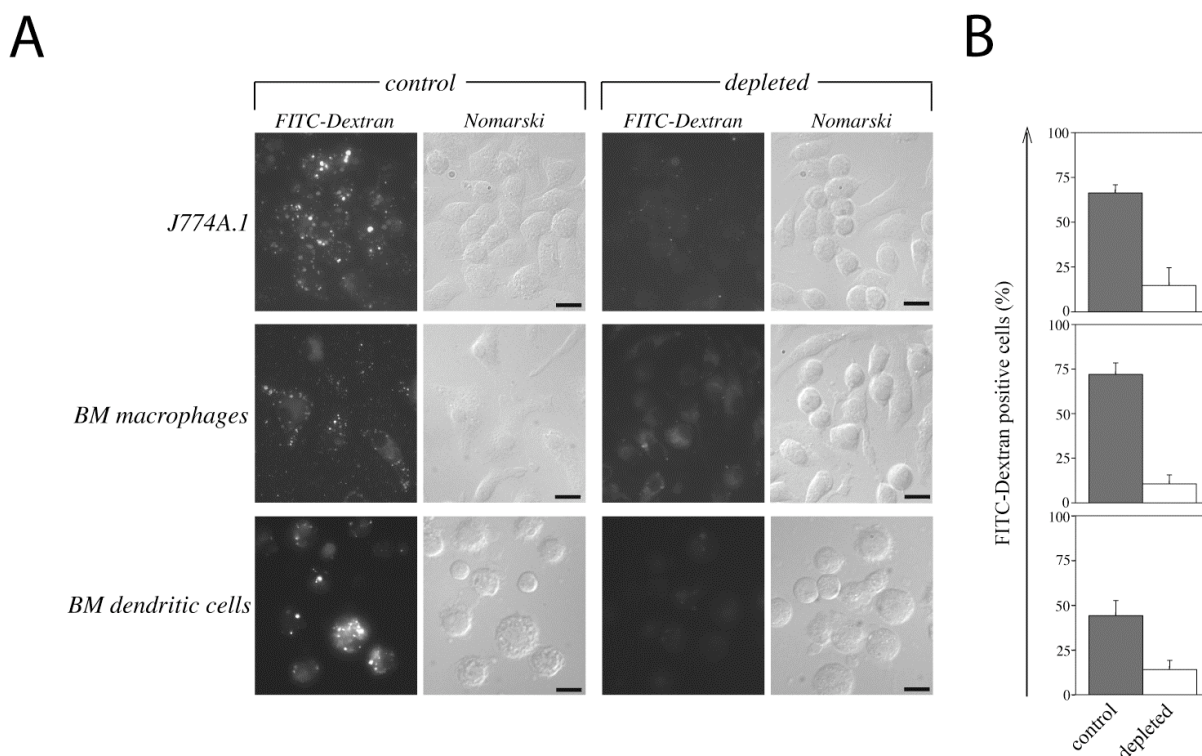


Figure 3.3. Effect of cholesterol-depletion on macropinocytosis analyzed by internalization of the fluid-phase marker FITC-Dextran.

A. Control (left) or cholesterol depleted (right) J774A.1 macrophages (upper panels), bone marrow derived macrophages (middle panels), both stimulated with PMA or dendritic cells (lower panels) were incubated with FITC-Dextran for 12 min, fixed and analyzed by fluorescence microscopy. Bar: 10 μ m.

B. For quantitation, cells (n= 150) were scored for the presence of internalized FITC-Dextran. Shown are mean values (+/- SD, n = 50) from three experiments.

Cholesterol is an important component of the plasma membrane where it has a key role in organization of membrane lipid domains that serve as platforms for cell signalling, protein organization and protein sorting.

To exclude the possibility that the impairment of cholesterol-depleted cells to exhibit macropinocytosis is due to an overall defect in common cellular processes, the influence of cholesterol-depletion on protein biosynthesis as well as on phagocytosis was examined.

To study protein synthesis, control and cholesterol-depleted cells were metabolically labeled for one hour with ^{35}S -methionine and cysteine, washed and lysed. Proteins from the lysates were precipitated with trichloroacetic acid and the amount of radioactivity incorporated into newly synthesized proteins was determined. As shown in figure 3.4.A, the rate of ^{35}S incorporation in J774A.1 and BM macrophages after cholesterol-depletion was only slightly affected, whereas in cholesterol depleted BM dendritic cells protein biosynthesis was reduced around 40% compared to non-treated cells.

Phagocytosis was examined by measuring the uptake of FITC-labeled latex beads in control and cholesterol-depleted cells. To that end, cells were incubated with latex beads for one hour at 37°C , chased for a further 30 min, washed and analyzed by flow cytometry to quantify phagocytosis.

As shown in figure 3.4.B, cholesterol depletion of J774A.1 cells and BM macrophages did not significantly interfere with the ability of these cells to internalize material via phagocytosis, which is consistent with earlier reports (Gatfield and Pieters, 2000). The same was observed using BM dendritic cells. Also cholesterol-depleted BM dendritic cells were able to internalized FITC-labeled latex beads to a similar extent as control BM dendritic cells suggesting that cholesterol depletion did not affect phagocytosis.

Together these results show that the removal of plasma membrane cholesterol blocked macropinocytosis without severely inhibiting other cellular processes such as protein biosynthesis or phagocytosis in antigen-presenting cells.

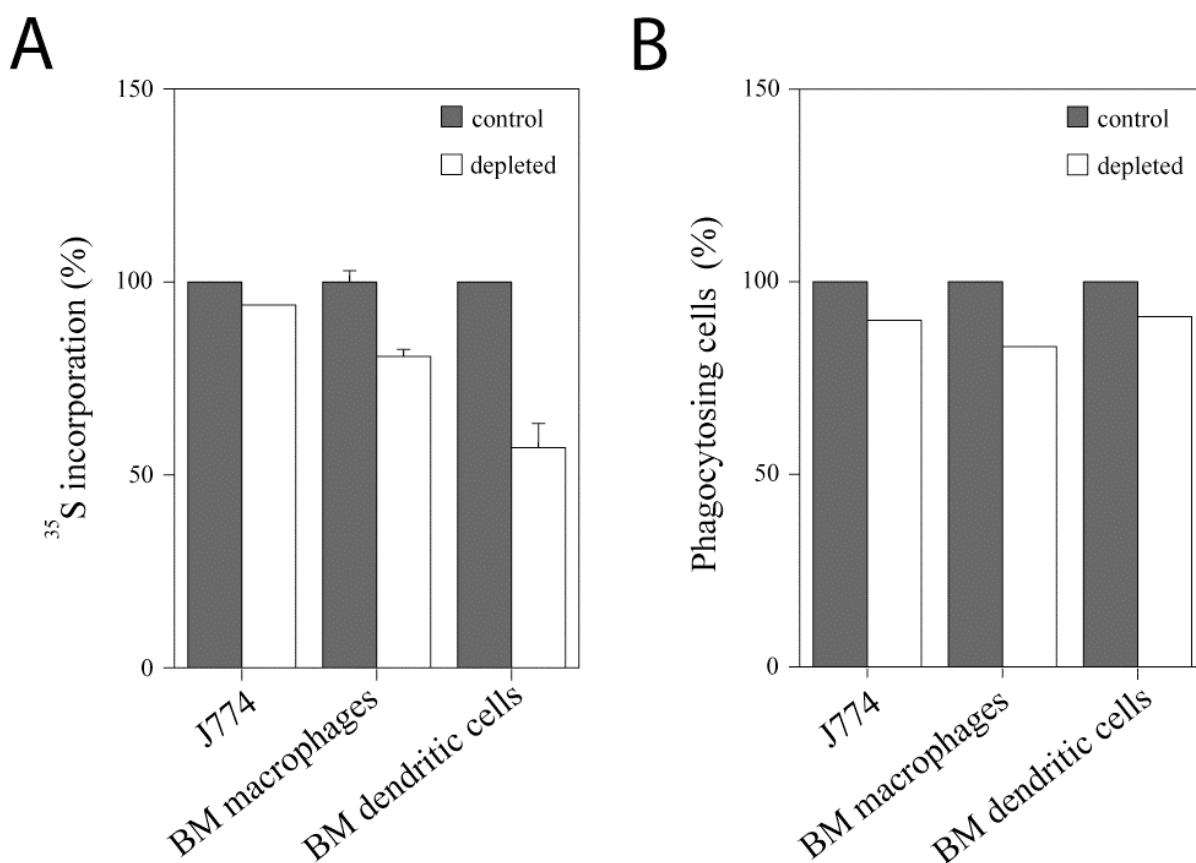


Figure 3.4. Effect of cholesterol-depletion on protein synthesis and phagocytosis.

A. Control (grey bars) and cholesterol-depleted (white bars) J774A.1 macrophages (left), bone marrow derived macrophages (middle) or bone marrow derived dendritic cells (right) were metabolically labeled for 1 hour with [³⁵S] methionine and cysteine, washed and lysed in TX-100 containing lysis buffer. Proteins from the lysate were TCA precipitated and the incorporated radioactivity determined in a liquid scintillation counter.

B. Control (grey bars) and cholesterol-depleted (white bars) J774A.1 macrophages (left), bone marrow derived macrophages (middle) or bone marrow derived dendritic cells (right) were allowed to internalize FITC-labeled beads for 1 hour at 37°C, chased for 30 min and washed to remove non-internalized material. Phagocytosis was quantified by flow-cytometry analysis and it is displayed as mean fluorescence intensity. Phagocytosis is corrected for background adherence occurring at 4°C and is expressed as percent phagocytosed beads compared with control macrophages.

To test whether macropinosome formation can be restored when cholesterol is re-added, cholesterol-depleted cells were incubated with methyl- β -cyclodextrin-cholesterol complex for one hour. Macropinosome activity was measured afterwards by internalization of FITC-Dextran. Shown in figure 3.5., treatment of cholesterol-depleted cells with methyl- β -cyclodextrin-cholesterol led to the replenishment of cholesterol (figure 3.5.A) fully restoring macropinosome activity of the cells (figure 3.5.B).

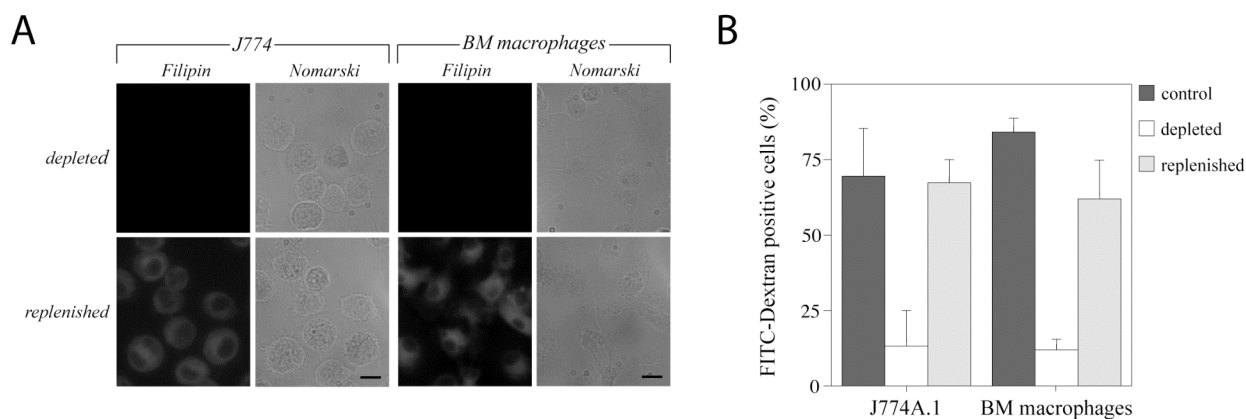


Figure 3.5. Effect of cholesterol re-addition to cholesterol-depleted macrophages.

A. Cholesterol-depleted (*upper panels*) and cholesterol-depleted J774A.1 macrophages and bone marrow derived macrophages treated for 1 hour with cholesterol:methyl- β -cyclodextrin complex (6 mg/ml) to allow re-insertion of cholesterol (*lower panels*) were fixed and labeled for cholesterol with filipin. Bar: 10 μ m.

B. Control (*dark grey bars*), cholesterol-depleted (*white bars*) or cholesterol-replenished J774A.1 macrophages and bone marrow derived macrophages (*light grey bars*) were incubated for 12 min with FITC-Dextran. After fixation, quantitation was performed by scoring cells (n=100) for the presence of internalized FITC-Dextran. Shown are mean values (+/- SD) from three experiments.

These results show that macropinosome formation in macrophages and dendritic cells is a cholesterol-dependent process.

3.3.2. Role for cholesterol in cross-presentation

Given the role of cholesterol in macropinocytosis, the involvement of cholesterol in cross-presentation was investigated. For that purpose we made use of the model antigen ovalbumin. Ovalbumin labeled with FITC, when added to macrophages, was efficiently internalized into macropinosomes (*figure 3.6.A/B*). Conversely, internalization of FITC-ovalbumin in cholesterol-depleted cells was greatly reduced.

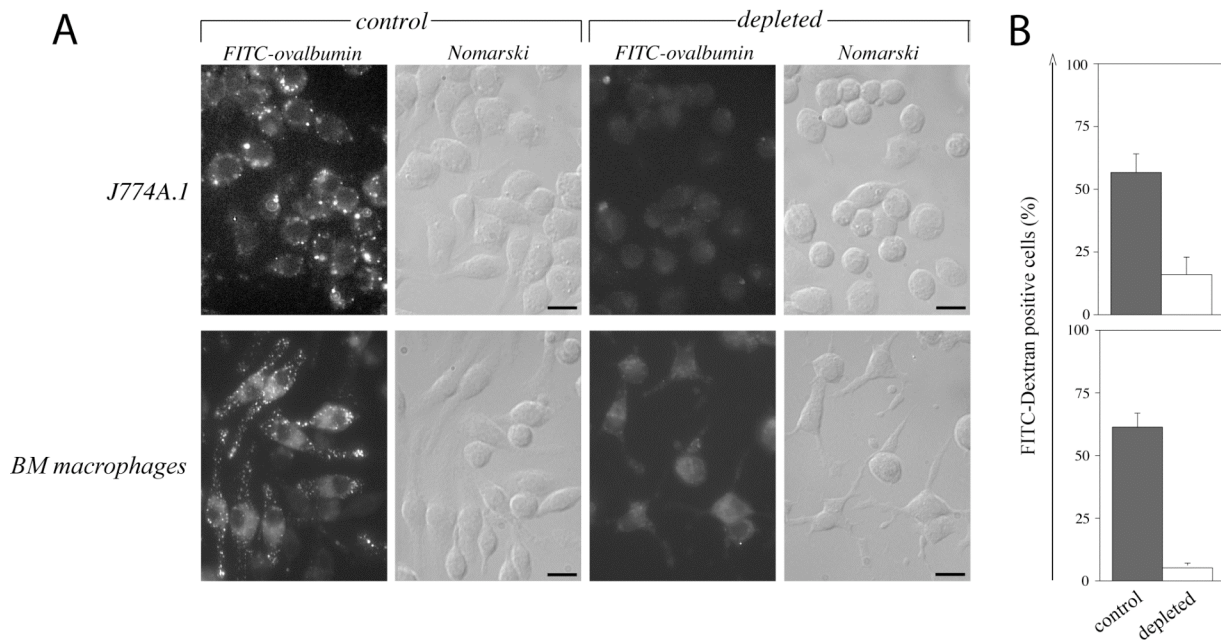


Figure 3. 6. Effect of cholesterol-depletion on the internalization of ovalbumin.

A. Macrophages (top panels: J774A.1, bottom panels: bone marrow derived macrophages) left untreated (control) or depleted for cholesterol (depleted) were incubated with 0.1 mg /ml FITC-ovalbumin for 12 min, fixed, and analyzed by fluorescence microscopy. Bar: 10 μ m.

B. Quantitation was carried out after fixation. Values represent the percentages of cells having internalized FITC-ovalbumin (+/- SD from triplicates; n=50).

To analyze cross-presentation, control or cholesterol-depleted macrophages were incubated with ovalbumin for three hours, washed, and the cell surface display of the ovalbumin derived MHC class I SIINFEKL epitope was measured using CD8⁺ T-cells obtained from OT-1 mice (see materials and methods). The capacity of the ovalbumin-loaded macrophages to stimulate OT-1 T-cells was quantified by measuring T-cell proliferation, which is a direct result of T-cell activation initiated by the recognition of the appropriate antigen on the surface of the antigen-presenting cell.

Whereas control macrophages stimulated T-cell proliferation, depletion of macrophages for cholesterol resulted in a severely reduced T-cell activation (*figure 3.7.A*). To analyze whether cholesterol depletion compromises the ability to present the SIINFEKL peptide *per se*, untreated and cholesterol depleted macrophages were pulsed with SIINFEKL peptide that does not require internalization prior to presentation to T-cells. As shown in *figure 3.7.B.*, both in control or cholesterol-depleted macrophages MHC class I presentation of exogenously added SIINFEKL peptide was comparable. Ovalbumin was indeed presented after cross-

presentation, as the inclusion of the proteasome inhibitor lactacystin, or fixation of the macrophages with paraformaldehyde abolished T-cell proliferation (*figure 3.7.C, D*).

From these results it can be concluded that cholesterol has a crucial role in cross-presentation of exogenous antigens by modulating their uptake and/or their translocation.

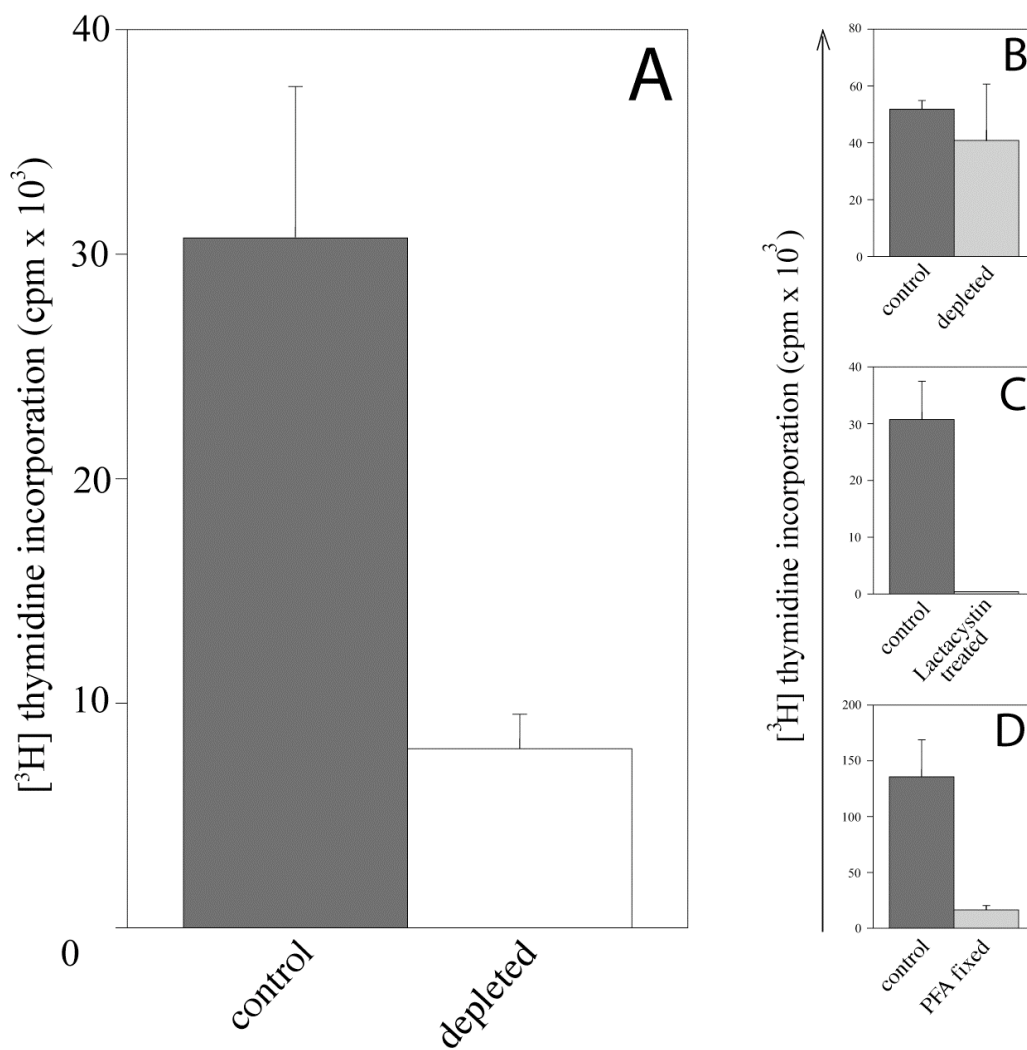


Figure 3.7. Effect of cholesterol depletion on cross-presentation of ovalbumin

A, D. Bone marrow derived macrophages were left untreated (*dark grey bars*) or depleted (*white bars*) for cholesterol and incubated with ovalbumin (10 mg/ml) (*A,C*) or SIINFEKL peptide (10 mM) (*B*) for three hours. In *C*, macrophages were treated with lactacystin. In *D*, macrophages were fixed with paraformaldehyde prior to addition of ovalbumin (5 mg/ml). Cells were washed and T-cells specific for the SIINFEKL epitope isolated from OT-1 mice were added. T-cell proliferation was measured after three days as described in materials and methods.

3.3.3. Modulation of internalization and cross-presentation of proteins by palmitoylation

The finding that macropinosomes are cholesterol-rich structures, lead us to explore the possibility that enhancement of the affinity of antigens for cholesterol improves internalization. One modification that targets proteins to cholesterol-enriched sites in the plasma membrane is palmitoylation (Wolfen *et al.*, 1997; Melkonian *et al.*, 1999; Zacharias *et al.*, 2002). As a model protein, the behaviour of horseradish peroxidase (HRP) after modification by palmitoylation was investigated. Horseradish peroxidase was internalized into macrophages via macropinocytosis and internalization was inhibited following cholesterol depletion (*figure 3.8*).

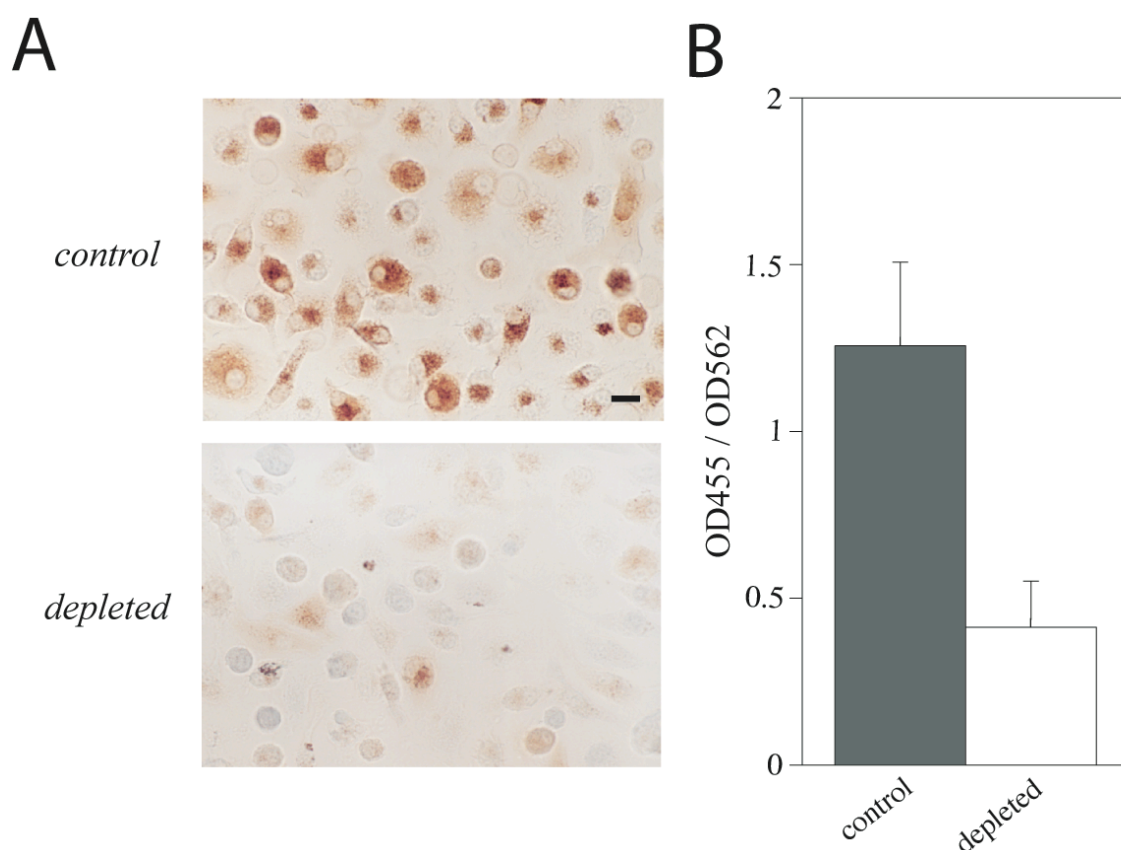


Figure 3.8. Internalization of horseradish peroxidase (HRP)

A. Control (*left panel*) or cholesterol-depleted (*right panel*) BM derived macrophages were incubated for one hour with HRP (5 mg/ml) and chased for 4 hours followed by fixation. The internalized HRP was visualized as described in methods. Bar: 10 μ m.

B. Control (*dark grey bar*) or cholesterol-depleted (*white bar*) BM derived macrophages were incubated for one hour with horseradish peroxidase (2 mg/ml). After washing, cells were lysed and the amount of internalized HRP in the lysate was determined as described in methods. Shown are the mean values (\pm SD) from three experiments.

To modify horseradish peroxidase by palmitoylation, HRP was incubated for 20 hours with the NHS ester of palmitic acid (figure 3.9.). After palmitoylation, the product was purified by hydrophobic interaction chromatography (figure 3.10.A). Mass spectrometry analysis showed a mass shift of 239 Da upon palmitoylation consistent with the addition of one palmitic acid residue. (figure 3.10.B). Incubation of macrophages with palmitoylated-HRP resulted in efficient internalization of HRP, whereas non-modified horseradish peroxidase was barely detectable at the same concentration (figure 3.10.C). Thus, palmitoylation leads to an enhanced uptake of exogenous proteins via macropinocytosis.

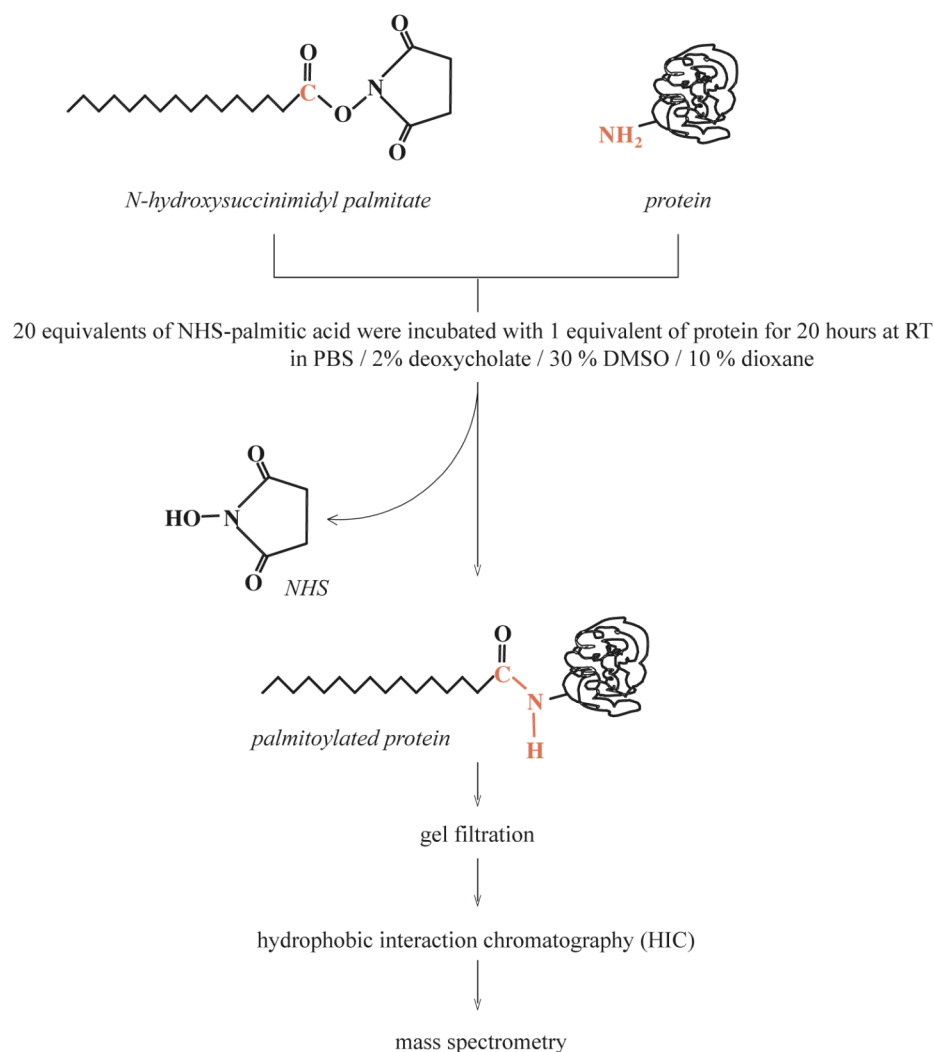


Figure 3.9. Palmitoylation of horseradish peroxidase (HRP) – Reaction scheme

Palmitoylation procedure of HRP. HRP was incubated with NHS-activated palmitic acid for 20 hours. Afterwards the unreacted NHS-palmitic acid was removed by gel filtration and palmitoylated protein was purified with hydrophobic interaction chromatography.

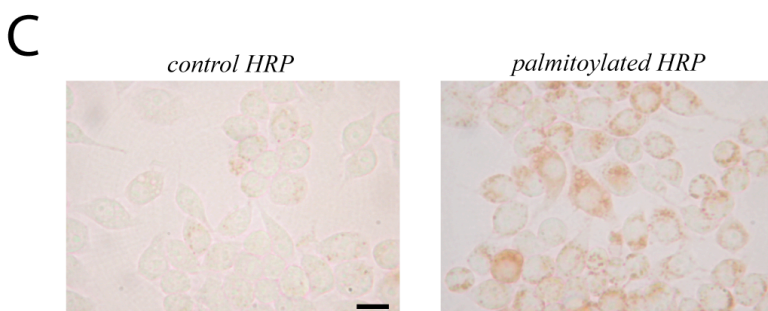
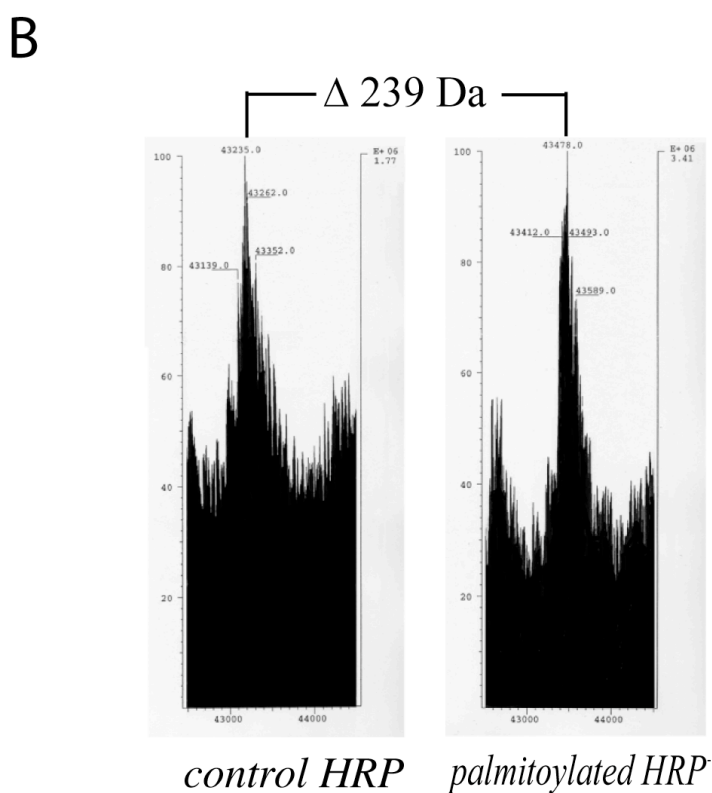
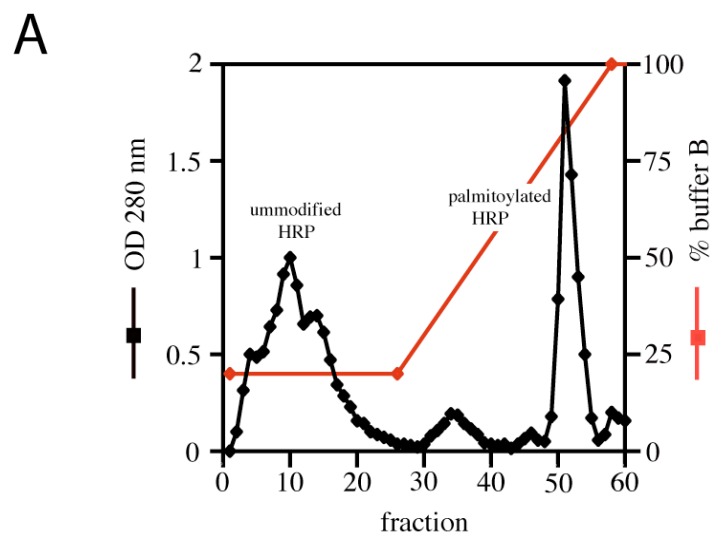


Figure 3.10. Palmitoylation of HRP – Purification, Analysis and Internalization

A. Hydrophobic interaction chromatography (HIC) profile. Loading of HRP onto a Phenyl Superose column (HR 10/10, pharmacia) was performed at high-salt concentration (1.4 M $(\text{NH}_4)_2\text{SO}_4$ in 50 mM sodium phosphate pH 7.0) allowing the exclusive binding of palmitoylated HRP whereas unmodified HRP did not bind and could be recovered in the wash fractions. Elution of palmitoylated HRP was achieved by decreasing the salt concentration.

B. Mass spectrometry analysis (MALDI-TOF) of control HRP (*left panel*) and palmitoylated HRP (purified by HIC) (*right panel*). A mass shift of 239 Da was detected corresponding to the attachment of one palmitic acid chain to the protein.

C. J774A.1 macrophages were incubated for one hour with 0.5 mg/ml HRP (*left panel*) or palmitoylated HRP (*right panel*), fixed and permeabilized. Internalized HRP was visualized as described in materials and methods. Bar: 10 μm .

Given the dependence of cross-presentation on cholesterol, we analyzed whether modification of the antigen by palmitoylation could modulate cross-presentation. To that end, ovalbumin was palmitoylated as described and the capacity of macrophages to internalize and cross-present palmitoylated ovalbumin was examined. As shown in figure 3.11.A/B, internalization of FITC labeled palmitoylated ovalbumin was three to four times increased compared to non-modified FITC-ovalbumin.

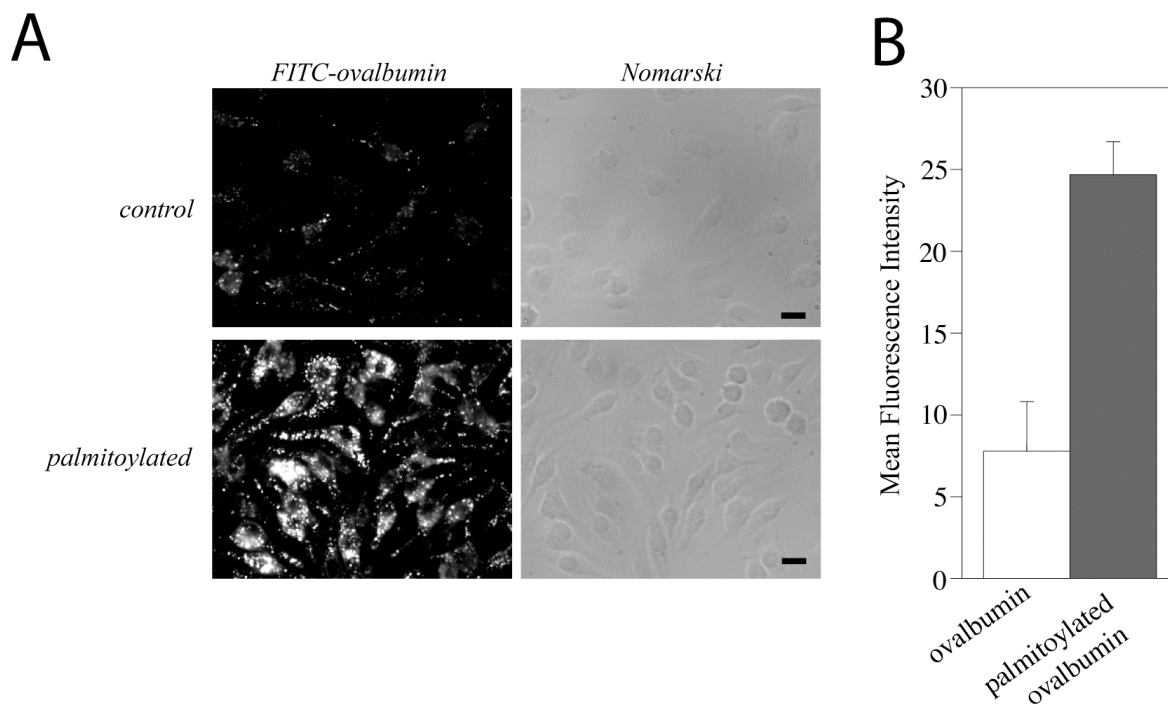


Figure 3.11. Effect of palmitoylation on internalization of ovalbumin.

A. Bone marrow derived macrophages were incubated with 0.1 mg/ml ovalbumin (*upper panels*) or palmitoylated ovalbumin (*lower panels*) that was labeled with FITC for 12 min, followed by fixation and analysis by fluorescence microscopy. Bar: 10 μ m.

B. Quantification of internalization was performed using flow cytometry. After incubation with FITC labeled ovalbumin (*white bars*) or palmitoylated ovalbumin (*dark grey bars*) for 20 min at 37°C, bone marrow derived macrophages were fixed and protein internalization analyzed by flow cytometry. Shown are mean values (+/- SD) from three experiments.

To analyze the effect of palmitoylation on cross-presentation, macrophages were pulsed with different concentrations of ovalbumin or palmitoylated ovalbumin. As shown in figure 3.12., T-cell proliferation of the SIINFEKL epitope was greatly enhanced for palmitoylated ovalbumin as compared to SIINFEKL presentation after internalization of the same concentrations of ovalbumin. The enhanced T-cell proliferation was due to internalization and processing of the palmitoylated ovalbumin, as palmitoylated SIINFEKL peptide was far less

potent in the stimulation of T-cell proliferation (*figure 3.12.B*), consistent with an earlier report (Andrieu *et al.*, 2000).

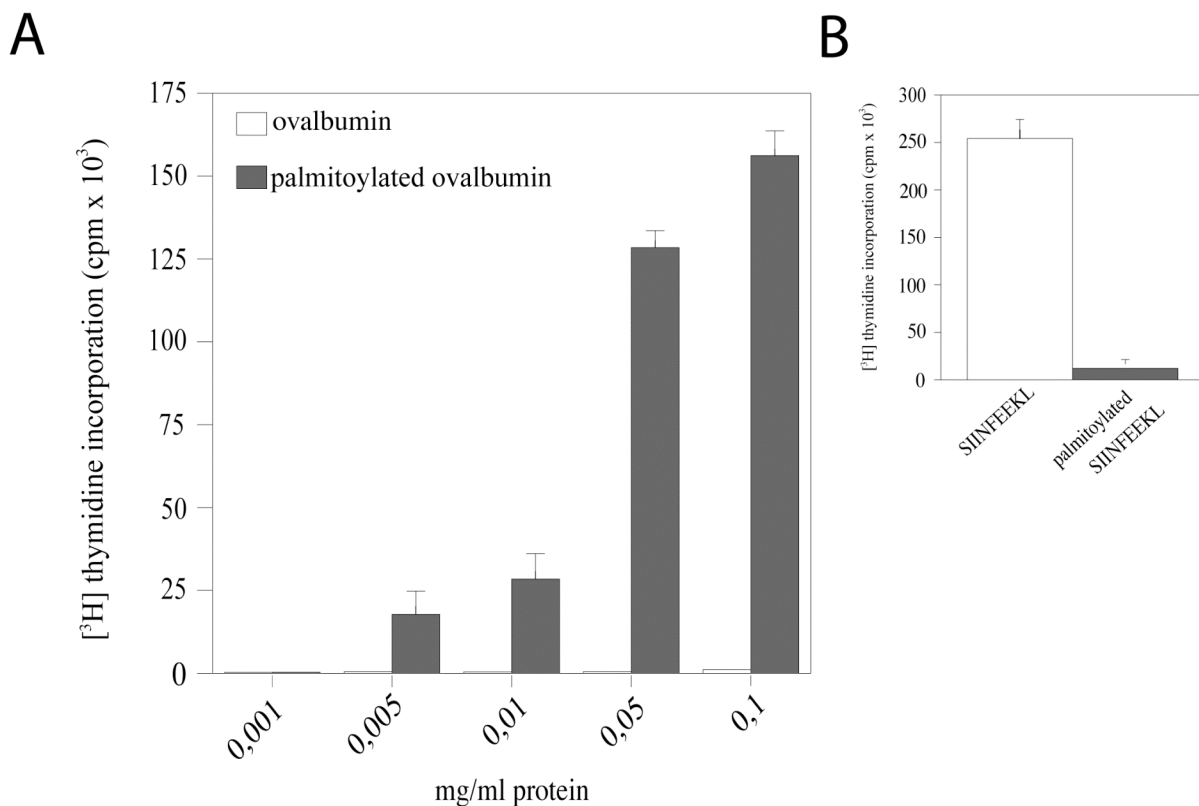


Figure 3.12. Effect of palmitoylation on cross-presentation of ovalbumin

A. Bone marrow derived macrophages were incubated for three hours with ovalbumin (*white bars*) or palmitoylated ovalbumin (*dark grey bars*). Cells were washed and T-cells specific for the SIINFEKL epitope isolated from OT-1 mice were added, and T-cell proliferation was measured as described in methods.

B. Bone marrow derived macrophages were incubated with 10 mM of SIINFEKL peptide or palmitoylated SIINFEKL peptide for 3 hours.

Together these results show that modification of ovalbumin by palmitoylation increases its ability to be internalized via macropinocytosis, be processed intracellularly and presented on MHC class I molecules to T-cells.

3.4. Discussion

Initiation of the immune response against infectious organisms occurs through the presentation of antigenic peptides by professional antigen presenting cells, such as macrophages and dendritic cells. Elimination of viruses occurs largely through the activity of cytotoxic T-cells that become activated after presentation of viral antigens on MHC class I

molecules. In recent years it is becoming clear that these MHC class I restricted antigens not only derive from endogenously synthesized proteins but that also exogenous proteins are a source for antigenic peptides presented via MHC class I (den Haan *et al.*, 2001; Ackerman *et al.*, 2005; Rodriguez *et al.*, 1999). This ‘cross-presentation’ of exogenous antigens ensures the generation of an immune response when an antigen-presenting cell is not infected by a virus itself and is thought to be important in the establishment of an immune response against tumours. In professional antigen presenting cells such as macrophages and dendritic cells, one mechanism to internalize antigens for cross-presentation occurs via macropinocytosis (Watts and Amigorena, 2000). This work shows that internalization of antigens into macrophages and dendritic cells via macropinocytosis requires the presence of cholesterol. Furthermore, modification of the model antigen ovalbumin with palmitoylation dramatically increased cross-presentation. These results suggest that modification of antigens to increase their affinity for cholesterol may be exploited to enhance the activation of CD8⁺ T-cells.

What role does cholesterol play in macropinosome formation? Phagocytosis is not affected in cholesterol-depleted macrophages (Gatfield and Pieters, 2000) and therefore cholesterol is not necessary for the membrane curvature during the process of macropinosome formation. Interestingly, in the epidermoid carcinoma cell line A431 the localization of Rac 1 is dependent on the presence of cholesterol at the plasma membrane (Grimmer *et al.*, 2002). Cholesterol-depletion of A431 cells prevents plasma membrane localization of Rac 1 upon phorbol ester treatment thereby blocking membrane ruffling and macropinosome formation. In macrophages and dendritic cells, depletion of cholesterol abolished macropinosome formation but does not affect membrane ruffling which is known to be independent of Rac 1 (West *et al.*, 2000). Therefore, cholesterol depletion may inhibit macropinosome formation by blocking plasma membrane localization of Rac1 also in professional antigen presenting cells such as macrophages and dendritic cells.

Besides a role for cholesterol in the internalization process of soluble antigens into macropinosomes it is likely that there is an additional role for cholesterol in the cytosolic translocation of these antigens to allow cross-presentation. This is based on our finding that while internalization of palmitoylated antigen was increased ~ 4-fold, presentation of ovalbumin-derived peptide was increased up to ~ 200 fold when the palmitoylated form of ovalbumin was administered. Cross-presentation of ovalbumin is dependent on the functioning of the proteasome, suggesting that translocation to the cytosol is required, but

exactly how antigens are entering the cytoplasm for processing and presentation on MHC class I molecules remains unclear.

Several models to explain MHC class I presentation of exogenous antigens have been put forward. First, antigens could be internalized through different forms of endocytosis, including phagocytosis and macropinocytosis, followed by antigen degradation within such organelles and antigenic peptide loading on recycling MHC class I molecules. Second, antigens could be transferred to the cytosol where the proteolytic activity of the proteasome would generate antigenic peptides to be translocated into the endoplasmic reticulum followed by presentation on endoplasmic reticulum resident MHC class I molecules (Ackerman *et al.*, 2004; Guermonprez and Amigorena, 2005).

Cross-presentation is blocked when antigen-presenting cells are incubated in the presence of proteasome inhibitors (Kovacsovic-Bankowski and Rock, 1995; Norbury *et al.*, 1995). As proteasomes are not known to reside within endocytic organelles, this suggests that cytosolic translocation of the antigen has to occur in order to generate the appropriate peptides. How do protein antigens acquire access from endosomal organelles such as phagosomes and macropinosomes to the cytosol? One recently proposed possibility involves the same machinery that is responsible for translocation of misfolded proteins from the endoplasmic reticulum, namely the Sec61 translocon. Interestingly, in *Dictyostelium discoideum* several resident endoplasmic reticulum proteins are necessary for phagocytosis (Muller-Taubenberger *et al.*, 2001). More recently, based on the localization of resident endoplasmic reticulum proteins within phagosomes (Gagnon *et al.*, 2002), it has been proposed that phagosomes intersect with the endoplasmic reticulum. The endoplasmic reticulum could thereby provide most of the processing and presentation components required for MHC class I restricted antigen presentation (Guermonprez *et al.*, 2003; Houde *et al.*, 2003; Ackerman *et al.*, 2003; Ackerman *et al.*, 2005).

Whether or not molecules of the Sec61 translocation complex are involved in transport of antigenic peptides generated by the proteasome as well as import of antigens into the cytosol is unknown. Interestingly, cholesterol renders the Sec61 translocon machinery unable to recognize and/or initiate translocation of nascent polypeptide chains (Nilsson *et al.*, 2001). As import of antigens from macropinosomes to the cytosol is topologically similar to retro-translocation, cholesterol may play a role in ensuring cytosolic import of substrates, while blocking the activity of the Sec61 complex for passage of nascent chains.

The requirement for cholesterol in delivering exogenous antigens to the MHC class I processing and presentation pathway could be utilized to enhance the immune response against defined antigens. As shown here, palmitoylation of ovalbumin to increase its affinity for cholesterol (Melkonian *et al.*, 1999; Zacharias *et al.*, 2002) dramatically enhanced the capacity of antigen presenting cells loaded with this modified antigen to stimulate T-cells. This is in contrast to the capacity of palmitoylated peptides that do require internalization and processing to trigger T-cell activation, which is similar to or even lower than the non-modified peptides (Andrieu *et al.*, 2000). The increase in T-cell stimulatory capacity far exceeded the enhanced internalization of palmitoylated ovalbumin, suggesting that cholesterol plays an important role in the actual translocation process.

The potential of palmitoylation to enhance the immunity against exogenous antigens could be used for vaccine development against viruses and tumours (Benmohamed *et al.*, 2000). This approach might especially be useful when using protein antigens which, compared to peptides, have a greatly increased stability *in vivo*.

3.5. References

- Ackerman, A.L., Kyritsis, C., Tampe, R., Cresswell, P. Access of soluble antigens to the endoplasmic reticulum can explain cross-presentation by dendritic cells. *Nat Immunol.* 2005, **6**: 107-13.
- Ackerman, A.L., Cresswell, P. Cellular mechanisms governing cross-presentation of exogenous antigens. *Nat Immunol.* 2004, **5**: 678-84. Review.
- Ackerman, A.L., Kyritsis, C., Tampe, R., Cresswell, P. Early phagosomes in dendritic cells form a cellular compartment sufficient for cross presentation of exogenous antigens. *Proc Natl Acad Sci U S A.* 2003, **100**: 12889-94.
- Amigorena, S., Drake, J.R., Webster, P., Mellman, I. Transient accumulation of new class II MHC molecules in a novel endocytic compartment in B lymphocytes. *Nature.* 1994, **369**: 113-20.
- Amyere, M., Mettlen, M., Van Der Smissen, P., Platek, A., Payrastra, B., Veithen, A., Courtoy, P.J. Origin, originality, functions, subversions and molecular signalling of macropinocytosis. *Int J Med. Microbiol.* 2002, **291**: 487-94. Review.
- Amyere, M., Payrastra, B., Krause, U., Van Der Smissen, P., Veithen, A., Courtoy, P.J. Constitutive macropinocytosis in oncogene-transformed fibroblasts depends on sequential permanent activation of phosphoinositide 3-kinase and phospholipase C. *Mol Biol Cell.* 2000, **11**: 3453-67.
- Andrieu, M., Loing, E., Desoutter, J.F., Connan, F., Choppin, J., Gras-Masse, H., Hanau, D., DautryVarsat, A., Guillet, J.G., Hosmalin, A. Endocytosis of an HIV-derived lipopeptide into human dendritic cells followed by class I-restricted CD8(+) T lymphocyte activation. *Eur J Immunol.* 2000, **30**: 3256-65.
- Androlewicz, M.J., Anderson, K.S., Cresswell, P. Evidence that transporters associated with antigen processing translocate a major histocompatibility complex class I-binding peptide into the endoplasmic reticulum in an ATP-dependent manner. *Proc Natl Acad Sci U S A.* 1993, **90**: 9130-4.

- Araki, N., Johnson, M.T., Swanson, J.A. A role for phosphoinositide 3-kinase in the completion of macropinocytosis and phagocytosis by macrophages. *J Cell Biol.* 1996, **135**: 1249-60.
- Banchereau, J., Steinman, R.M. Dendritic cells and the control of immunity. *Nature.* 1998, **392**: 245-52. Review.
- Baumeister, W., Walz, J., Zuhl, F., Seemuller, E. The proteasome: paradigm of a self-compartmentalizing protease. *Cell.* 1998, **92**: 367-80. Review.
- Benmohamed, L., Thomas, A., Bossus, M., Brahimi, K., Wubben, J., Gras-Masse, H., Druilhe, P. High immunogenicity in chimpanzees of peptides and lipopeptides derived from four new *Plasmodium falciparum* pre-erythrocytic molecules. *Vaccine.* 2000, **18**: 2843-55.
- Bevan, M.J. Minor H antigens introduced on H-2 different stimulating cells cross-react at the cytotoxic T cell level during in vivo priming. *J Immunol.* 1976, **117**: 2233-8.
- Bornig, H., Geyer, G. Staining of cholesterol with the fluorescent antibiotic "filipin". *Acta Histochem.* 1974, **50**:110-5.
- Boes, M., Cerny, J., Massol, R., Op den Brouw, M., Kirchhausen, T., Chen, J., Ploegh, H.L. T-cell engagement of dendritic cells rapidly rearranges MHC class II transport. *Nature.* 2002, **418**: 983-8.
- Brossart, P., Bevan, M.J. Presentation of exogenous protein antigens on major histocompatibility complex class I molecules by dendritic cells: pathway of presentation and regulation by cytokines. *Blood.* 1997, **90**: 1594-9.
- Cardelli, J. Phagocytosis and macropinocytosis in *Dictyostelium*: phosphoinositide-based processes, biochemically distinct. *Traffic.* 2001, **2**: 311-20. Review.
- Cella, M., Engering, A., Pinet, V., Pieters, J., Lanzavecchia, A. Inflammatory stimuli induce accumulation of MHC class II complexes on dendritic cells. *Nature.* 1997, **388**: 782-7.
- Cresswell, P. Invariant chain structure and MHC class II function. *Cell.* 1996, **84**: 505-7. Review.
- den Haan, J.M., Bevan, M.J. Antigen presentation to CD8+ T cells: cross-priming in infectious diseases. *Curr Opin Immunol.* 2001, **13**: 437-41. Review.
- Dharmawardhane, S., Schurmann, A., Sells, M.A., Chernoff, J., Schmid, S.L., Bokoch, G.M. Regulation of macropinocytosis by p21-activated kinase-1. *Mol Biol Cell.* 2000, **11**: 3341-52.
- Drabikowski, W., Lagwinska, E., Sarzala, M.G. Filipin as a fluorescent probe for the location of cholesterol in the membranes of fragmented sarcoplasmic reticulum. *Biochim Biophys Acta.* 1973, **291**:61-70.
- Gagnon, E., Duclos, S., Rondeau, C., Chevet, E., Cameron, P.H., Steele-Mortimer, O., Paiement, J., Bergeron, J.J., Desjardins, M. Endoplasmic reticulum-mediated phagocytosis is a mechanism of entry into macrophages. *Cell.* 2002, **110**: 119-31.
- Gatfield, J., Pieters, J. Essential role for cholesterol in entry of mycobacteria into macrophages. *Science.* 2000, **288**: 1647-50.
- Germain, R.N. MHC-dependent antigen processing and peptide presentation: providing ligands for T lymphocyte activation. *Cell.* 1994, **76**: 287-99. Review.
- Grimmer, S., van Deurs, B., Sandvig, K. Membrane ruffling and macropinocytosis in A431 cells require cholesterol. *J Cell Sci.* 2002, **115**: 2953-62.
- Guermonprez, P., Amigorena, S. Pathways for antigen cross presentation. *Springer Semin Immunopathol.* 2005, **26**: 257-71.

- Guermónprez, P., Saveanu, L., Kleijmeer, M., Davoust, J., Van Endert, P., Amigorena, S. ER-phagosome fusion defines an MHC class I cross-presentation compartment in dendritic cells. *Nature*. 2003, **425**: 397-402.
- Heath, W.R., Carbone, F.R. Cross-presentation in viral immunity and self-tolerance. *Nat Rev Immunol*. 2001, **1**: 126-34. Review.
- Hewlett, L.J., Prescott, A.R., Watts, C. The coated pit and macropinocytic pathways serve distinct endosome populations. *J Cell Biol*. 1994, **124**: 689-703.
- Houde, M., Bertholet, S., Gagnon, E., Brunet, S., Goyette, G., Laplante, A., Princiotta, M.F., Thibault, P., Sacks, D., Desjardins, M. Phagosomes are competent organelles for antigen cross-presentation. *Nature*. 2003, **425**: 402-6.
- Klein, U., Gimpl, G., Fahrenholz, F. Alteration of the myometrial plasma membrane cholesterol content with beta-cyclodextrin modulates the binding affinity of the oxytocin receptor. *Biochemistry*. 1995, **34**: 13784-93.
- Koopmann, J.O., Hammerling, G.J., Momburg, F. Generation, intracellular transport and loading of peptides associated with MHC class I molecules. *Curr Opin Immunol*. 1997, **9**: 80-8. Review.
- Kovacsovics-Bankowski, M., Rock, K.L. A phagosome-to-cytosol pathway for exogenous antigens presented on MHC class I molecules. *Science*. 1995, **267**: 243-6.
- Melkonian, K.A., Ostermeyer, A.G., Chen, J.Z., Roth, M.G., Brown, D.A. Role of lipid modifications in targeting proteins to detergent-resistant membrane rafts. Many raft proteins are acylated, while few are prenylated. *J Biol Chem*. 1999, **274**: 3910-7.
- Miki, H., Yamaguchi, H., Suetsugu, S., Takenawa, T. IRSp53 is an essential intermediate between Rac and WAVE in the regulation of membrane ruffling. *Nature*. 2000, **408**: 732-5.
- Miki, H., Suetsugu, S., Takenawa, T. WAVE, a novel WASP-family protein involved in actin reorganization induced by Rac. *EMBO J*. 1998, **17**: 6932-41.
- Monaco, J.J. Pathways for the processing and presentation of antigens to T cells. *J Leukoc Biol*. 1995, **57**: 543-7. Review.
- Muller-Taubenberger A, Lupas AN, Li H, Ecke M, Simmeth E, Gerisch G. Calreticulin and calnexin in the endoplasmic reticulum are important for phagocytosis. *EMBO J*. 2001, **20**: 6772-82.
- Nilsson, I., Ohvo-Rekila, H., Slotte, J.P., Johnson, A.E., von Heijne, G. Inhibition of protein translocation across the endoplasmic reticulum membrane by sterols. *J Biol Chem*. 2001, **276**: 41748-54.
- Norbury, C.C., Chambers, B.J., Prescott, A.R., Ljunggren, H.G., Watts, C. Constitutive macropinocytosis allows TAP-dependent major histocompatibility complex class I presentation of exogenous soluble antigen by bone marrow-derived dendritic cells. *Eur J Immunol*. 1997, **27**: 280-8.
- Norbury, C.C., Hewlett, L.J., Prescott, A.R., Shastri, N., Watts, C. Class I MHC presentation of exogenous soluble antigen via macropinocytosis in bone marrow macrophages. *Immunity*. 1995, **3**: 783-91.
- Pierre, P., Turley, S.J., Gatti, E., Hull, M., Meltzer, J., Mirza, A., Inaba, K., Steinman, R.M., Mellman, I. Developmental regulation of MHC class II transport in mouse dendritic cells. *Nature*. 1997, **388**: 787-92.
- Pieters, J. MHC class II compartments: specialized organelles of the endocytic pathway in antigen presenting cells. *Biol Chem*. 1997, **378**: 751-8. Review.
- Racoosin, E.L., Swanson, J.A. Macropinosome maturation and fusion with tubular lysosomes in macrophages. *J Cell Biol*. 1993, **121**: 1011-20.

- Reis e Sousa, C., Germain, R.N. Major histocompatibility complex class I presentation of peptides derived from soluble exogenous antigen by a subset of cells engaged in phagocytosis. *J Exp Med.* 1995, **182**: 841-51.
- Ridley, A.J., Paterson, H.F., Johnston, C.L., Diekmann, D., Hall, A. The small GTP-binding protein rac regulates growth factor-induced membrane ruffling. *Cell.* 1992, **70**: 401-10.
- Rock, K.L., Gamble, S., Rothstein, L. Presentation of exogenous antigen with class I major histocompatibility complex molecules. *Science.* 1990, **249**: 918-21.
- Rodriguez A, Regnault A, Kleijmeer M, Ricciardi-Castagnoli P, Amigorena S. Selective transport of internalized antigens to the cytosol for MHC class I presentation in dendritic cells. *Nat Cell Biol.* 1999, **1**: 362-8.
- Rupper, A., Lee, K., Knecht, D., Cardelli, J. Sequential activities of phosphoinositide 3-kinase, PKB/Akt, and Rab7 during macropinosome formation in Dictyostelium. *Mol Biol Cell.* 2001, **12**: 2813-24.
- Sallusto, F., Cella, M., Danieli, C., Lanzavecchia, A. Dendritic cells use macropinocytosis and the mannose receptor to concentrate macromolecules in the major histocompatibility complex class II compartment: downregulation by cytokines and bacterial products. *J Exp Med.* 1995, **182**: 389-400.
- Simons, M., Keller, P., DeStrooper, B., Beyreuther, K., Dotti, C.G., Simons, K. Cholesterol depletion inhibits the generation of beta-amyloid in hippocampal neurons. *Proc Natl Acad Sci U S A.* 1998, **95**: 6460-4.
- Spies, T., Bresnahan, M., Bahram, S., Arnold, D., Blanck, G., Mellins, E., Pious, D., DeMars, R. A gene in the human major histocompatibility complex class II region controlling the class I antigen presentation pathway. *Nature.* 1990, **348**: 744-7.
- Steinman, R.M., Swanson, J. The endocytic activity of dendritic cells. *J Exp Med.* 1995, **182**: 283-8. Review.
- Swanson, J.A. Phorbol esters stimulate macropinocytosis and solute flow through macrophages. *J Cell Sci.* 1989, **94**: 135-42.
- Townsend, A., Ohlen, C., Bastin, J., Ljunggren, H.G., Foster, L., Karre, K. Association of class I major histocompatibility heavy and light chains induced by viral peptides. *Nature.* 1989, **340**: 443-8.
- Trombetta, E.S., Mellman, I. Cell biology of antigen processing in vitro and in vivo. *Annu Rev Immunol.* 2005, **23**: 975-1028.
- Tulp, A., Verwoerd, D., Dobberstein, B., Ploegh, H.L., Pieters, J. Isolation and characterization of the intracellular MHC class II compartment. *Nature.* 1994, **369**: 120-6.
- Watts, C, Amigorena, S. Antigen traffic pathways in dendritic cells. *Traffic.* 2000, **1**: 312-7. Review.
- Watts, C., Powis, S. Pathways of antigen processing and presentation. *Rev Immunogenet.* 1999, **1**: 60-74. Review.
- Watts, C. Inside the gearbox of the dendritic cell. *Nature.* 1997, **388**: 724-5.
- West, M.A., Prescott, A.R., Eskelinen, E.L., Ridley, A.J., Watts, C. Rac is required for constitutive macropinocytosis by dendritic cells but does not control its downregulation. *Curr Biol.* 2000, **10**: 839-48.
- West, M.A., Lucocq, J.M., Watts, C. Antigen processing and class II MHC peptide-loading compartments in human B-lymphoblastoid cells. *Nature.* 1994, **369**: 147-51.
- West, M.A., Bretscher, M.S., Watts, C. Distinct endocytotic pathways in epidermal growth factor-stimulated human carcinoma A431 cells. *J Cell Biol.* 1989, **109**: 2731-9.

Wolven, A., Okamura, H., Rosenblatt, Y., Resh, M.D. Palmitoylation of p59fyn is reversible and sufficient for plasma membrane association. *Mol Biol Cell*. 1997, **8**: 1159-73.

Zacharias, D.A., Violin, J.D., Newton, A.C., Tsien, R.Y.: Partitioning of Lipid-Modified Monomeric GFPs into Membrane Microdomain of Live Cells. *Science* 2002, **296**: 913-916.

- Chapter 4 -

Lipid Modification of Antigens to improve Cross- presentation

Imke Albrecht ¹, Oliver Schwardt ², Beat Ernst ², Reto Schumacher ³, Giulio Spagnoli ³ and Jean Pieters ¹

Biozentrum¹, Institute of Pharmacology, Pharmazentrum²,
and Department of Surgery ³
University of Basel, CH-4056 Basel, Switzerland

unpublished

4.1. Abstract

Palmitoylation of ovalbumin increases the delivery of this protein into the MHC class I presentation pathway in antigen-presenting cells, thereby improving the ability of these cells to activate CD8⁺ T-cells (Chapter 3). To understand the role of palmitoylation in cross-presentation, the effect of different lipid modifications was investigated. In this chapter experiments are described to chemically modify proteins with lipid moieties. Furthermore it was investigated whether palmitoylation can be used as a general method to improve cross-presentation of soluble proteins to possibly lead to a better vaccine development against viruses and tumours.

4.2. Introduction

The establishment of immunity against many intracellular pathogens and cancer cells is dependent on the generation of a cellular immune response. In particular, it requires the induction of MHC class I restricted cytotoxic CD8⁺ T-cells (CTLs). As activation of naïve CTLs can only be performed by professional antigen-presenting cells (APCs) (Bernhard *et al.*, 2002), vaccinations for viral infections and cancer immunotherapies must target these professional antigen-presenting cells to be successful.

Inefficient targeting to professional APCs might be one reason why immunization with small peptides of 8-11 residues, which do not need further processing for association with the MHC class I (Wiesmüller *et al.*, 1995) are poor in the induction of CTLs (Deres *et al.*, 1989; Bourgault *et al.*, 1994; van Endert *et al.*, 2001). Therefore different transport techniques such as liposomes, bacteria or virosomes were used which allowed the direct transport of exogenous materials into the cytoplasm of the APCs (Bungener *et al.*, 2002; Schoen *et al.*, 2004; Daemen *et al.*, 2005).

The delivery of antigens to the MHC class I processing pathway can also be achieved via a physiological route, as professional APCs possess the unique ability to cross-present exogenous antigens. Methods, which would allow the specific targeting of antigens into the cross-presentation pathway could be therefore attractive for new vaccine design.

Using palmitoylated soluble ovalbumin, we could show that internalization of the protein in macrophages as well as subsequent cross-presentation was strongly enhanced (Chapter 3). Palmitoylation is a posttranslational modification, which is described to promote the

association of proteins with cholesterol-enriched microdomains, the so-called lipid rafts (Brown and Rose, 1992; Simons and Ikonen, 1997; Wolven *et al.*, 1997; Melkonian *et al.*, 1999; Zacharias *et al.*, 2002). Given the cholesterol dependence of cross-presentation of soluble antigens (chapter 3), targeting of antigens to rafts might therefore facilitate cross-presentation. To further test this hypothesis, the effect of other lipid moieties on cross-presentation was decided to be studied. Furthermore we investigated whether palmitoylation of soluble proteins can be used as a general means to provide antigens for the cross-presentation pathway.

4.3. Results

4.3.1. Synthesis of activated lipids for protein modification

For studying the role of lipid modification on cross-presentation, different lipids (summarized in table 4.1.) were chosen on the basis of their ability to promote or to inhibit the association with cholesterol-enriched microdomains (Wolven *et al.*, 1997; Galbiati *et al.*, 1999; Melkonian *et al.*, 1999; Zacharias *et al.*, 2002).

Introduction of the lipid modification into the proteins was performed chemically by reaction of the protein with N-hydroxysuccinimide (NHS) activated lipids (*Chapter 3, figure 3.9*). NHS esters containing compounds are highly reactive towards amine nucleophiles, and upon release of the NHS leaving group, generate acylated products. In protein molecules, NHS-ester groups primarily react with the α -amine at the N-terminus and the ϵ -amines of lysine side chains. In a first step, the activated NHS lipids were synthesized.

4.3.1.1. Activation of farnesol with succinimidyl carbonate (SC)

Activation of *trans, trans*-farnesol was performed according to a method previously used for the derivatization of polyethylene glycol (PEG) (Miron and Wilchek, 1993). Like PEG, farnesol is an alcohol containing no carboxyl group for attachment of a NHS group. However reaction of the hydroxyl group with an anhydride compound allows the introduction of a carboxyl group. In the method of Miron and Wilchek, the reaction was performed with the anhydride N',N'-disuccinimidyl carbonate (DSC). DSC has the advantage that the carboxyl group, which is introduced is already coupled to a NHS group.

The synthesis of succinimidyl carbonate (SC) farnesol was performed as summarized in figure 4.1. Farnesol was incubated with disuccinimidyl carbonate in the presence of the catalyst,

4-(dimethylamino)-pyridine (DMAP), overnight at room temperature and the generated SC-farnesol was purified afterwards by silica gel chromatography as described in materials and methods.

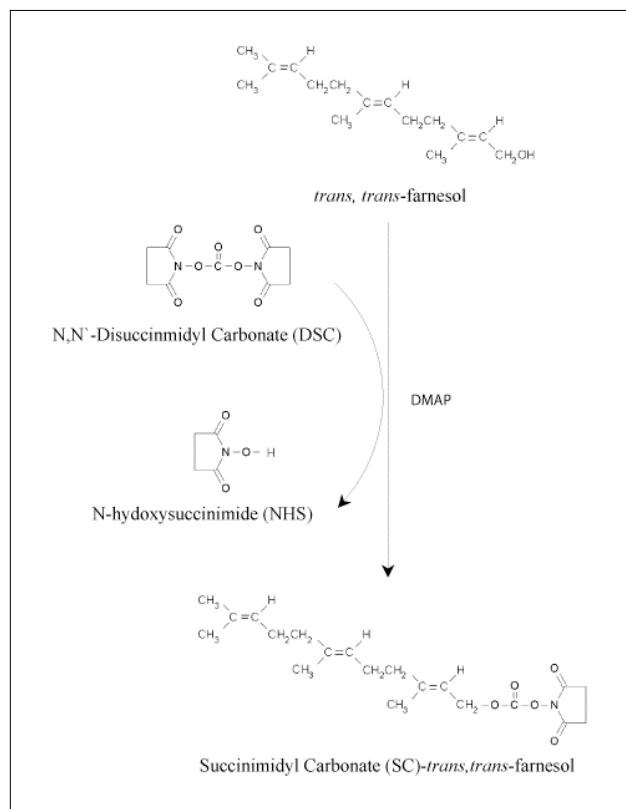


Figure 4.1. Activation of farnesol with succinimidyl carbonate (SC) – reaction scheme

The identity of succinimidyl carbonate derivative of farnesol was confirmed by nuclear magnetic resonance spectroscopy (NMR) analysis. Each peak in the ^1H - and ^{13}C -NMR spectrum (figure 4.2.) could be assigned to the corresponding H or C-atom of the product, showing that SC-farnesol was successfully synthesized.

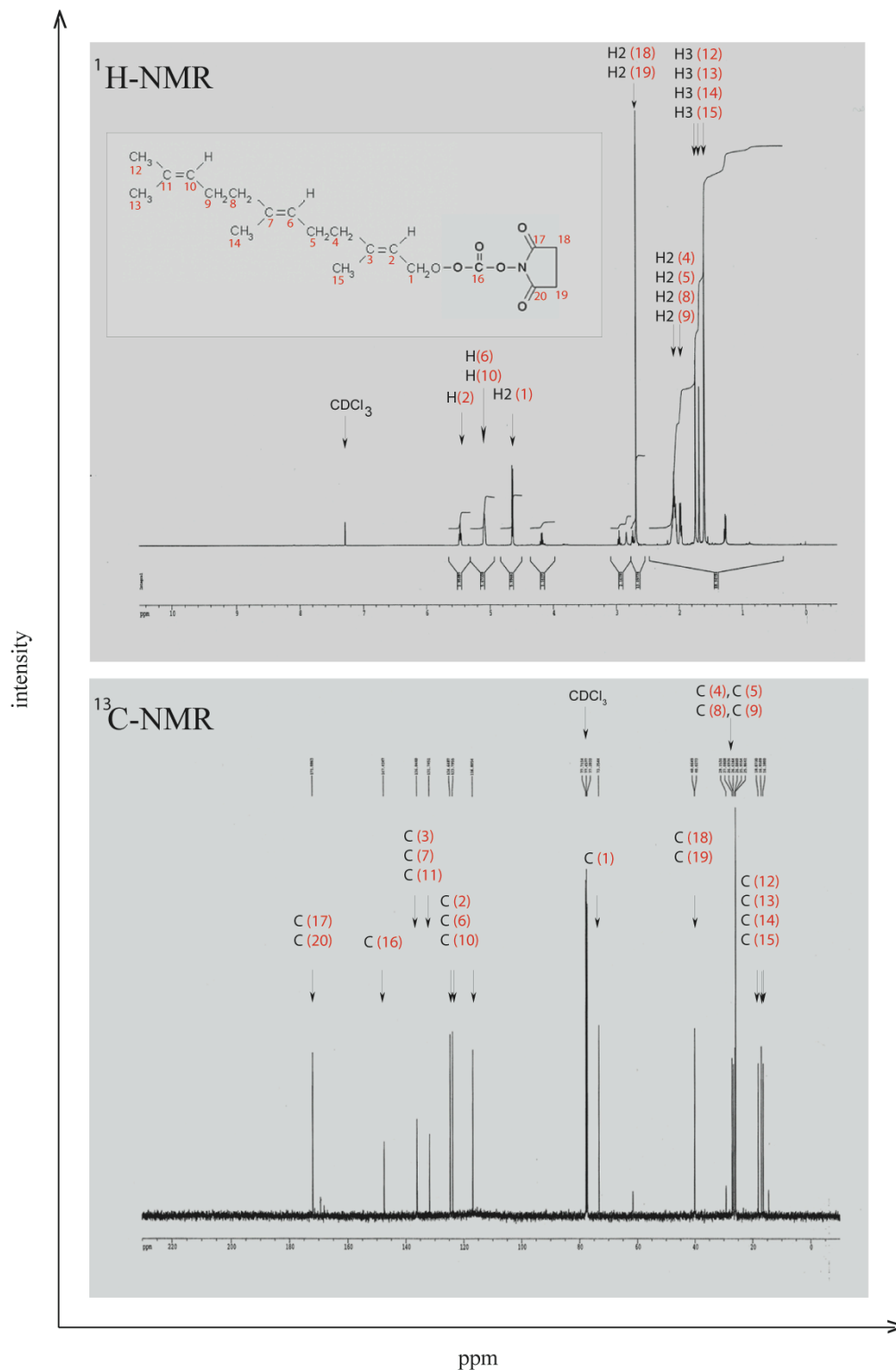


Figure 4.2. Synthesis of succinimidyl carbonate (SC)-farnesol – NMR-analysis

Spectra were recorded on a Bruker Advance DMX-500 (500Hz) spectrometer. Assignment of the ¹H- and ¹³C-NMR spectra was performed with the help of 2D methods (COSY and HSQC). Chemical shifts are expressed in ppm.

4.3.1.2. Synthesis of lipid N-hydroxysuccinimide (NHS) ester

Synthesis of the NHS esters of saturated and unsaturated fatty acids (listed in table 4.1.) was performed as previously described (Huang *et al.*, 1980). To that end, the fatty acids were incubated with N-hydroxysuccinimide (NHS) in the presence of the catalyst dicyclohexyl carbodiimide (DCC) overnight at room temperature (*figure 4.3.*).

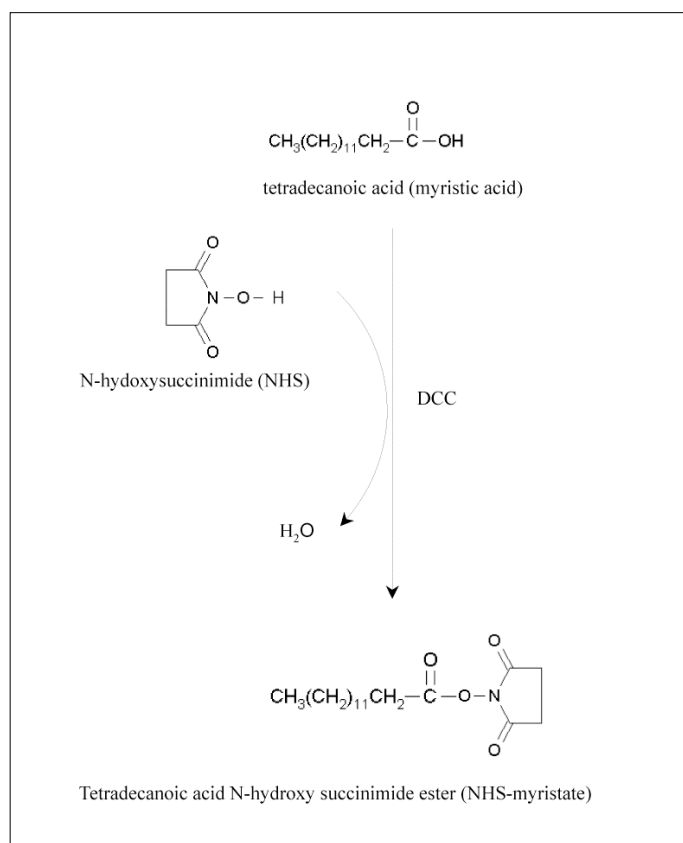


Figure 4.3. Synthesis of NHS ester of myristic acid – reaction scheme

The NHS ester of stearic acid and myristic acid were further purified by re-crystallization as described in materials and methods. As unsaturated fatty acids are very sensitive towards light and oxygen, re-crystallization of these acids was not performed to avoid saturation.

Coupling of the NHS group to the lipids was analyzed by thin layer chromatography (TLC) combined with a staining for NHS-groups. As shown in figure 4.4. for the modification of myristic acid, coupling of the NHS-group to the fatty acid was successful as indicated by the positive NHS stain of the modified fatty acid.

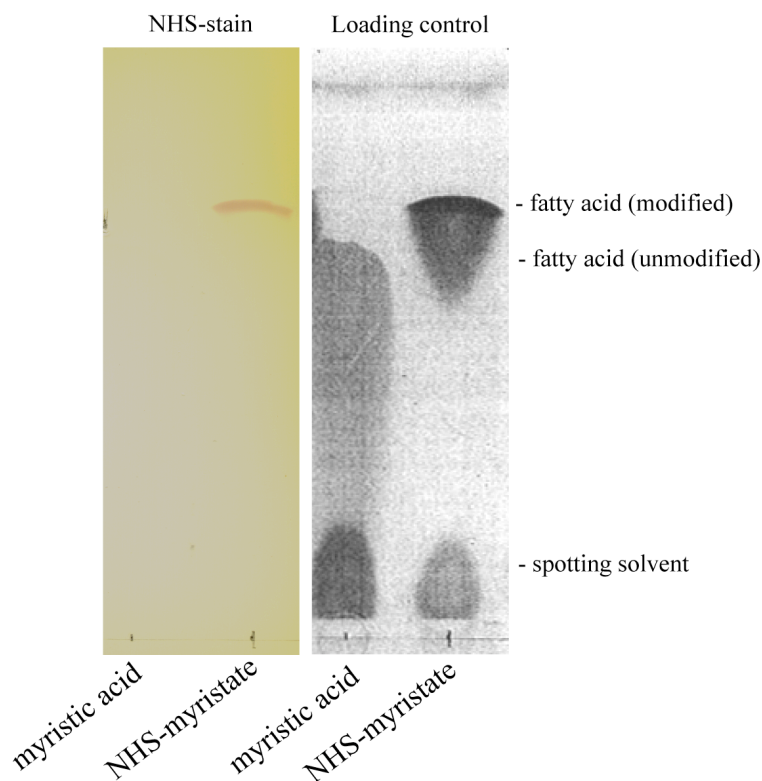


Figure 4.4. Thin layer chromatography analysis.

Thin layer chromatography (TLC) of myristic acid and NHS-myristate. Samples were separated with chloroform /petrol ether mixture (8:2). Staining of the NHS group (*left panel*) was performed as described in material and methods, for loading control the sample were visualized with iodine (*right panel*).

In conclusion, as listed in table 4.1., for all fatty acids the corresponding NHS esters could be successfully synthesized. Subsequently NHS activated fatty acids were used for modification of peptides and proteins.

4.3.2. Coupling of activated lipids to peptides and proteins

To test the coupling efficiency, the activated lipids were incubated either with a short peptide containing a primary amino group (NH₂-GSGSGSK[Acetyl]) or with horseradish peroxidase as described in materials and methods. Successful coupling was assessed by mass spectrometry by detection of the appropriate shift in the molecular mass, as shown in figure 4.5. for myristoylation of GSGSGSK(Acetyl).

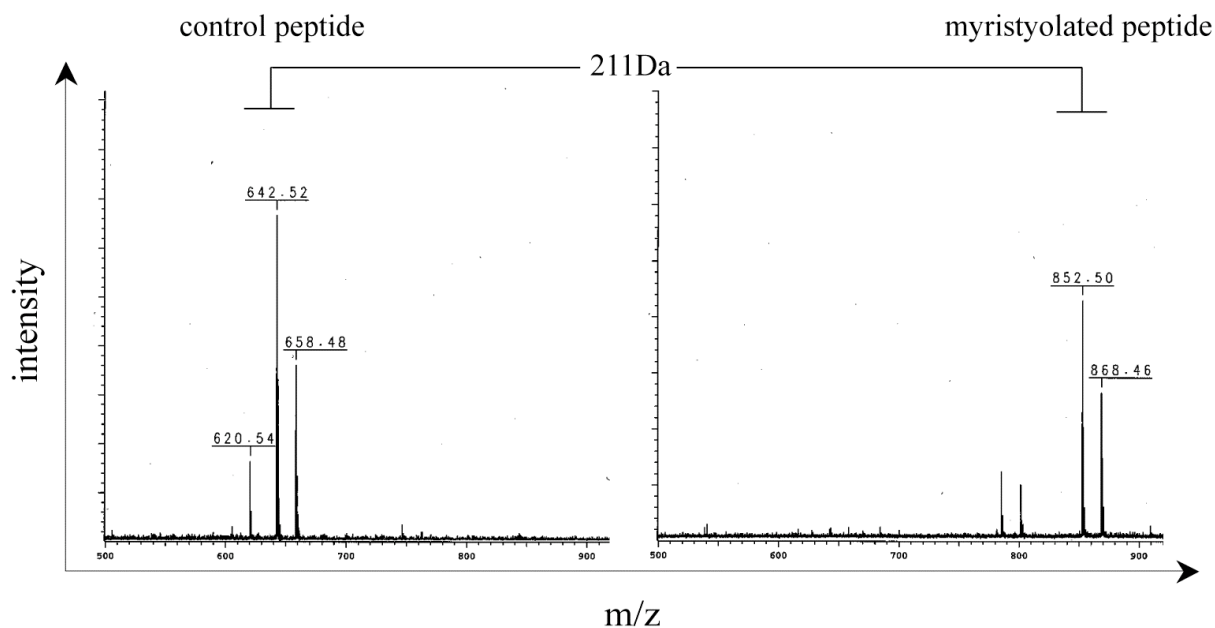


Figure 4.5. Mass spectrometry analysis

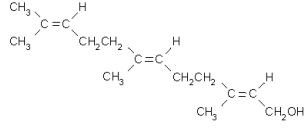
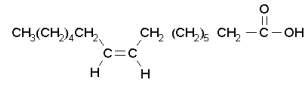
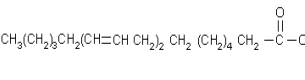
Mass spectrometry analysis (MALDI-TOF) of control and modified $\text{NH}_2\text{-GSGSGSK[Acetyl]}$ peptide. Mass shift of 211 Da indicates the attachment of one myristic acid to the peptide. The three peaks seen in the spectra of the control peptide represent the peptide (620 kDa), its sodium (642 kDa) and its potassium salt (658 kDa). In the case of the modified peptide only the two latter ones were detected.

The results for all coupling reactions are summarized in table 4.1. Saturated fatty acids (myristic and stearic acid) could be coupled to peptides giving raise to the desired product with a yield of 50% as quantified by mass-spectrometry (electron spray ionization). However, modification of horseradish peroxidase with the saturated fatty acids was not successful for unknown reasons.

Whereas modification of peptides with unsaturated fatty acids was achieved, unsaturated fatty acids were unstable and became oxidized over time resulting in the accumulation of by-products. Therefore, it was not possible to obtain protein modified with unsaturated fatty acids for further investigations.

Coupling of SC-farnesol to the peptide or protein resulted in the formation of a product with a three fold lower molecular mass than expected. Although the SC-farnesol, according to NMR analysis, was pure, it cannot be excluded that the lower mass shift resulted from the reaction with contaminations still present in the SC-farnesol fraction.

Table 4.1. Summary of synthesis of activated lipids

Substrate	Synthesis of NHS ester derivatives	Coupling to peptide NH ₂ -GSGSGSK(Acetyl) (analyzed by Mass spec)	Coupling to HRP (analyzed by Mass spec)
<p><i>trans, trans</i>-Farnesol</p> 	Yes	<p>expected mass shift: Δ250 Da measured mass shift: Δ65-72Da</p>	<p>expected a mass shift: Δ250 Da measured mass shift: Δ 65-72Da</p>
<p>Tetradecanoic acid (myristic acid)</p> $\text{CH}_3(\text{CH}_2)_{11}\text{CH}_2-\overset{\text{O}}{\parallel}{\text{C}}-\text{OH}$	Yes	<p>expected mass shift: Δ211 Da measured mass shift: Δ211 Da</p>	no mass shift
<p><i>cis</i>-9-Hexadecanoic acid (palmitoleic acid)</p> 	Yes	<p>expected mass shift: Δ237 Da measured mass shift: Δ237 Da (NHS-substrate was not stable)</p>	NHS-substrate was not stable
<p>Octadecanoic acid (stearic acid)</p> $\text{CH}_3(\text{CH}_2)_{15}\text{CH}_2-\overset{\text{O}}{\parallel}{\text{C}}-\text{OH}$	Yes	<p>expected mass shift: Δ267 Da measured mass shift: Δ267 Da</p>	no mass shift
<p><i>cis, cis</i>-9,12-Octadecanoic acid (linoleic acid)</p> 	Yes	<p>expected mass shift: Δ263 Da measured mass shift: Δ263 Da (NHS-substrate was not stable)</p>	NHS-substrate was not stable

In summary, the chemical modification of proteins with lipid tails was only partially. Thus, the initial question about the influence of different lipid modifications on cross-presentation could not be further addressed using this approach.

4.3.3. Palmitoylation of exogenous proteins: A general method to improve cross-presentation?

As cross-presentation of soluble ovalbumin is significantly improved by palmitoylation (described in Chapter 3), the question was raised whether palmitoylation could be used as a general method to increase cross-presentation of soluble proteins.

To address this question, cross-presentation of the influenza virus matrix protein (IM) in a human system was studied. In humans, several cytotoxic T-cells clones specific for epitopes of this viral protein have been identified (Gotch *et al.*, 1987; Vitiello *et al.*, 1996; Tamura *et al.*, 1998; Tourdot *et al.*, 2001), among them the HLA-A2-restricted immunodominant 58-GILGFVTLV-66 (IM₅₈₋₆₆) peptide. Furthermore, it was shown that the influenza matrix protein is cross-presented by dendritic cells, which have acquired the antigen from apoptotic and necrotic virus-infected cells (Larsson *et al.*, 2001).

4.3.3.1. Expression and purification of influenza matrix protein

To study cross-presentation, a truncated form of the influenza virus matrix protein (referred to IM 1-164) containing a mutated nuclear localization sequence (NLS), was expressed in *E. coli* and purified as described in materials and methods (Arzt *et al.*, 2004). The mutation in the NLS region (95-101aa) significantly increases the protein solubility (Elster *et al.*, 1997). As the mutated region does not flank the IM₅₈₋₆₆ epitope, it should not influence the presentation of this epitope used for detection of cross-presentation of IM (1-164).

4.3.3.2. Cross-presentation of unmodified influenza matrix protein

Cross-presentation of IM (1-164) was measured as follows. Immature dendritic cells generated from peripheral blood monocytes (PBMC) of an HLA-A0201 positive healthy donor were pulsed with IM (1-164) or control antigens for 24 hours in the presence of LPS. After removal of non-internalized and non-bound antigens, T-cells (CD4⁺ and CD8⁺) isolated from peripheral blood of the same donor were added and co-cultured for seven days. The induction of IM₅₈₋₆₆ specific CD8⁺ T-cells within the culture was determined by flow cytometry using HLA-A0201/IM₅₈₋₆₆ PE-tetramer binding and anti-CD8 staining.

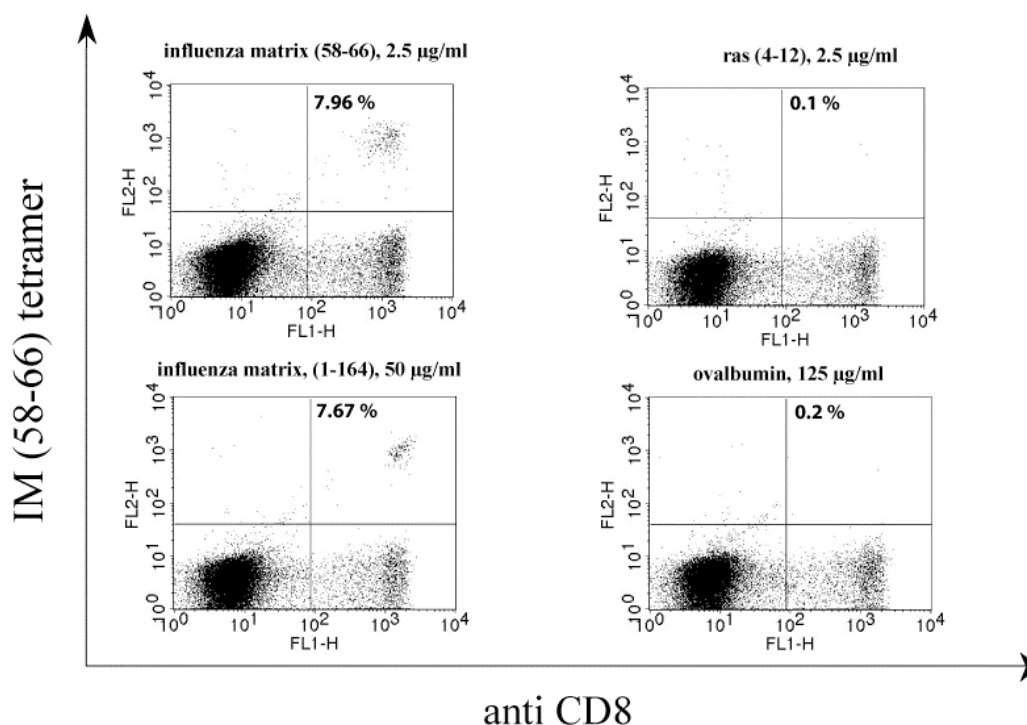


Figure 4.6. Cross-presentation analysis of influenza matrix protein derived antigens.

Immature dendritic cells derived from PBMC from a healthy donor were incubated with 2.5 µg/ml IM (58-66) [GILGFVTLTV], 2.5 µg/ml ras (4-12), 50 µg/ml purified IM (1-164) or 125 µg/ml ovalbumin for 24 hours in the presence of LPS. After removal of the exogenous antigens, CD14⁻ cells (CD4⁺ and CD8⁺ T-cells) purified from the PB of a healthy donor were added and co-cultured with the antigen pulsed dendritic cells for further 7 days. At day 4, 5, and 6 Il-2 (10 U/ml) was added. The percentages of IM (58-66) specific CD8⁺ T-cells in the cultured cell population were quantified by flow cytometry using HLA-A0201/IM₅₈₋₆₆ PE tetramer (y-axis) and FITC labeled anti-CD8 antibody (x-axis). Results from one representative experiment are shown.

As shown in figure 4.6., no HLA-A0201/IM₅₈₋₆₆ tetramer specific positive CD8⁺ T-cells could be detected when dendritic cells were pulsed with the control protein ovalbumin (*right panel, lower row*), or with the control peptide ras (*right panel, upper row*). In contrast, incubation of the dendritic cells with the IM (1-164) led to expansion of the HLA-A0201/IM₅₈₋₆₆ tetramer positive cells within the CD8⁺ T-cell population. Around 8% of all CD8⁺ T cells show specific tetramer binding (*left panel, lower row*). Pulsing dendritic cells with an equimolar amount of IM (58-66) peptides, which can directly bind to surface MHC class I and do not need intracellular processing, resulted in a similar expansion of HLA-A0201/IM₅₈₋₆₆ tetramer positive CD8⁺ T-cells (*left panel, upper row*). These results show that the soluble IM (1-164) protein can be efficiently cross-presented.

4.3.3.3. Palmitoylation of influenza matrix protein

To study the influence of palmitoylation on the cross-presentation of IM (1-164), palmitoylation of IM (1-164) was performed as described in materials and methods. The degree of palmitoylation was determined by mass spectrometry analysis. As seen in figure 4.7.B, a mass shift of $\sim 1,9$ kDa was detected comparing control and palmitoylated IM (1-164), which corresponds to the attachment of up to eight palmitic acid moieties.

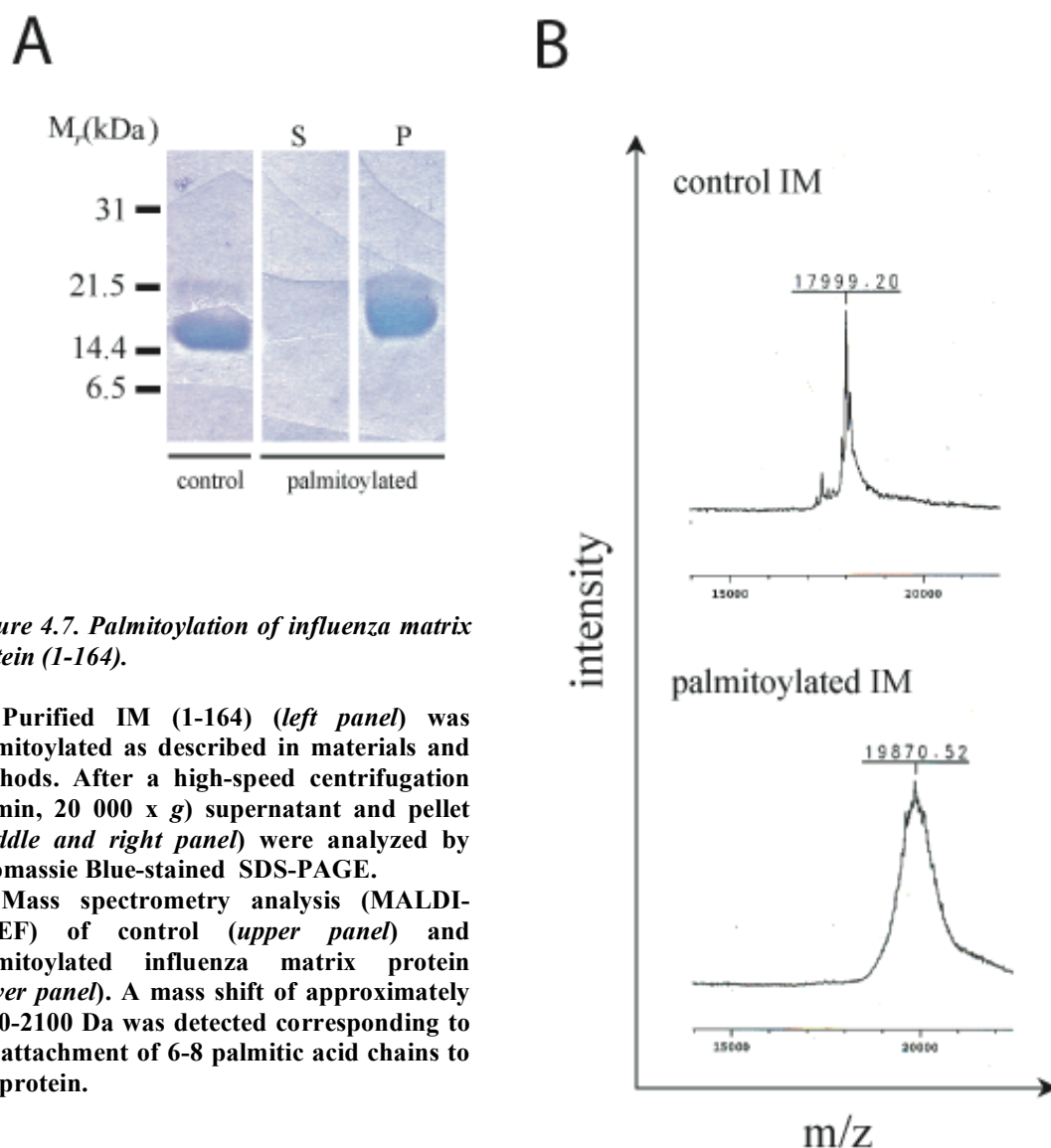


Figure 4.7. Palmitoylation of influenza matrix protein (1-164).

A. Purified IM (1-164) (*left panel*) was palmitoylated as described in materials and methods. After a high-speed centrifugation (5 min, 20 000 x g) supernatant and pellet (*middle and right panel*) were analyzed by Coomassie Blue-stained SDS-PAGE.

B. Mass spectrometry analysis (MALDI-TOEF) of control (*upper panel*) and palmitoylated influenza matrix protein (*lower panel*). A mass shift of approximately 1600-2100 Da was detected corresponding to the attachment of 6-8 palmitic acid chains to the protein.

However, during palmitoylation IM (1-164) precipitated and no soluble protein could be recovered after a high-speed centrifugation (20 000 x g, 5 min) in the supernatant (*figure 4.7.A.*). As it was not possible to obtain soluble palmitoylated IM (1-164), no further investigations could be performed.

Analysis of a further antigen, the melanoma-associated antigen MART-1, could also not be completed as palmitoylation of recombinant expressed MART-1 resulted in an insoluble protein.

In summary, improving cross-presentation of a soluble protein by palmitoylation is not suitable for all proteins as palmitoylation increases the hydrophobicity of proteins, which can affect protein solubility.

4.4. Discussion

Activated fatty acids were synthesized in order to modify ovalbumin with different lipid tails via a chemical approach. Although the synthesis of the NHS-lipids was successful, it was not possible to obtain lipidated protein for further analysis. This was due to inefficient coupling of the lipids to the proteins as well as to the instability of some of the lipids and undesired side reactions during the coupling reaction.

Further investigations may overcome these technical difficulties by considering an alternative activation of the lipids or a different coupling strategy. Although this may prove exceeding technically challenging, the potential benefits of improved immunization protocols may justify time and effort spent.

What role does palmitoylation play in cross-presentation? Peptide epitopes covalently linked to palmitic acid moieties have been used for some time for immunization against intracellular infectious agents. Compared to non-modified peptides, these lipopeptides have been shown to be highly immunogenic both in animal models as well as in humans inducing CTL immune responses (Deres *et al.*, 1989; Livingston *et al.*, 1997; Vitiello *et al.*, 1995; Mortara *et al.*, 1999; Pialoux *et al.*, 2001). Less is known about their mode of action. They were originally designed to mediate direct entry into the cytoplasm through the plasma membrane (Martinon *et al.*, 1992; Thiam *et al.*, 1999). But now it is becoming evident, that some are endocytosed by the APC prior to their transport into the cytoplasm, which nevertheless could occur passively mediated by the palmitic acid moieties (Andrieu *et al.*, 2000; Andrieu *et al.*, 2003). Together these reports suggest a possible role of palmitic acid for the delivery of antigens into the MHC class I processing pathway. Thereby the mode of action of palmitic acid moieties in peptides and proteins may be different, as latter ones cannot diffuse through membranes.

Whether in our case the action of the lipid tail helps to concentrate the protein at the plasma membrane where it can be taken up more easily or whether targeting to specific membrane domains can explain the improved cross-presentation needs further investigations.

Targeting of exogenous antigens into the MHC class I processing pathway, an aim of many vaccines, is necessary for the development of an efficient immune response against viruses and cancer. Given the enhanced T-cell stimulation when palmitoylated antigens were used as described in Chapter 3, palmitoylation might offer a way to improve delivery of soluble protein antigens into the MHC class I pathway, which was so far only applied to peptides. The use of intact proteins would offer several advantages over peptide for immunization. Proteins are normally more stable than peptides and contain several T-cell epitopes allowing activation of a broader range of T-cells simultaneously.

Similar to the use of peptides, lipid modification of proteins could be performed chemically by coupling palmitic acid residues to primary amino groups of the protein as we and others have shown (Huang *et al.*, 1980). In contrast to enzymatic modification, chemical modification has the advantage that a consensus sequence is not needed and can therefore, in principle, be performed independent of a primary sequence. However, attachment of a hydrophobic tail such as palmitic acid can severely affect protein solubility. Whereas proteins such as ovalbumin and horseradish peroxidase remained soluble after palmitoylation perhaps due to their high degree of glycosylation, modification of the influenza matrix protein and the melanoma-associated antigen MART-1 resulted in insoluble protein. Thus, palmitoylation as a means for delivery of proteins into the cross-presentation pathway is not suited for every protein. Improving protein solubility or using different chemical coupling strategies might overcome the difficulties.

4.5. References

- Andrieu, M., Desoutter, J.F., Loing, E., Gaston, J., Hanau, D., Guillet, J.G., Hosmalin, A. Two human immunodeficiency virus vaccinal lipopeptides follow different cross-presentation pathways in human dendritic cells. *J Virol.* 2003, **77**: 1564-70.
- Andrieu, M., Loing, E., Desoutter, J.F., Connan, F., Choppin, J., Gras-Masse, H., Hanau, D., Dautry-Varsat, A., Guillet, J.G., Hosmalin, A. Endocytosis of an HIV-derived lipopeptide into human dendritic cells followed by class I-restricted CD8(+) T lymphocyte activation. *Eur J Immunol.* 2000, **30**: 3256-65.
- Arzt, S., Petit, I., Burmeister, W.P., Ruigrok, R.W., Baudin, F. Structure of a knockout mutant of influenza virus M1 protein that has altered activities in membrane binding, oligomerisation and binding to NEP (NS2). *Virus Res.* 2004, **99**: 115-9.

- Bernard, A., Lamy, A., Alberti, I. The two-signal model of T-cell activation after 30 years *Transplantation*. 2002, **73**: S31-5. Review.
- Bourgault, I., Chirat, F., Tartar, A., Levy, J.P., Guillet, J.G., Venet, A. Simian immunodeficiency virus as a model for vaccination against HIV. Induction in rhesus macaques of GAG- or NEF-specific cytotoxic T lymphocytes by lipopeptides. *J Immunol*. 1994, **152**: 2530-7.
- Brown, D.A., Rose, J.K. Sorting of GPI-anchored proteins to glycolipid-enriched membran subdomain during transport to the apical cell surface. *Cell*. 1992, **68**: 533-44.
- Bungener, L., Huckriede, A., Wilschut, J., Daemen, T. Delivery of protein antigens to the immune system by fusion-active virosomes: a comparison with liposomes and ISCOMs. *Biosci Rep*. 2002, **22**: 323-38. Review.
- Daemen, T., de Mare, A., Bungener, L., de Jonge, J., Huckriede, A., Wilschut, J. Virosomes for antigen and DNA delivery. *Adv Drug Deliv Rev*. 2005, **57**: 451-63. Review.
- Deres, K., Schild, H., Wiesmuller, K.H., Jung, G., Rammensee, H.G. In vivo priming of virus-specific cytotoxic T lymphocytes with synthetic lipopeptide vaccine. *Nature*. 1989, **342**: 561-4.
- Elster, C., Larsen, K., Gagnon, J., Ruigrok, R.W., Baudin, F. Influenza virus M1 protein binds to RNA through its nuclear localization signal. *J Gen Virol*. 1997, **78**: 1589-96.
- Galbiati, F., Volonte, D., Meani, D., Milligan, G., Lublin, D.M., Lisanti, M.P., Parenti, M. The dually acylated NH2-terminal domain of g α is sufficient to target a green fluorescent protein reporter to caveolin-enriched plasma membrane domains. Palmitoylation of caveolin-1 is required for the recognition of dually acylated g-protein α subunits in vivo. *J Biol Chem*. 1999, **274**: 5843-50.
- Gotch, F., J. Rothbard, K., Howland, A., Townsend, A. McMichael. Cytotoxic T lymphocytes recognize a fragment of influenza virus matrix protein in association with HLA-A2. *Nature*, 1987, **326**: 881-882.
- Larsson, M., Fonteneau, J.F., Somersan, S., Sanders, C., Bickham, K., Thomas, E.K., Mahnke, K., Bhardwaj, N. Efficiency of cross presentation of vaccinia virus-derived antigens by human dendritic cells. *Eur J Immunol*. 2001, **31**: 3432-42.
- Livingston, B.D., Crimi, C., Grey, H., Ishioka, G., Chisari, F.V., Fikes, J., Grey, H., Chesnut, R.W., Sette, A. The hepatitis B virus-specific CTL responses induced in humans by lipopeptide vaccination are comparable to those elicited by acute viral infection *J Immunol*. 1997, **159**: 1383-92.
- Huang, A., Huang, L., Kennel, S.J. Monoclonal antibody covalently coupled with fatty acid. A reagent for in vitro liposome targeting. *J Biol Chem*. 1980, **255**: 8015-8.
- Martinon, F., Gras-Masse, H., Boutillon, C., Chirat, F., Deprez, B., Guillet, J.G., Gomard, E., Tartar, A., Levy, J.P. Immunization of mice with lipopeptides bypasses the prerequisite for adjuvant. Immune response of BALB/c mice to human immunodeficiency virus envelope glycoprotein. *J Immunol*. 1992, **149**: 3416-22.
- Melkonian, K.A., Ostermeyer, A.G., Chen, J.Z., Roth, M.G., Brown, D.A. Role of lipid modifications in targeting proteins to detergent-resistant membrane rafts. Many raft proteins are acylated, while few are prenylated. *J Biol Chem*. 1999, **274**: 3910-7.
- Miron, T., Wilchek, M. A simplified method for the preparation of succinimidyl carbonate polyethylene glycol for coupling to proteins. *Bioconjug Chem*. 1993, **4**: 568-9.
- Mortara, L., Gras-Masse, H., Rommens, C., Venet, A., Guillet, J.G., Bourgault-Villada, I. Type 1 CD4(+) T-cell help is required for induction of antipeptide multispecific cytotoxic T lymphocytes by a lipopeptidic vaccine in rhesus macaques. *J Virol*. 1999, **73**: 4447-51.

- Pialoux, G., Gahery-Segard, H., Sermet, S., Poncelet, H., Fournier, S., Gerard, L., Tartar, A., Gras-Masse, H., Levy, J.P., Guillet, J.G. Lipopeptides induce cell-mediated anti-HIV immune responses in seronegative volunteers. *AIDS*. 2001, **15**: 1239-49.
- Simons K, Ikonen E. Functional rafts in cell membranes. *Nature*. 1997, **387**: 569-72. Review.
- Schoen, C., Stritzker, J., Goebel, W., Pilgrim, S. Bacteria as DNA vaccine carriers for genetic immunization. *Int J Med Microbiol*. 2004, **294**: 319-35. Review.
- Tamura, M., Kuwano, K., Kurane, I., Ennis, F.A. Definition of amino acid residues on the epitope responsible for recognition by influenza A virus H1-specific, H2-specific, and H1- and H2-cross-reactive murine cytotoxic T-lymphocyte clones. *J Virol* 1998, **72**: 9404-9406.
- Thiam, K., Loing, E., Verwaerde, C., Auriault, C., Gras-Masse, H. IFN-gamma-derived lipopeptides: influence of lipid modification on the conformation and the ability to induce MHC class II expression on murine and human cells. *J Med Chem*. 1999, **42**: 3732-6.
- Tourdot, S., Herath, S., Gould, K.G. Characterization of a new H-2D(k)-restricted epitope prominent in primary influenza A virus infection. *J Gen Virol* 2001, **82**: 1749-1755.
- van Endert, P.M. Designing peptide vaccines for cellular cross-presentation. *Biologicals*. 2001, **29**: 285-8.
- Vitiello, A., Yuan, L.L., Chesnut, R.W., Sidney, J., Southwood, S., Farness, P. Immunodominance analysis of CTL responses to influenza PR8 virus reveals two new dominant and subdominant Kb-restricted epitopes. *J Immunol* 1996, **157**: 5555-5562.
- Vitiello, A., Ishioka, G., Grey, H.M., Rose, R., Farness, P., LaFond, R., Yuan, L., Chisari, F.V., Furze, J., Bartholomeuz, R. Development of a lipopeptide-based therapeutic vaccine to treat chronic HBV infection. I. Induction of a primary cytotoxic T lymphocyte response in humans. *J Clin Invest*. 1995, **95**: 341-9.
- Wiesmuller, K.H., Brich, M., Jung, G., Sparbier, K., Walden, P. Peptide binding to MHC class I molecules analyzed by confocal microscopy. *Eur J Cell Biol*. 1995, **66**: 389-93.
- Wolven, A., Okamura, H., Rosenblatt, Y., Resh, M.D. Palmitoylation of p59fyn is reversible and sufficient for plasma membrane association. *Mol Biol Cell*. 1997, **8**: 1159-73.
- Zacharias, D.A., Violin, J.D., Newton, A.C., Tsien, R.Y. Partitioning of lipid-modified monomeric GFPs into membrane microdomains of live cells. *Science*. 2002, **296**: 913-6.

- Chapter 5 -

Characterisation of Coronin 1 Interaction Sites with the F-Actin Cytoskeleton and the Plasma Membrane

Imke Albrecht ¹, John Gatfield ¹, Bettina Zanolari ¹, Michel O. Steinmetz ²
and Jean Pieters ¹

Biozentrum ¹, University of Basel, Klingelbergstrasse 50,
CH-4056 Basel, Switzerland and Paul Scherrer Institut, Biomolecular Research
², Structural Biology, CH-5232 Villigen, Switzerland

Parts of the results presented here are published in

Mol Biol Cell 2005, 16(6): 2786-98

5.1. Abstract

Coronin 1 is a member of the coronin protein family specifically expressed in leukocytes and accumulates at sites of rearrangements of the F-actin cytoskeleton. This chapter describes that interaction of coronin 1 with the plasma membrane and with the cytoskeleton occurs via two distinct domains. Association with the F-actin cytoskeleton was mediated by trimerization of a stretch of positively charged residues within a linker region between the N-terminal WD repeat-containing domain and the C-terminal coiled coil. Interaction of coronin 1 with the plasma membrane required the presence of the N-terminal WD repeat-containing domain. The capacity of coronin 1 to link the leukocyte cytoskeleton to the plasma membrane may serve to integrate outside-inside signaling with modulation of the cytoskeleton.

5.2. Introduction

Coronin 1 is predominantly expressed by leukocytes (Suzuki *et al.*, 1995; Ferrari *et al.*, 1999; Nal *et al.*, 2004) and is a member of the WD repeat protein family termed coronins, which are collectively defined as F-actin-associated proteins widely expressed in the eukaryotic kingdom (de Hostos, 1999; Rybakin *et al.*, 2005). In *Dictyostelium discoideum*, coronin co-localizes with F-actin filaments at crown-shaped phagocytic cups and macropinosomes (de Hostos *et al.*, 1991; de Hostos *et al.*, 1993; Maniak *et al.*, 1995; Fukui *et al.*, 1999). *Dictyostelium* deleted for coronin displays a strong reduction in cell locomotion, phagocytosis, macropinocytosis and cytokinesis indicating that in this slime mold coronin is functionally involved in F-actin-based motility-related processes (de Hostos *et al.*, 1993). In *S. cerevisiae*, the single coronin isoform Crn1p was found to localize to cortical F-actin patches in an actin-dependent manner (Heil-Chapdelaine *et al.*, 1998). *In vitro*, Crn1p can nucleate and crosslink F-actin filaments and bind to microtubules (Goode *et al.*, 1999). Recently, yeast Crn1p was proposed to promote the formation of actin filament networks based on its interaction with the Arp2/3 complex (Humphries *et al.*, 2002). Unlike the *Dictyostelium* coronin-null mutant, a *S. cerevisiae* Crn1p-null-mutant does not show any phenotype in actin-dependent processes (Heil-Chapdelaine *et al.*, 1998) suggesting that in this organism coronin does not perform an essential function in regulating the actin cytoskeleton. While single cell eukaryotes have one coronin gene, data base searches have revealed the existence of several coronins in humans

and mice (denoted coronins 1 to 7) (Okumura *et al.*, 1998; de Hostos, 1999; Rybakina *et al.*, 2004).

In leukocytes, coronin 1 concentrates at sites of rearrangement of the cytoskeleton. In macrophages, coronin 1 accumulates during phagocytosis at the cytosolic face of phagosomes. Expression of dominant-negative coronin 1 constructs and RNAi downregulation of coronin 1 in macrophages suggested a role of coronin 1 in early steps of phagosome formation by promoting actin polymerization (Yan *et al.*, 2005). During phagosome maturation coronin 1 dissociates from the phagosome in a process controlled by phosphorylation (Itoh *et al.*, 2002). By actively retaining coronin 1 at the phagosomal membrane, pathogenic mycobacteria can prevent lysosomal delivery allowing these bacteria to survive within the cell (Ferrari *et al.*, 1999; Gatfield and Pieters, 2000). In neutrophils, coronin 1 interacts with a cytosolic subunit of the NADPH oxidase complex (Grogan *et al.*, 1997). In lymphocytes, coronin 1 assembles at the immunological synapse formed during activation of T cells (Nal *et al.*, 2004). Together these studies suggest that coronin 1 may have a function in the modulation of cytoskeletal rearrangements during leukocyte-specific processes.

Based on sequence comparison among members of the coronin family in different species, three conserved domain structures were identified by us and others (de Hostos, 1999). Figure 5.1. shows a schematic drawing of the proposed domain structure for coronin 1.

The approximately 400 residue long N-terminal domain contains five highly conserved WD (tryptophan-aspartate) repeats reminiscent of the ones found in the β -subunits of G proteins (Neer *et al.*, 1994; Lambright *et al.*, 1996; Sondek *et al.*, 1996). Like in the G-protein, secondary structure prediction suggests that N-terminal domain of the coronin 1 folds into a seven-bladed β -propeller whereby each blade (marked in figure 5.1. as B1-B7) is formed by 4-antiparallel β -sheets.

The most C-terminally located 30-40 residues are strongly predicted to fold into a α -helical coiled coil structure. For the *Xenopus* coronin homologues (Xcoronins), as well as coronin 3, the coiled coil has been shown to mediate the formation of higher molecular weight complexes (de Hostos, 1999; Asano *et al.*, 2001; Spoerl *et al.*, 2002) whose exact oligomerization states are not fully clear. Using size exclusion chromatography, analytical ultracentrifugation and electron microscopy it was shown in our lab, that coronin 1 occurs *in vivo* as a homotrimeric complex whose formation is mediated by the coiled coil domain.

The N-terminal domain is connected via a unique linker with the coiled coil domain. This linker region has no predicted secondary structure, it varies greatly in length (50-200 amino acids) and sequence among coronin homologues (de Hostos, 1999).



Figure 5.1. Schematic representation of the proposed domain organization of coronin 1.

The N-terminal domain containing the seven predicted propeller blades is shown in light grey, the linker domain is shown in white, and the C-terminal coiled-coil domain is shown in dark grey.

Besides this sequence information and their classification as actin-associated proteins, little is known about the structure-function relationship of the different coronins in mammals (Suzuki *et al.*, 1995; Spoerl *et al.*, 2002; Oku *et al.*, 2003).

This chapter describes experiments aimed to delineate the role of the single coronin 1 domains in the interaction with the F-actin cytoskeleton and the plasma membrane.

5.3. Results

5.3.1. Subcellular localization of coronin 1 upon expression in HEK293 cells

Immunofluorescence and biochemical studies of the subcellular localization of coronin 1 in leukocytes revealed that coronin 1 interacts both with the plasma membrane as well as with the F-actin cytoskeleton (Gatfield *et al.*, 2005). As coronin 1 consists of three domains, this raised the questions about the role of the individual coronin 1 domains in this interaction. To avoid interference with endogenously expressed coronin 1, studies were performed in the human embryonic kidney (HEK) 293 cells, which do not express endogenous coronin 1 (*figure 5.4.A*). First of all it was tested whether coronin 1 displays a similar subcellular localization upon expression in HEK293 cells as coronin 1 in leukocytes.

To that end, coronin 1 containing a C-terminal hemagglutinin tag (Cor1-HA, *see figure 5.5*) was expressed in HEK293 cells. Twenty-four hours after transfection, the cells were fixed, permeabilized and stained for coronin 1, for the F-actin cytoskeleton and for a plasma membrane associated protein, the Na/K-ATPase.

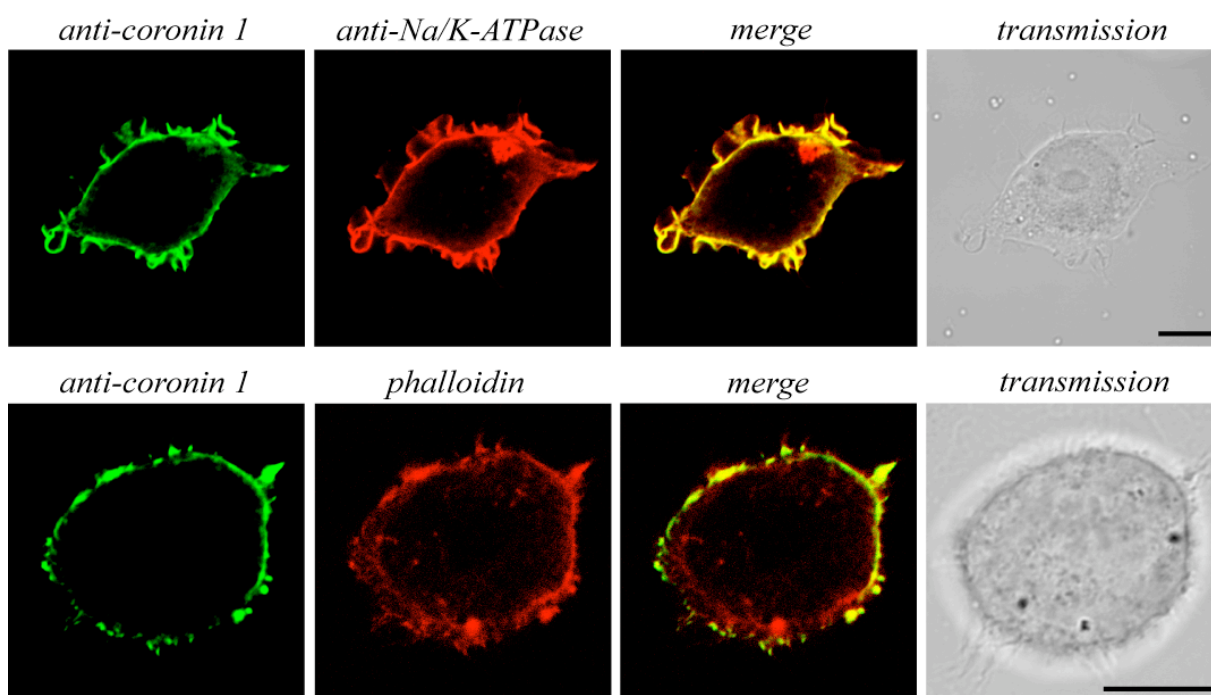


Figure 5.2. Subcellular localization of coronin 1 after expression in HEK293 cells.

Cor1-HA transfected HEK293 cells were stained with anti-coronin 1 antiserum (*left panel*), anti-Na/K-ATPase (*second left panel, upper row*) or phalloidin (*second left panel, lower row*). The right panel shows the corresponding Nomarski image. Bar: 10 μ m.

Analysis by immunofluorescence microscopy revealed a plasma membrane localization of Cor1-HA (*figure 5.2., upper row*) upon expression in HEK293 cells. Furthermore Cor1-HA co-localizes with the cortical F-actin cytoskeleton (*figure 5.2., lower row*) indicating that plasma membrane binding might be actin-dependent.

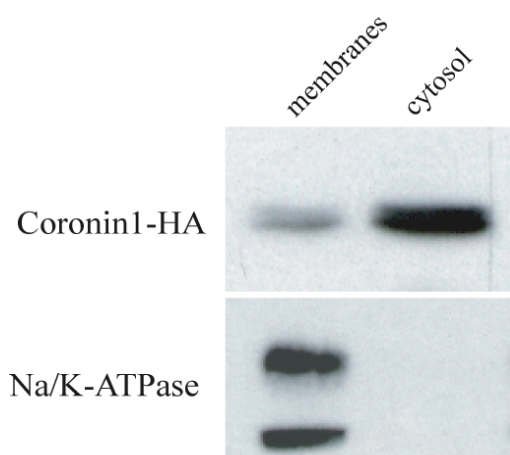


Figure 5.3. Biochemical analysis of coronin 1 interaction with HEK293 cell membranes.

The postnuclear supernatant of a Cor1-HA transfected HEK293 cell homogenate was separated into membrane fraction and cytosol (100 000 x g, 30 min) and analyzed for the presence of coronin 1 and the Na/K-ATPase by SDS-PAGE and immunoblotting.

To further analyze the subcellular distribution of Cor1-HA in HEK293 cells, cell fractionation was performed. Cor1-HA expressing HEK293 cells were homogenized in sucrose-containing buffer, and membrane and cytosolic fractions were prepared.

SDS-PAGE of membrane and cytosol fractions followed by immunoblotting using anti-coronin 1 antiserum and anti-Na/K-ATPase antibody revealed that the Cor1-HA proteins distributed between membrane (Na/K-ATPase positive) fraction and cytosolic fraction (*Figure 5.3.*). This membrane-cytosol distribution of Cor1-HA is similar to the distribution of endogenous coronin 1 in J774 mouse macrophages seen before (Gatfield *et al.*, 2005). To analyze the cytoskeletal association of Cor1-HA, the cytoskeleton of HEK293 cells was isolated by cell lysis in

1% TX-100 / 80 mM PIPES and low speed centrifugation (3000 x g, 2 min).

Immunoblotting of pellet and supernatant showed that ~ 50 % of all coronin molecules were found in the sedimented detergent-insoluble fraction (*figure 5.4.B*). This partial TX-100 insolubility of Cor1-HA is in contrast to endogenous coronin 1 in J774 mouse macrophages where coronin 1 is completely insoluble in cytoskeletal isolation buffer (Gatfield *et al.*, 2005). Treatment of the Cor1-HA transfected HEK293 cells for 30 min with 20 μ M of the F-actin depolymerising drug latrunculin B, prior to isolation of the cytoskeleton, resulted in the simultaneous release of actin and Cor1-HA into the supernatant (*figure 5.4.B*). We conclude that as in J774 cells, the TX-100 insolubility of Cor1-HA in HEK293 cells is due to association of Cor1-HA with the F-actin cytoskeleton.

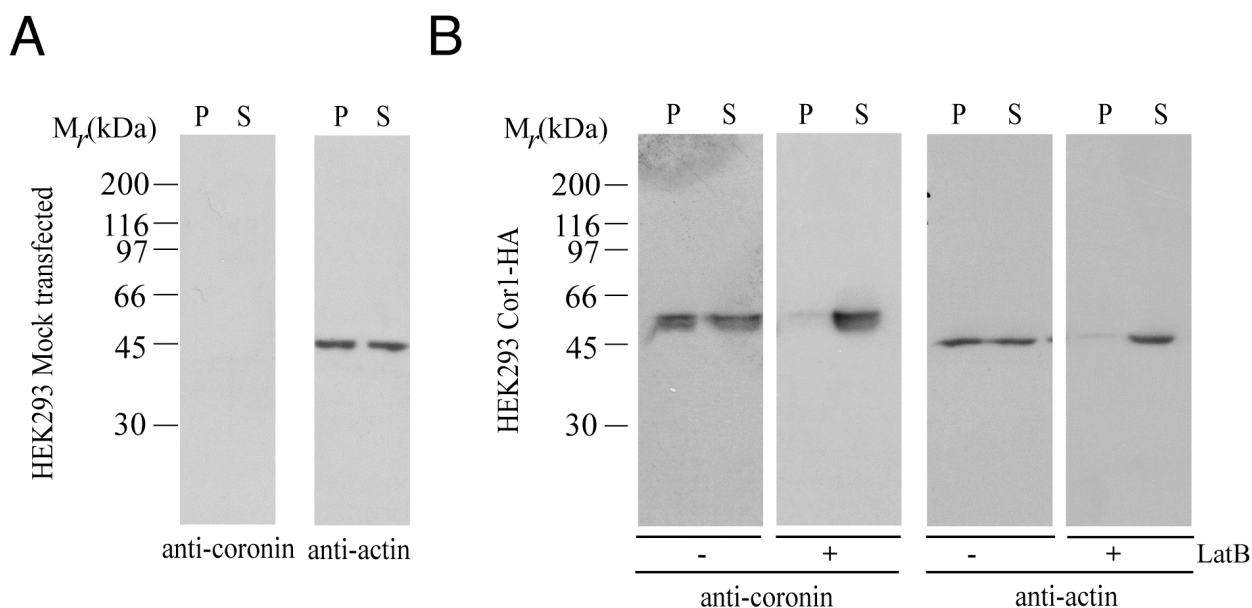


Figure 5.4. Biochemical analysis of coronin 1 localization in the detergent-insoluble fraction of HEK293 cells transfected with Cor1-HA.

A+B. HEK293 cells mock transfected (A) or transfected with Cor1-HA expression construct (B) were lysed in cytoskeleton isolation buffer containing 1% Triton X-100 and directly subjected to low speed centrifugation (3000 x g, 2 min, see materials and methods). Subsequently, the detergent-insoluble pellets and the supernatants were analyzed by SDS-PAGE and immunoblotting for detection of coronin 1 and actin.

For depolymerization of the F-actin cytoskeleton HEK293 Cor1-HA cells were treated for 30 min with 20 μ m latrunculin B.

In summary, these results show that Cor1-HA expressed in HEK293 cells displays a similar subcellular localization as endogenously expressed coronin 1 in J774 cells. Therefore this system is well suited to further investigate F-actin cytoskeleton and plasma membrane association of coronin 1 in intact cells.

Coronin 1 consists of three domains, a N-terminal β -propeller domain connected via a linker with the C-terminal coiled coil. To determine which domains of coronin 1 are responsible for mediating of the F-actin cytoskeleton and the plasma membrane interaction, truncated forms of coronin 1 were expressed in HEK293 cells and their ability to interact with the F-actin cytoskeleton as well as with the plasma membrane was examined.

5.3.2. Role of the coiled coil domain of coronin 1 in the interaction with the F-actin cytoskeleton

Analysis of endogenous coronin 1 in macrophages by size exclusion chromatography and by electron microscopy revealed that coronin 1 occurs *in vivo* as a homotrimeric complex (Gatfield *et al.*, 2005). For the *Xenopus* coronin homologues (Xcoronins), as well as for coronin 3, it was shown that the coiled coil mediates the oligomerization (de Hostos, 1999; Asano *et al.*, 2001; Spoerl *et al.*, 2002). To analyze the role of the C-terminal coiled coil of coronin 1, a hemagglutinin tagged coronin 1 mutant lacking the coiled coil domain was constructed (referred to as Cor1- Δ CC-HA, *figure 5.5.A*) and expressed in HEK293 cells. First the oligomerization state of Cor1- Δ CC-HA upon expression in HEK293 cells was determined using size exclusion chromatography. Therefore cytosol isolated from Cor-1-HA and Cor1- Δ CC-HA transfected HEK293 cells was separated on a Superdex200 column, and the presence of coronin 1 in the single fractions was analyzed by immunoblotting. As shown in *figure 5.5.B*, whereas full length Cor1-HA (*upper panel, figure 5.5.B*) migrated at a position corresponding to a molecular weight of 160kDa, Cor1- Δ CC-HA could be detected in fractions corresponding to a molecular weight of 50kDa (*lower panel, figure 5.5.B*). This result suggested that Cor-1-HA occurs in HEK293 cells as a trimer and furthermore that trimerization is mediated by the coiled coil domain. Next it was tested whether deletion of the coiled coil domain affects the interaction of coronin 1 with the F-actin cytoskeleton.

Isolation of the TX-100 insoluble F-actin cytoskeleton fraction of Cor1-HA or Cor1- Δ CC-HA transfected HEK293 cells and subsequent immunoblotting using coronin 1 antiserum revealed that Cor1- Δ CC-HA is completely soluble in the TX-100 cytoskeleton isolation buffer (*figure 5.5.C*) indicating that Cor1- Δ CC-HA cannot associate anymore with the F-actin cytoskeleton. Thus interaction of coronin 1 with the F-actin cytoskeleton is dependent on the presence of the coiled coil.

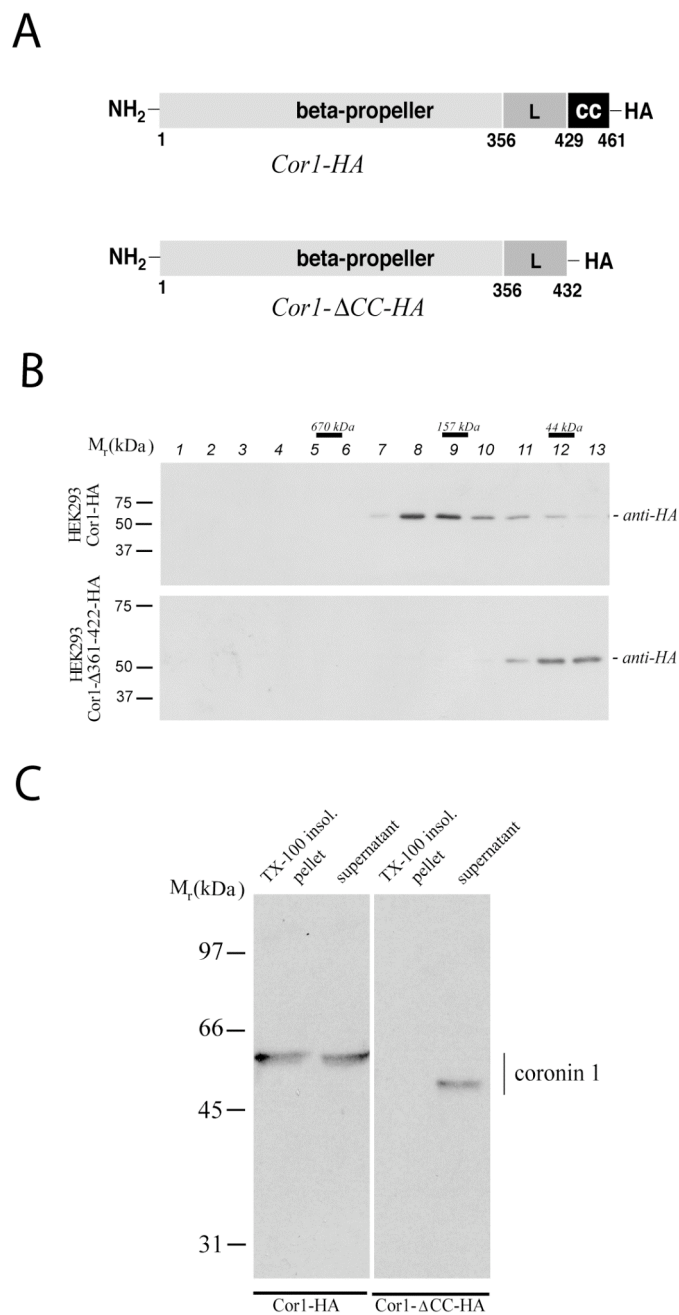


Figure 5.5. Functional analysis of the coiled coil domain of coronin 1.

A. Schematic representation of coronin 1 deletion mutant used in this study.

B. HEK293 cells were transiently transfected with the indicated constructs, and after 24 hours, the cytosol was solubilized in 2% octylglucopyranoside and subjected to size exclusion chromatography on a Superdex 200 column. The presence of transcriptionally active coronin 1 constructs was analyzed using immunoblotting following SDS-PAGE of the fractions indicated. The positions of proteins of known molecular weight (M_r) are indicated.

C. Biochemical analysis of F-actin association of coronin 1. HEK293 cells transiently transfected with Cor1-HA or Cor1- Δ CC-HA were lysed in cytoskeleton isolation buffer containing 1% Triton X-100 and a detergent-insoluble fraction was obtained by low speed centrifugation (see methods). Subsequently, detergent-insoluble pellets and supernatants were analyzed by SDS-PAGE and immunoblotting using an anti-coronin 1 antiserum.

To analyze whether the coiled coil is responsible for the association with the F-actin cytoskeleton, a Cor1-(430-461)-HA construct compromising the coiled coil domain was generated. As this construct failed to be expressed in HEK293 cells (data not shown), the coiled coil domain of coronin 1 was fused to the C-terminus of an enhanced green fluorescent protein (EGFP) and after expression in HEK293 cells the TX-100 solubility of this fusion protein was determined. EGFP and EGFP fused to an unrelated coiled coil of the extracellular protein matrilin 4 (*figure 5.6. A*) were used as a control. The matrilin 4 coiled coil was chosen because it mediates trimerization but as an extracellular matrix protein does not interact with F-actin (Frank *et al.*, 2002).

As can be seen in figure 5.6 B, whereas most of the EGFP protein and the EGFP-CC_{matrilin4} fusion protein could be recovered in the supernatant (*figure 5.6. B, left and right panel*), a significant part of the EGFP-CC_{coronin1} protein was found in TX-100 insoluble cytoskeletal fraction.

To investigate whether this increased TX-100 insolubility of the EGFP-CC_{coronin1} fusion protein was due to F-actin cytoskeleton association mediated by the coiled coil domain, EGFP-CC_{coronin1} expressing HEK293 cells were treated with latrunculin B prior to isolation of the F-actin cytoskeleton. Treatment with latrunculin B completely released actin into the supernatant, but had no effect on the supernatant-pellet distribution of EGFP-CC_{coronin1} indicating that the TX-100 insolubility of EGFP-CC_{coronin1} was not the result of an association with the F-actin cytoskeleton.

From these results it can be concluded that the coiled coil domain is necessary for the interaction of coronin 1 with the F-actin cytoskeleton, but it is not sufficient for this interaction.

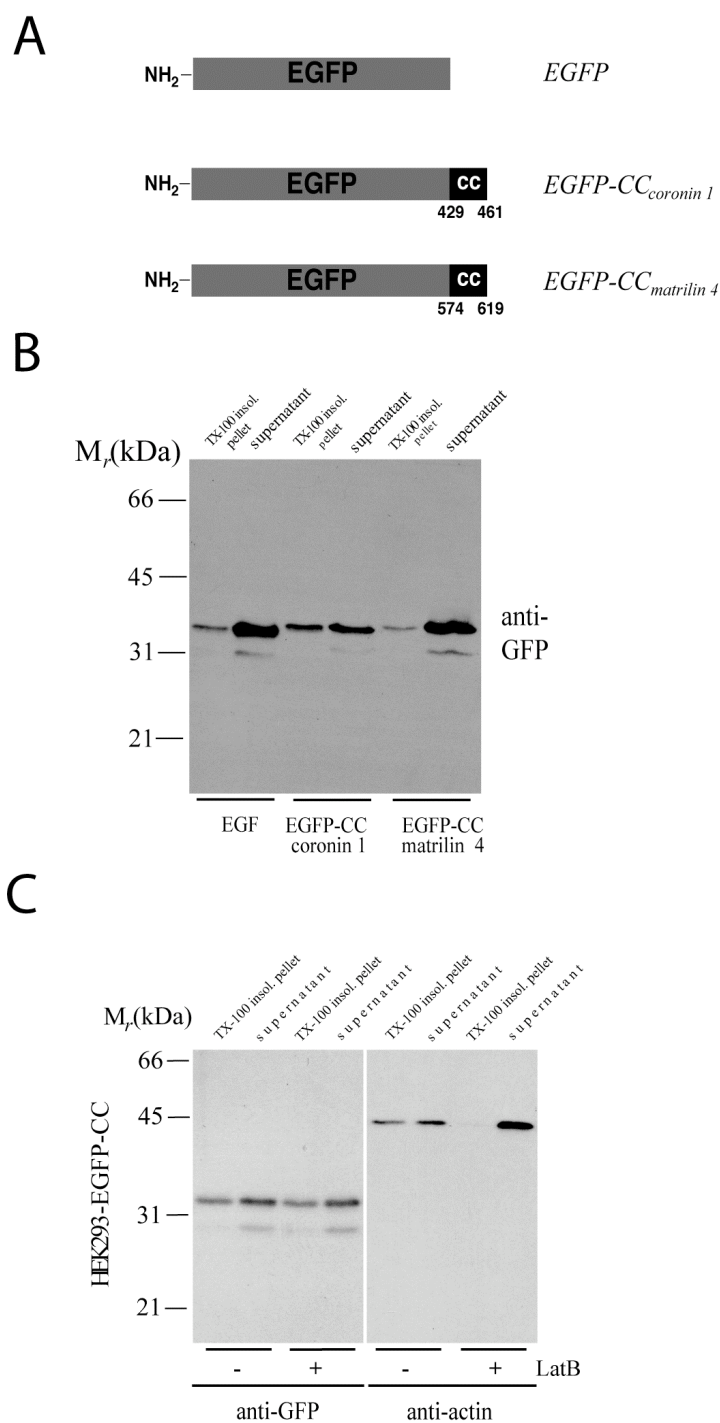


Figure 5.6. Role of the coiled coil domain of coronin 1 in the interaction with the F-actin cytoskeleton.

A. Schematic representation of enhanced green fluorescent (EGFP) fusion proteins used in this study.

B. HEK293 cells were transiently transfected with expression constructs for EGFP, for the EGFP-CC_{coronin1} or for the EGFP-CC_{matrilin4} fusion proteins. Twenty-four hours after transfection HEK293 cells were lysed in cytoskeleton isolation buffer containing 1% Triton X-100 and directly subjected to low speed centrifugation (3000 x g, 2 min). Subsequently, the detergent-insoluble pellets and the supernatants were analyzed by SDS-PAGE and immunoblotting using an anti-GFP antibody.

C. Isolation of TX-100 insoluble fractions from control and latrunculin B treated HEK293 cells transiently transfected with EGFP-CC fusion protein.

5.3.3. Role of the N-terminal β -propeller domain of coronin 1 in the interaction with the F-Actin cytoskeleton

We next investigated whether the N-terminal β -propeller domain of coronin 1 participates in the interaction with the F-actin cytoskeleton.

As expression of a HA-tagged Cor1 β -propeller in HEK293 cells was not successful investigations were performed with coronin 1 proteins lacking the N-terminal β -propeller domain (referred in figure 5.7 as to Cor1^{L+C}-HA).

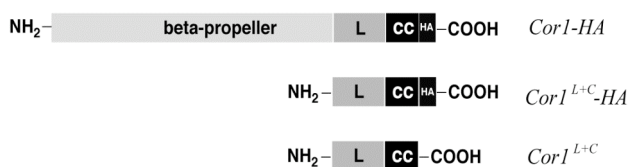


Figure 5.7. Schematic representation of Cor1-HA, Cor1^{L+C}-HA and Cor1^{L+C}.

The linker and coiled-coil domain (L+C) comprise the amino acid sequence from 357 to 461.

To check whether deletion of the N-terminal β -propeller interfered with the proper oligomerization of the protein, Cor1^{L+C}-HA expressed in HEK293 cells was subjected to size exclusion chromatography (*figure 5.8.A*). As shown in *figure 5.8.A*, Cor1^{L+C}-HA migrated at a position corresponding to a molecular mass laying between 60 and 80 kDa. The molecular mass of Cor1^{L+C}-HA monomer is 12 kDa, suggesting an oligomerization state of a pentamer or a hexamer instead of a trimer. Besides, as the gel filtration was performed with total cytosol, there is the possibility that Cor1^{L+C}-HA interacts with other proteins resulting in a high molecular mass complex.

However as migration in a gel filtration column is shape dependent, it does not allow always a precise determination of the molecular mass. Therefore, recombinant Cor1^{L+C} (*figure 5.7, lower row*) which was purified from *E. coli* was investigated by static light scattering (SLS). Using SLS the molecular mass of the Cor1^{L+C} was determined to be 34.4 kDa showing that the recombinant Cor1^{L+C} protein indeed occurred as a trimer.

As the recombinant Cor1^{L+C} protein shows the same migration behaviour in size exclusion analysis (*figure 5.8.B*) like the Cor1^{L+C}-HA, it was concluded that also Cor1^{L+C}-HA forms trimers upon expression in HEK293 cells and is therefore suitable for further analysis.

Next, the association of Cor1^{L+C}-HA with the F-actin cytoskeleton was investigated by determination of the TX-100 solubility of Cor1^{L+C}-HA construct expressed in HEK293 cells.

As summarized in figure 5.9.A, deletion of the N-terminal β -propeller resulted in the complete TX-100 solubility of Cor1^{L+C}-HA protein.

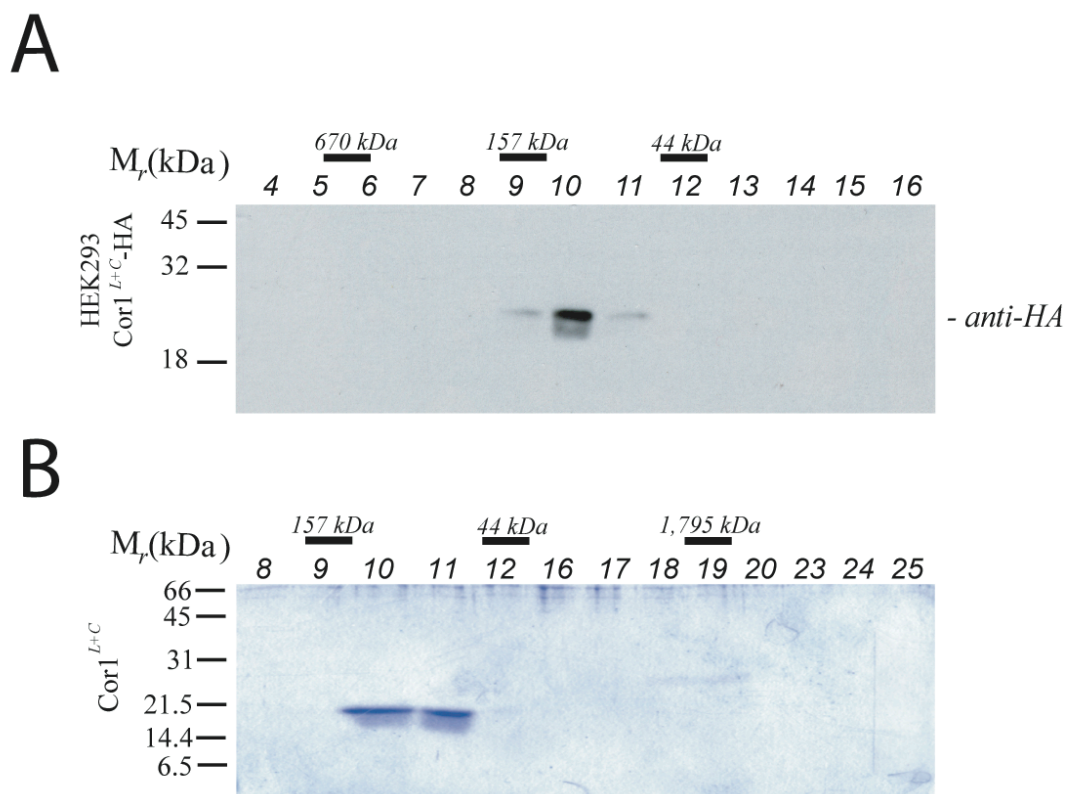


Figure 5.8. Oligomerization of Cor1^{L+C}

A. Size exclusion chromatography analysis of cytosol from Cor1^{L+C}-HA expressing HEK293 cells. Cytosol was isolated twenty-four hours after transfection and subjected to size exclusion chromatography on a Superdex 200 column. The eluted fractions were assayed for the presence of Cor1^{L+C}-HA by SDS-PAGE and immunoblotting. The positions of proteins of known molecular weight (M_r) are indicated.

B. Size exclusion chromatography analysis of recombinant expressed coronin 1 linker-coiled coil domain (Cor1^{L+C}). Cor1^{L+C} was purified from *E. coli* as described in material and methods and subjected to size exclusion chromatography on a Superdex 200 column. The eluted fractions were analyzed by Coomassie Blue-stained SDS-PAGE.

The availability of the recombinant Cor1^{L+C} made it possible also to investigate the F-actin association *in vitro* using a F-actin co-sedimentation assay. In contrast to monomeric actin, polymerized actin can be sedimented by high-speed centrifugation allowing the co-sedimentation of proteins, which bind to F-actin. To test whether recombinant Cor1^{L+C} can interact with F-actin, the protein was incubated for 45 min with polymerized actin, subsequently the F-actin was pelleted by ultracentrifugation and then supernatant and pellet were analyzed by Coomassie Blue-stained SDS-PAGE. As seen in figure 5.9.B, Cor1^{L+C} could not be detected in the pellet fraction, indicating that the linker-coiled coil domain is not sufficient for the F-actin interaction.

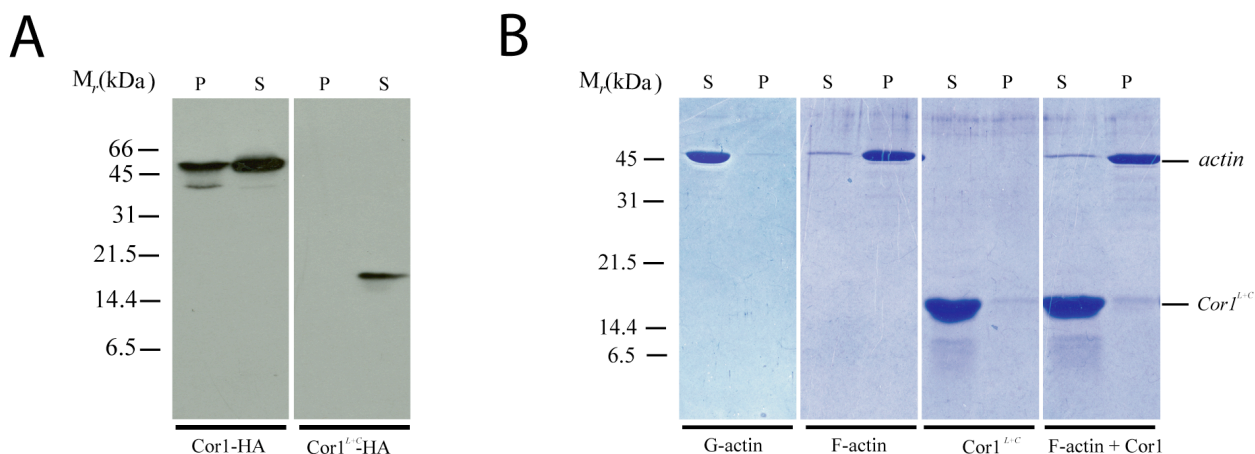


Figure 5.9. Interaction of Cor1^{L+C} with the F-actin cytoskeleton.

A. HEK293 cells were transiently transfected with expression constructs for Cor1-HA and Cor1^{L+C}-HA. Twenty-four hours after transfection the TritonX-100 insoluble fractions were isolated and analyzed by SDS-PAGE and immunoblotting using an anti-coronin 1 antibody.

B. Co-sedimentation assay of Cor1^{L+C} with F-actin. F-actin (5 μM) was incubated with Cor1^{L+C} (50 μM) for 45 min at room temperature, centrifuged for 30 min at 100 000 x g to pellet F-actin and pellets (P) and supernatants (S) were analyzed by Coomassie Blue-stained SDS-PAGE.

Together these results suggest that the linker domain and the C-terminal coiled coil are not sufficient for the association of coronin 1 with the F-actin cytoskeleton.

5.3.4. Involvement of coronin 1 linker domain in the association with the F-actin cytoskeleton

To determine a function for the linker region in cytoskeletal binding, a mutant coronin 1 was constructed, (Cor1-Δ361-422), lacking the complete linker domain. However, expression of this construct in HEK293 cells leads to coronin 1 aggregation, as revealed by size exclusion chromatography (*figure 5.10.*) and therefore this construct was not suited for further analysis.

As this linker region contains a stretch of positively charged amino acid residues that may be responsible for such cytoskeletal interaction (Tang *et al.*, 1996; Wohnsland *et al.*, 2000), a Cor1-Δ400-416-HA construct was produced in which these residues are deleted (*figure 5.11.*).

This construct was correctly oligomerized upon expression in HEK293 cells (*figure 5.11.B*).

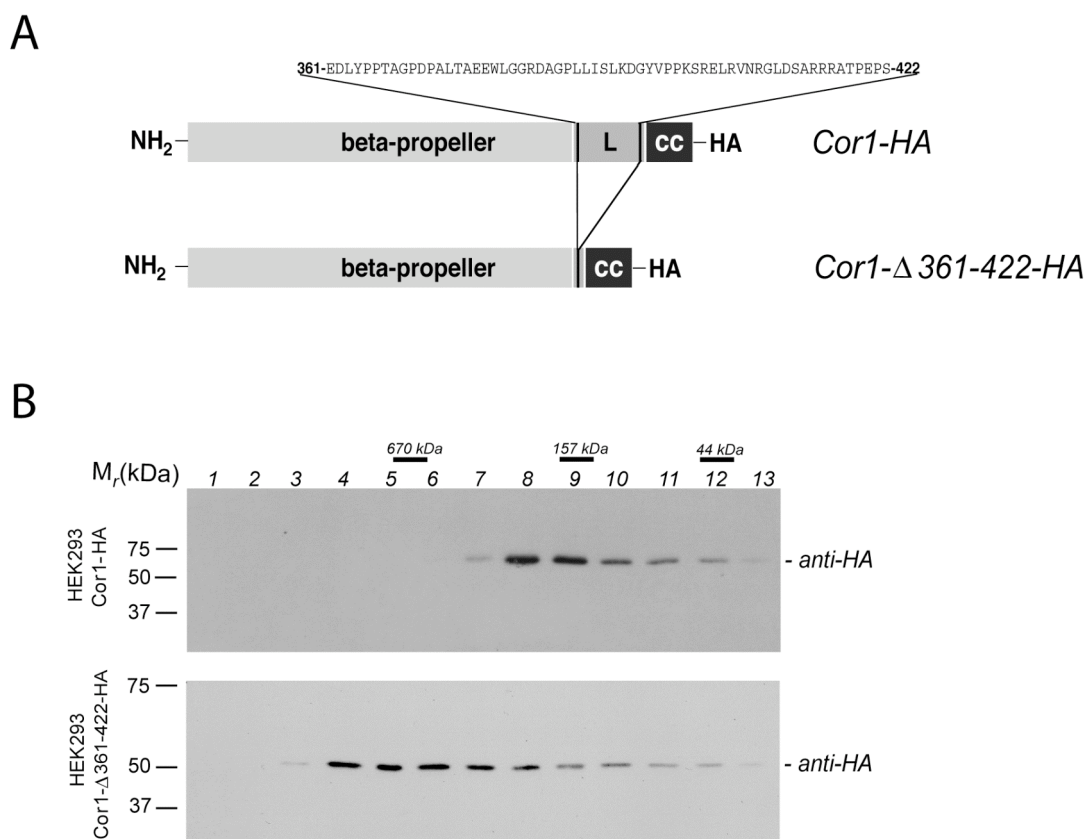


Figure 5.10. Interaction of *Cor1*^{L+C} with the F-actin cytoskeleton.

A. Schematic representation of coronin 1 deletion mutant *Cor1-Δ(361-422)-HA*.

B. Size exclusion chromatography analysis of cytosol from *Cor1-HA* and *Cor1-Δ(361-422)-HA* expressing HEK293 cells. Cytosol was isolated twenty-four hours after transfection and subjected to size exclusion chromatography on a Superdex 200 column. The eluted fractions were assayed for the presence of *Cor1*^{L+C}-HA by SDS-PAGE and immunoblotting. The positions of proteins of known molecular mass (M_r) are indicated.

When the cytoskeletal association was analyzed by isolation of TX-100 insoluble cytoskeleton, this mutant was retrieved in the soluble fraction (*figure 5.11.C, right panel*), indicating that F-actin cytoskeleton association of this coronin 1 mutant was lost. Furthermore it supported the previous results showing that neither the N-terminal β -propeller region nor the coiled coil alone are sufficient for mediation of coronin 1 interaction with the F-actin cytoskeleton.

Summarizing these results, it can be concluded that the stretch of positively charged residues within the linker domain is the actual site of cytoskeletal association. To be functional, this site requires clustering which is achieved by trimerization of the molecules through the coiled coil domain. The function of the N-terminal β -propeller domain is less clear, but it might be

important for keeping the molecule in a conformation, which supports the clustering of the positively charged amino acids (see also *figure 5.15.*).

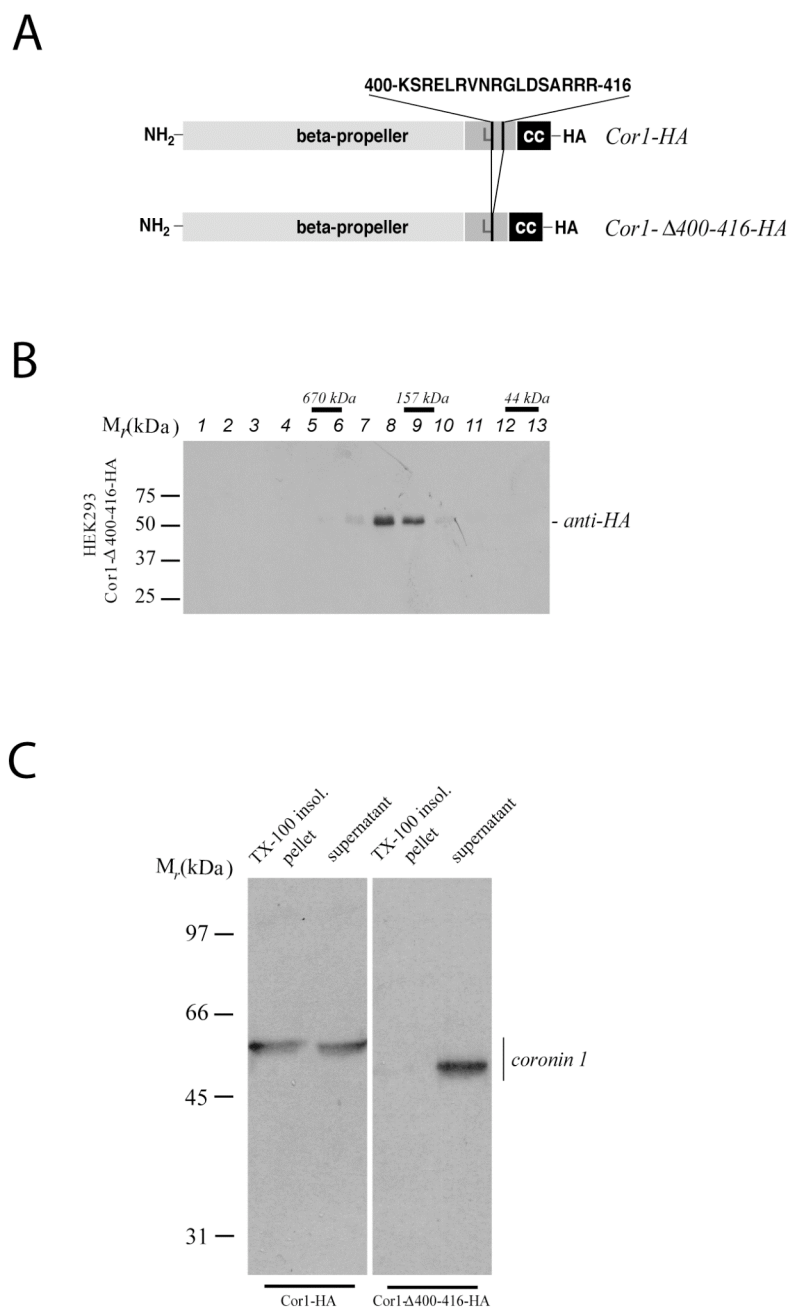


Figure 5.11. Involvement of coronin 1 linker in the association with the F-actin cytoskeleton

A. Schematic representation of coronin 1 deletion mutant Cor1- Δ 400-416-HA.

B. Size exclusion chromatography analysis of cytosol from Cor1- Δ 400-416-HA expressing HEK293 cells. Size exclusion chromatography was performed as described previously.

C. HEK293 cells transiently transfected with Cor1-HA or Cor1- Δ 400-416-HA were lysed in cytoskeleton isolation buffer containing 1% Triton X-100 and a detergent-insoluble fraction was obtained by low speed centrifugation (see materials and methods). Subsequently, detergent-insoluble pellets and supernatants were analyzed by SDS-PAGE and immunoblotting using an anti-coronin 1 antiserum.

5.3.5. Association of coronin 1 with the plasma membrane

In HEK293 cells transfected with coronin 1, as well as in macrophages, coronin molecules interact with the plasma membrane (*figure 5.2 /5.3.*).

To analyze the region of coronin 1 required for plasma membrane association, HEK293 cells were transfected with cDNA constructs encoding Cor1-HA, Cor1- Δ CC-HA or Cor1- Δ 400-416-HA. Cells were then homogenized, membrane and cytosolic fractions were prepared as described previously and analyzed by immunoblotting using an anti-HA antibody.

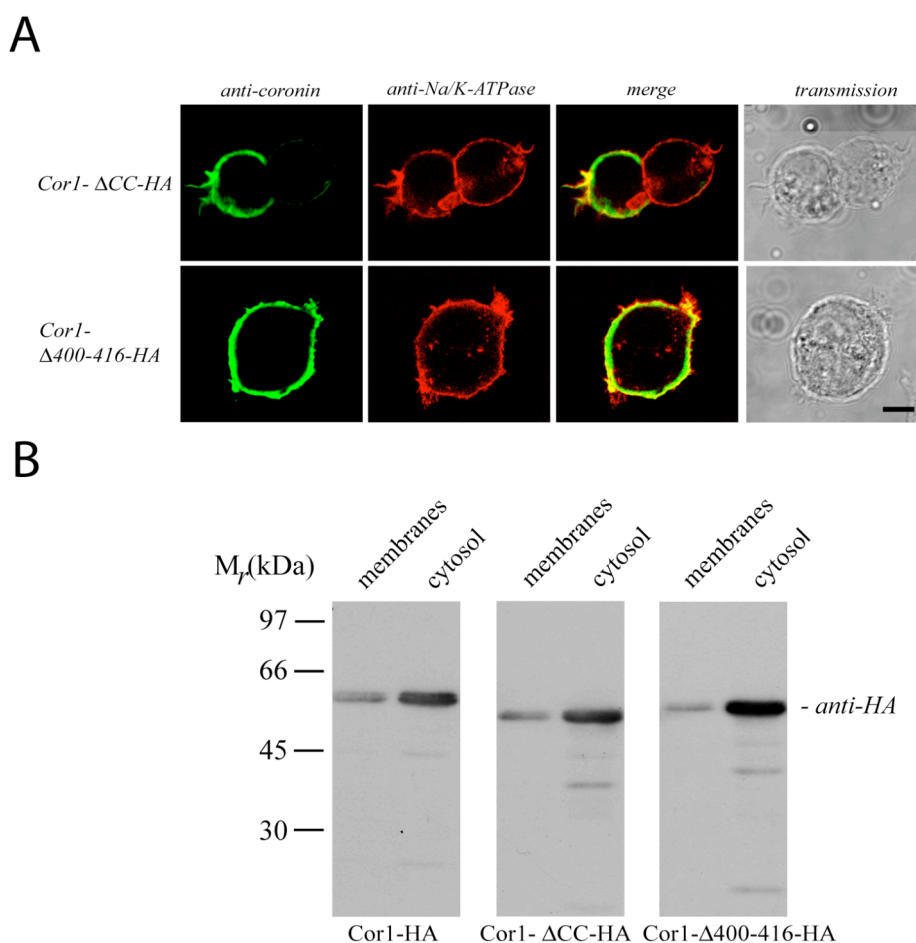


Figure 5.12. Association of coronin 1 with the plasma membrane.

A. Immunofluorescence analysis of coronin 1 and Na/K-ATPase localization in HEK293 cells expressing Cor1- Δ CC-HA or Cor1- Δ 400-416-HA. Twenty-four hours after transfection cells were fixed, permeabilized and stained for coronin 1 and Na/K-ATPase using an anti-coronin 1 antiserum and anti-Na/K-ATPase antibody. Bar: 10 μ m.

B. The post nuclear supernatants of HEK293 cells transfected with Cor1-HA, Cor1- Δ CC-HA or Cor1- Δ 400-416-HA expression constructs were subjected to subcellular fractionation (100 000 \times g, 30 min). Membrane and cytosolic fractions were analyzed for the presence of coronin 1 by SDS-PAGE and immunoblotting with an anti-HA antibody.

The coronin 1 molecules lacking the coiled coil or lacking the cytoskeleton binding site in the linker region were distributed in a similar manner as wild type coronin 1 between membranes and cytosol (*figure 5.12.B*). Furthermore, immunofluorescence analysis of Cor1- Δ CC-HA or Cor1- Δ 400-416-HA expressing HEK293 cells (*figure 5.12.A*) stained with anti-coronin antiserum and anti-Na/K-ATPase antibody revealed co-localization of coronin 1 and the plasma membrane associated Na/K-ATPase.

Together these data suggest that the coiled coil domain and the stretch of positively charged amino acids within the linker region are not required for plasma membrane association.

To test whether coronin 1 plasma membrane binding is mediated by the N-terminal β -propeller domain, the subcellular localization of Cor1^{L+C}-HA protein in HEK293 cells was analyzed. Both the immunofluorescence (*figure 5.13.A*) as well as the biochemical analysis (*figure 5.13.B*) clearly showed that deletion of the N-terminal β -propeller domain resulted in the loss of coronin 1 plasma membrane binding indicating that coronin 1 binds to the plasma membrane by its N-terminal β -propeller domain.

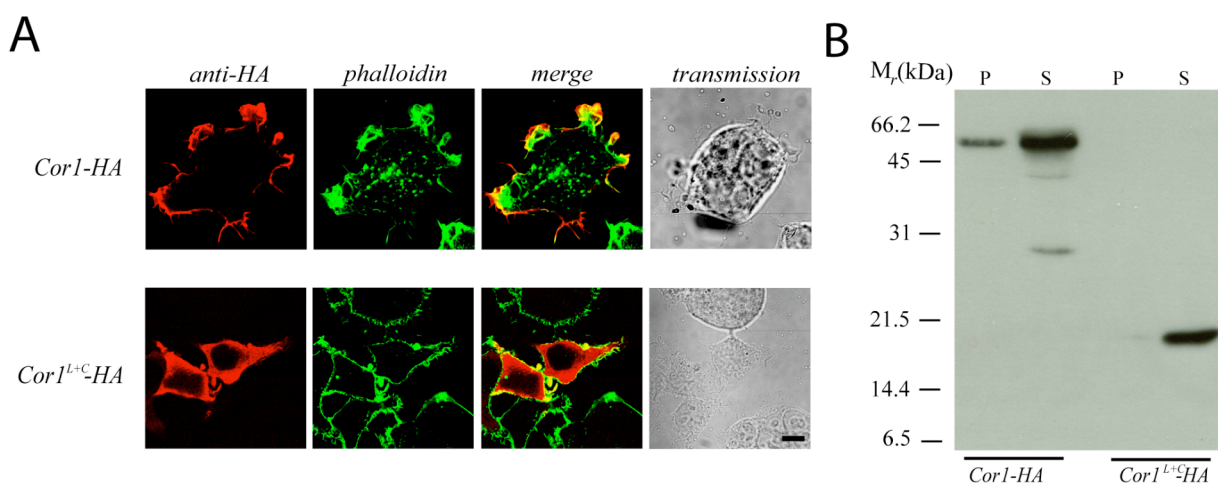


Figure 5.13. Role of the N-terminal β -propeller domain of coronin 1 in plasma membrane binding.

A. Immunofluorescence analysis of Cor1-HA (upper panels) and Cor1^{L+C}-HA (lower panels) localization in HEK293 cells. Twenty-four hours after transfection, HEK293 cells were fixed, permeabilized and stained with an anti-HA antibody (secondary reagent: goat-anti-mouse-Ig2b-Texas red) and phalloidin-488. Bar: 10 μ m

B. The post nuclear supernatants of HEK293 cells transfected with Cor1-HA, or Cor1^{L+C}-HA expression constructs were subjected to subcellular fractionation (100 000x g, 30 min). Membrane and cytosolic fractions were analyzed for the presence of coronin 1 by SDS-PAGE and immunoblotting with an anti-HA antibody.

How does coronin bind to the plasma membrane? The co-localization of coronin 1 with the cortical actin (figure 5.2.) raised the question whether plasma membrane binding is dependent on F-actin association. To that end, HEK293 cells transfected with Cor1-HA, Cor1- Δ CC-HA or Cor1- Δ 400-416-HA were treated with latrunculin B for 30 min, fixed and stained for hemagglutinin and F-actin. As shown in figure 5.14., the cortical coronin 1 staining remained unaffected while the actin cytoskeleton was efficiently depolymerized as indicated by a lack of phalloidin fluorescence.

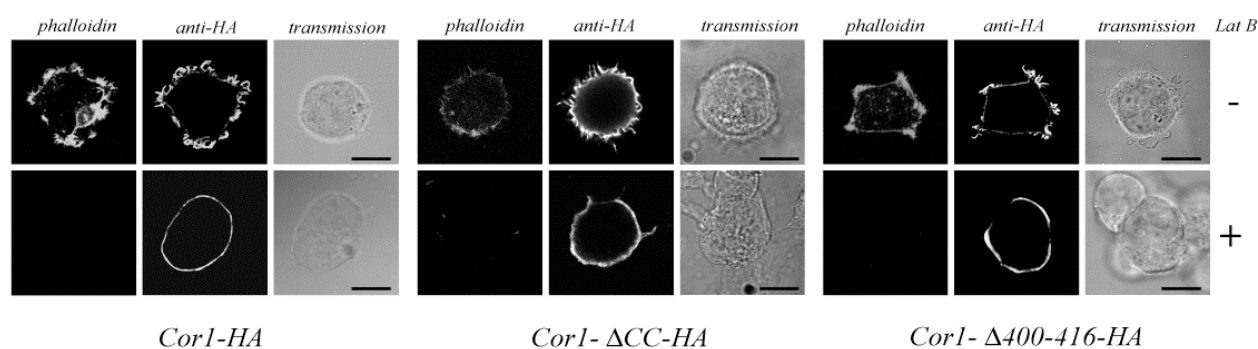


Figure 5.14. Association of coronin 1 with the plasma membrane is independent of the F-actin cytoskeleton.

Immunofluorescence analysis of coronin 1 and F-actin localization in latrunculin B-treated HEK293 cells. Cells were transfected with the indicated constructs and after 24 hours were treated with 20 μ M latrunculin B (30 min) or left untreated. Cells were fixed with formaldehyde followed by saponin permeabilization and stained for coronin 1 and F-actin using anti-HA (secondary reagent: goat-anti-mouse-AlexaFluor-488), and phalloidin-Texas red. Bar: 10 μ m.

These observations demonstrate that coronin 1 association with the plasma membrane is independent of F-actin.

5.4. Discussion

The ability of a multicellular organism to defend itself against the invasion of pathogens is based on its capability to produce an effective and appropriate immune response against the pathogen. During generation of an host immune response immune cells have to fulfil a variety of functions, many of them are dependent on processes, which require the reorganisation of the F-actin cytoskeleton, including phagocytosis and macropinocytosis, cellular movement, formation of immunological synapse and T-cell activation (Meiri *et al.*, 2004; Fenteany *et al.*, 2004; Das *et al.*, 2002; Vincente-Manzanares *et al.*, 2003).

Coronin 1 is a member of the coronin family of actin-binding proteins, which is specifically expressed in cells of the immune system. Therefore it may have a specific function in immunological processes where the actin cytoskeleton is involved. To better understand how coronin 1 exhibits its function and to get insight how this is related to its structure, the interaction of coronin 1 with the F-actin cytoskeleton and the plasma membrane was studied in this chapter. By analysing the subcellular localization of wildtype and truncated coronin 1 proteins expressed in HEK293 cells, which do not contain endogenous coronin 1, it was possible to dedicate a function to each coronin 1 domain as summarized in figure 5.15.

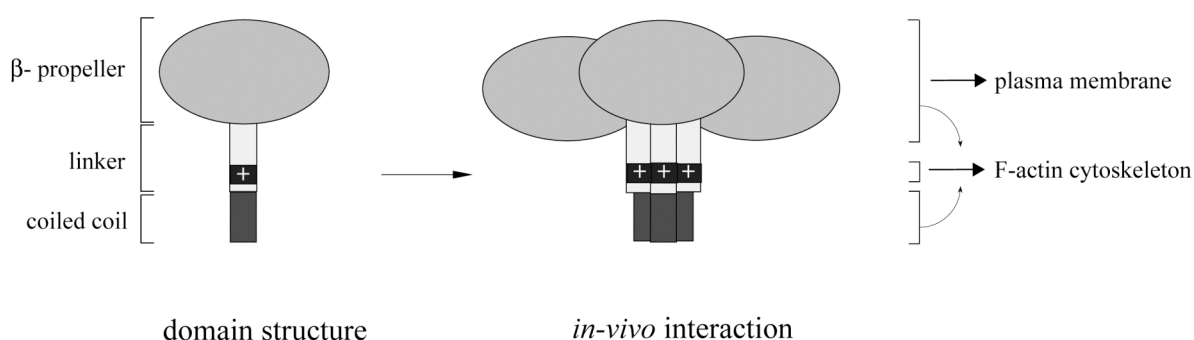


Figure 5.15. Function of coronin domains in association with the plasma membrane and the F-actin cytoskeleton.

Coronin 1 is a parallel homotrimeric protein consisting of three globular N-terminal β -propellers (dark grey) assembled via the C-terminal coiled coil (dark). Association of coronin 1 with the cytoskeleton occurs via a stretch of positively charged residues in the linker region (light grey) and is dependent on trimerization and the presence of the N-terminal β -propeller. The F-actin independent binding to the plasma membrane is mediated via the N-terminal globular β -propeller domain.

5.4.1. Interaction of coronin 1 with the F-actin cytoskeleton

In vivo interaction of coronin 1 with the F-actin cytoskeleton is dependent on the presence of all three domains (figure 5.15.). The actual interaction site with the F-actin cytoskeleton was identified as a short stretch of positively charged amino acids (400-416 aa) located in the linker region. The ability of positively charged peptides or basic amino acids stretches within a protein to interact with the F-actin cytoskeleton has been shown before (Tang *et al.*, 1996; Wohnsland *et al.*, 2000), nevertheless a single stretch of positively charged amino acids was not sufficient to mediate the interaction of coronin 1 with the F-actin cytoskeleton. Coronin1 has to trimerize to interact with the F-actin cytoskeleton, indicating that clustering of the basic amino acids within the linker region is required. Clustering of actin binding sites may allow coronin 1 to cross-link F-actin filaments leading to the generation of F-actin bundles or three-

dimensional actin networks. Interestingly, coronin 3 has been shown to bundle actin *in vitro* (Spoerl *et al.*, 2002), but this was not dependent on the oligomerization state of coronin 3. However, a number of coronin homologues also contain in their linker domain a region enriched with positively charged amino acid, similar to that found in coronin 1, suggesting that all these molecules interact with the F-actin cytoskeleton in a similar manner.

mCor 1:	356-SDLFQEDLYPPTAGPDPALTAEEWLGGRDAGPLLISLKDGYVPPK SR ELRVN RGLDSARRR ATPEPSGTPSS-472
mCor 2:	356-SDLFQDDLYPDTAGPEAALEAEDWVSGQDANPILISLREAYVPS KQ RDLK VSRR NVLS SDSR PASYS RS GASTATAVTDVPSGNLAGAGEA-446
mCor 3:	354-SDLFQDDLYPDTAGPEAALEAEWFE GKN ADPILISLKHGYIP GKN RDLK VVKN ILDS KPA ANK KSE FSCAP KKP TDAS-434
mCor 5:	356-SDSYQEDIYPMT PGTE PAL TPDE WLGGIN RDP V LS ML KEGY --- K - KSS K VV F KAP I RE KK S VV V NG ID LLEN V PPRT -430
mCor 6A:	358-SDLFQDDLYPDT PGPE PALEA DEW LSGQ DAE PV LIS L KEGY VPP KH REL RVTK RN ILDV RPAS PRRS QSAS-429

Figure 5.16. Sequence alignment of mouse coronin linker domains.

The F-actin association of coronin 1 depends furthermore on the presence of the N-terminal β -propeller domain as deletion of this domain abolished coronin 1 interaction with the F-actin cytoskeleton both *in vivo* and *in vitro*. About the function of this domain in F-actin cytoskeleton interaction it can so far only be speculated. It might help to keep the molecule in a certain three-dimensional conformation allowing the stretches of basic amino acids to be in proximity to one another or it might be important *in vivo* for localization of coronin 1 to locations in the cell where it can interact with actin.

In contrast to a previous report (Oku *et al.*, 2003), which located two F-actin binding site in the N-terminal β -propeller domain of coronin 1, we could not find any evidence that these regions interact with the F-actin cytoskeleton *in vivo*. This might be due to the different approaches chosen for investigation. Oku *et al.* used truncated proteins of the N-terminal β -propeller domain to study *in vitro* F-actin co-sedimentation. As truncation might interfere with the proper folding of the β -propeller *in vitro*, the accessibility of the mapped binding sites to actin might be completely different *in vivo*.

How does coronin 1 interact with the F-actin cytoskeleton is not known so far. It can occur directly (Oku *et al.*, 2003) or indirectly by binding to F-actin filaments via Arp 2/3 complexes. So it was shown in *S. cerevisiae* that the C-terminal part including the linker region and the coiled coil domain of Crn1p can bind and modulate Arp2/3 activity *in vitro* (Humphries *et al.*, 2002; Rodal *et al.*, 2005).

To better understand the role of coronin 1 in the interaction with the F-actin cytoskeleton further *in vitro* studies with recombinant coronin 1 protein, which could not be obtained so far, are necessary.

5.4.2. Interaction of coronin 1 with the plasma membrane

Besides interaction with the F-actin cytoskeleton, coronin 1 binds to the plasma membrane. As shown in this chapter, the globular N-terminal β -propeller domain of coronin 1 mediates this binding. In contrast to coronin 3 (Spoerl *et al.*, 2002), plasma membrane association of coronin 1 does not depend on the oligomerization state. Furthermore it is F-actin independent as deletion of actin-binding site (construct Cor1- Δ 400-416-HA) as well as disruption of the F-actin cytoskeleton by latruncilin B treatment does not interfere with the plasma membrane interaction of coronin 1. It is not yet known how coronin 1 binds to the plasma membrane. Possible binding partners might include lipid moieties (Gatfield and Pieters, 2000) or integral or peripheral proteins which may interact with WD40 repeats of the N-terminal β -propeller domain.

In addition, it is unclear how the subcellular localization of coronin 1 is controlled. Regulation of membrane and cytoskeletal association via a switch in the coronin 1 oligomerization state is unlikely because trimers are the only detected species in macrophages but it may be regulated by phosphorylation (Itoh *et al.*, 2002).

5.4.3. What is the function of coronin 1 in immune cells?

Signaling through many receptors found on immune cells can trigger rapid rearrangement of the actin cytoskeleton. Among these are lymphocyte antigen receptors, phagocytic receptors as well as cell adhesion molecules (Allen and Aderem, 1996; Fischer *et al.*, 1998; Fuller *et al.*, 2003; Gruenheid and Finlay, 2003). Plasma membrane-cytoskeletal linkers connect extracellular signals from these receptors with the intracellular remodelling of the F-actin cytoskeleton. Like many plasma membrane-cytoskeletal linker molecules such as filamin (platelets), myosin1 (non-muscle cells), ezrin (epithelial cells) and dystrophin (muscle cells) coronin 1 contains two isolated binding sites for the plasma membrane and for the F-actin cytoskeleton indicating that it may fulfil a similar function (Rafael *et al.*, 1996; Jontes and Milligan, 1997; Stossel *et al.*, 2001; Schafer, 2002; Ivetic and Ridley, 2004).

Such a role for coronins as integrators of cellular structural components has also been suggested before for *S. cerevisiae* Crn1p (Heil-Chapdelaine *et al.*, 1998) which has binding sites for the actin cytoskeleton and microtubules. By linking the plasma membrane to the underlying actin cytoskeleton in immune cells, coronin 1, either via direct or indirect binding to transmembrane receptors, may facilitate the integration of extracellular signals with F-actin remodelling.

5.5. References

- Allen, L.A., Aderem, A. Mechanisms of phagocytosis. *Curr Opin Immunol.* 1996, **8**: 36-40. Review.
- Asano, S., Mishima, M., Nishida, E. Coronin forms a stable dimer through its C-terminal coiled coil region: an implicated role in its localization to cell periphery. *Genes Cells.* 2001, **6**: 225-35.
- Das, V., Nal, B., Roumier, A., Meas-Yedid, V., Zimmer, C., Olivo-Marin, J.C., Roux, P., Ferrier, P., Dautry-Varsat, A., Alcover, A. Membrane-cytoskeleton interactions during the formation of the immunological synapse and subsequent T-cell activation. *Immunol Rev.* 2002, **189**: 123-35. Review.
- de Hostos, E.L. The coronin family of actin-associated proteins. *Trends Cell Biol.* 1999, **9**: 345-50. Review.
- de Hostos, E.L., Rehfuess, C., Bradtke, B., Waddell, D.R., Albrecht, R., Murphy, J., Gerisch, G. Dictyostelium mutants lacking the cytoskeletal protein coronin are defective in cytokinesis and cell motility. *J Cell Biol.* 1993, **120**: 163-73.
- de Hostos, E.L., Bradtke, B., Lottspeich, F., Guggenheim, R., Gerisch, G. Coronin, an actin binding protein of Dictyostelium discoideum localized to cell surface projections, has sequence similarities to G protein beta subunits. *EMBO J.* 1991, **10**: 4097-104.
- Fenteany, G., Glogauer, M. Cytoskeletal remodeling in leukocyte function. *Curr Opin Hematol.* 2004, **11**: 15-24. Review.
- Ferrari, G., Langen, H., Naito, M., Pieters, J. A coat protein on phagosomes involved in the intracellular survival of mycobacteria. *Cell.* 1999, **97**: 435-47.
- Fischer, K.D., Tedford, K., Penninger, J.M. Vav links antigen-receptor signaling to the actin cytoskeleton. *Semin Immunol.* 1998, **10**: 317-27. Review.
- Frank, S., Schulthess, T., Landwehr, R., Lustig, A., Mini, T., Jenö, P., Engel, J., Kammerer, R.A. Characterization of the matrilin coiled-coil domains reveals seven novel isoforms. *J Biol Chem.* 2002, **277**: 19071-9.
- Fukui, Y., Engler, S., Inoue, S., de Hostos, E.L. Architectural dynamics and gene replacement of coronin suggest its role in cytokinesis. *Cell Motil Cytoskeleton.* 1999, **42**: 204-17.
- Fuller, C.L., Braciale, V.L., Samelson, L.E. All roads lead to actin: the intimate relationship between TCR signaling and the cytoskeleton. *Immunol Rev.* 2003, **191**: 220-36. Review.
- Gatfield, J., Albrecht, I., Zanolari, B., Steinmetz, M.O., Pieters, J. Association of the Leukocyte Plasma Membrane with the Actin Cytoskeleton through Coiled Coil-mediated Trimeric Coronin 1 Molecules. *Mol Biol Cell.* 2005, **16**: 2786-98.
- Gatfield, J., Pieters, J. Essential role for cholesterol in entry of mycobacteria into macrophages. *Science.* 2000, **288**: 1647-50.
- Grogan, A., Reeves, E., Keep, N., Wientjes, F., Totty, N.F., Burlingame, A.L., Hsuan, J.J., Segal, A.W. Cytosolic phox proteins interact with and regulate the assembly of coronin in neutrophils. *J Cell Sci.* 1997, **110**: 3071-81.
- Goode, B.L., Wong, J.J., Butty, A.C., Peter, M., McCormack, A.L., Yates, J.R., Drubin, D.G., Barnes, G. Coronin promotes the rapid assembly and cross-linking of actin filaments and may link the actin and microtubule cytoskeletons in yeast. *J Cell Biol.* 1999, **144**: 83-98.
- Gruenheid, S., Finlay, B.B. Microbial pathogenesis and cytoskeletal function. *Nature.* 2003, **422**: 775-81. Review.

- Heil-Chapdelaine, R.A., Tran, N.K., Cooper, J.A. The role of *Saccharomyces cerevisiae* coronin in the actin and microtubule cytoskeletons. *Curr Biol.* 1998, **19**: 1281-4.
- Humphries, C.L., Balcer, H.I., D'Agostino, J.L., Winsor, B., Drubin, D.G., Barnes, G., Andrews, B.J., Goode, B.L: Direct regulation of Arp2/3 complex activity and function by the actin binding protein coronin. *J Cell Biol.* 2002, **159**: 993-1004.
- Ivetic, A., Ridley, A.J. Ezrin/radixin/moesin proteins and Rho GTPase signalling in leucocytes. *Immunology.* 2004, **112**: 165-76. Review.
- Itoh, S., Suzuki, K., Nishihata, J., Iwasa, M., Oku, T., Nakajin, S., Nauseef, W.M., Toyoshima, S. The role of protein kinase C in the transient association of p57, a coronin family actin-binding protein, with phagosomes. *Biol Pharm Bull.* 2002, **25**: 837-44.
- Jontes, J.D., Milligan, R.A. Brush border myosin-I structure and ADP-dependent conformational changes revealed by cryoelectron microscopy and image analysis. *J Cell Biol.* 1997 **139**: 683-93.
- Lambright, D.G., Sondek, J., Bohm, A., Skiba, N.P., Hamm, H.E., Sigler, P.B. The 2.0 Å crystal structure of a heterotrimeric G protein. *Nature.* 1996, **379**: 311-9.
- Maniak, M., Rauchenberger, R., Albrecht, R., Murphy, J., Gerisch, G. Coronin involved in phagocytosis: dynamics of particle-induced relocalization visualized by a green fluorescent protein Tag. *Cell.* 1995, **83**: 915-24.
- Meiri, K.F. Membrane/cytoskeleton communication. *Subcell Biochem.* 2004, **37**: 247-82. Review.
- Miletic, A.V., Swat, M., Fujikawa, K., Swat, W. Cytoskeletal remodeling in lymphocyte activation. *Curr Opin Immunol.* 2003, **15**: 261-8. Review.
- Nal, B., Carroll, P., Mohr, E., Verthuy, C., Da Silva, M.I., Gayet, O., Guo, X.J., He, H.T., Alcover, A., Ferrier, P. Coronin-1 expression in T lymphocytes: insights into protein function during T cell development and activation. *Int Immunol.* 2004, **16**: 231-40.
- Neer, E.J., Schmidt, C.J., Nambudripad, R., Smith, T.F. The ancient regulatory-protein family of WD-repeat proteins. *Nature.* 1994, **371**: 297-300. Review.
- Oku, T., Itoh, S., Okano, M., Suzuki, A., Suzuki, K., Nakajin, S., Tsuji, T., Nauseef, W.M., Toyoshima, S. Two regions are responsible for the actin binding of p57, a mammalian coronin family actin-binding protein. *Biol Pharm Bull.* 2003, **26**: 409-16.
- Okumura, M., Kung, C., Wong, S., Rodgers, M., Thomas, M.L. Definition of family of coronin-related proteins conserved between humans and mice: close genetic linkage between coronin-2 and CD45-associated protein. *DNA Cell Biol.* 1998, **17**: 779-87.
- Rafael, J.A., Cox, G.A., Corrado, K., Jung, D., Campbell, K.P., Chamberlain J.S. Forced expression of dystrophin deletion constructs reveals structure-function correlations. *J Cell Biol.* 1996, **134**: 93-102.
- Rodal, A.A., Sokolova, O., Robins, D.B., Daugherty, K.M., Hippenmeyer, S., Riezman, H., Grigorieff, N., Goode, B.L. Conformational changes in the Arp2/3 complex leading to actin nucleation. *Nat Struct Mol Biol.* 2005, **12**: 26-31.
- Rybakin, V., Clemen, C.S. Coronin proteins as multifunctional regulators of the cytoskeleton and membrane trafficking. *Bioessays.* 2005, **27**: 625-632.
- Rybakin, V., Stumpf, M., Schulze, A., Majoul, I.V., Noegel, A.A., Hasse, A. Coronin 7, the mammalian POD-1 homologue, localizes to the Golgi apparatus. *FEBS Lett.* 2004, **573**: 161-7.
- Schafer, D.A. Coupling actin dynamics and membrane dynamics during endocytosis. *Curr Opin Cell Biol.* 2002, **14**: 76-81. Review.

- Sondek, J., Bohm, A., Lambright, D.G., Hamm, H.E., Sigler, P.B. Crystal structure of a G-protein beta gamma dimer at 2.1A resolution. *Nature*. 1996, **379**: 369-74.
- Spoerl, Z., Stumpf, M., Noegel, A.A., Hasse, A. Oligomerization, F-actin interaction, and membrane association of the ubiquitous mammalian coronin 3 are mediated by its carboxyl terminus. *J Biol Chem*. 2002, **277**: 48858-67.
- Stossel, T.P., Condeelis, J., Cooley, L., Hartwig, J.H., Noegel, A., Schleicher, M., Shapiro, S.S. Filamins as integrators of cell mechanics and signalling. *Nat Rev Mol Cell Biol*. 2001, **2**: 138-45. Review.
- Suzuki, K., Nishihata, J., Arai, Y., Honma, N., Yamamoto, K., Irimura, T., Toyoshima, S. Molecular cloning of a novel actin-binding protein, p57, with a WD repeat and a leucine zipper motif. *FEBS Lett*. 1995, **364**: 283-8.
- Tang, J.X., Janmey, P.A. The polyelectrolyte nature of F-actin and the mechanism of actin bundle formation. *J Biol Chem*. 1996, **271**: 8556-63.
- Vicente-Manzanares, M., Sancho, D., Yanez-Mo, M., Sanchez-Madrid, F. The leukocyte cytoskeleton in cell migration and immune interactions. *Int Rev Cytol*. 2002, **216**: 233-89. Review.
- Wohnsland, F., Schmitz, A.A., Steinmetz, M.O., Aebi, U., Vergeres, G. Interaction between actin and the effector peptide of MARCKS-related protein. Identification of functional amino acid segments. *J Biol Chem*. 2000, **275**: 20873-9.
- Yan, M., Collins, R.F., Grinstein, S., Trimble, W.S. Coronin-1 Function Is Required for Phagosome Formation. *Mol Biol Cell*. 2005.

- Chapter 6 -

Summary

The function of the immune system lies within pathogen recognition and the subsequent clearance of the pathogens from the body. This requires constant monitoring of the extra- and intracellular space for the presence of foreign materials. In the case of an infection, the immune system can immediately disarm pathogens (innate immunity) or, in the later phases of the infection, can induce a more pathogen specific immune response (adaptive immunity).

Antigen-presenting cells play a central role in the induction of an adaptive immune response as they are crucial for sampling, processing and presentation of antigens to naïve T-cells. Only upon recognition of the appropriate antigen, T-cells become activated and differentiate into effector T-cells. The two subsets of T-cells, the CD8⁺ and the CD4⁺ T-cells together ensure the elimination of both intracellular as well as extracellular pathogens. Whereas CD8⁺ T-cells after activation destroy infected cells, CD4⁺ T-cells mediate the host defense against extracellular microbes in concert with phagocytic cells and antibody producing B-cells.

The work presented in this thesis focuses on processes involved in the presentation of exogenous antigens whereby a role of cholesterol in these processes was defined. In addition, it was investigated how coronin 1 mediates the interaction between the plasma membrane and the cytoskeleton in antigen-presenting cells.

In the first part (Chapters 3 and 4) antigen internalization and processing was studied, addressing the issue of how exogenous antigens can gain access to the MHC class I processing pathway. This pathway, termed cross-presentation, was for a long time thought to be limited to endogenous cytosolic antigens. One way used by antigen-presenting cells to sample antigens for this cross-presentation is via macropinocytosis, an actin-dependent process resulting in the uptake of non-particulate material.

We found that in macrophages and dendritic cells, macropinosomes are cholesterol-rich structures. Removal of cellular cholesterol by pharmacological treatment led to a four-fold decrease in the uptake of fluid-phase markers. Time-lapse microscopy revealed that in cholesterol-depleted cells the formation of macropinosomes was impaired. Re-addition of cholesterol to cholesterol-depleted cells restored their macropinocytic activity indicating that cholesterol is required for macropinosome formation. In addition, inhibition of macropinosome formation interfered with the ability of macrophages to cross-present

exogenous antigens. In cholesterol-depleted macrophages, the model antigen ovalbumin could no longer be delivered into the MHC class I pathway.

The involvement of cholesterol in sampling of soluble antigens for cross-presentation raised the question of whether it is possible to specifically target exogenous antigens for MHC class I presentation by increasing their affinity to cholesterol. To achieve this, ovalbumin was chemically modified by palmitoylation. The covalent attachment of palmitic acid moieties to proteins is known to intracellularly promote the association of proteins with cholesterol-enriched plasma membrane domains. When ovalbumin was modified with palmitic acid, an enhanced internalization of ovalbumin in bone marrow-derived macrophages and an improved cross-presentation of this exogenous antigen was detected.

Defining a role of the palmitic acid moiety in cross-presentation can be performed by studying the effect of other lipid moieties on internalization and cross-presentation. Chapter 4 describes an attempt to introduce lipid tails into proteins via a chemical approach. Due to technical difficulties in the synthesis of activated lipids, needed for this protein modification, the question of specificity could not be addressed, and further investigations will be needed to perform the analysis.

The delivery of antigens into the MHC class I presentation pathway to induce a CTL response is necessary for the generation of immunity against many intracellular pathogens as well as against cancer and therefore vaccination strategies aim to enhance cross-presentation. The usage of palmitoylation as a general means to improve the MHC class I delivery of soluble proteins might have the potential for development of new vaccines, but as our results show, it is not suitable for every protein due to decreased solubility of palmitoylated proteins.

The second part of this thesis investigated the interaction of coronin 1, an actin-associated protein of the coronin 1 family, with the plasma membrane and the F-actin cytoskeleton. Due to its distinct expression pattern restricted mainly to leukocytes, coronin 1 could play a role in the regulation of cytoskeleton remodelling during an immune response by connecting extracellular signals with intracellular events.

Similar to other members of this family, coronin 1 possesses three domains; an N-terminal domain containing 5 WD40 repeats, predicted to form a seven bladed β -propeller, a short linker domain and a C-terminal coiled coil. In chapter 5 we show how each of the single coronin 1 domain contributes to binding of coronin 1 to the plasma membrane binding and to

the F-actin cytoskeleton. The F-actin interaction site was mapped in the linker region consisting of a stretch of positively charged amino acids. Interaction with the F-actin cytoskeleton via this site was dependent on the oligomerization state of coronin 1. Only upon trimerization of coronin 1 that was mediated by the coiled coil, association with the F-actin cytoskeleton could be observed. In addition, also the N-terminal β -propeller domain was shown to be necessary for cytoskeletal interaction. Furthermore, the β -propeller is the domain via which coronin 1 interaction with the plasma membrane is mediated. Together the results present a first step towards understanding how coronin 1 functions inside the cell.

-Appendix-

Appendix I: Abbreviations

aa	amino acid
amp ^r	ampicillin resistance
AP-1	activator protein
APC	antigen-presenting cell
APS	ammonium persulfate
Arp2/3	actin related protein
ATP	adenosintriphosphate
BCA	bicinchoninic acid
BM	bone marrow
BMDC	bone marrow derived dendritic cells
BMMØ	bone marrow derived macrophages
bp	base pair
BSA	bovine serum albumin
CC	coiled coil
CD	clusters of differentiation
CLIP	class II linked invariant chain peptide
CLAAP	chymostatin, <i>leupeptin</i> , <i>aprotinin</i> , <i>antipain</i> , <i>pepstatin</i>
Cor1	coronin 1
COSY	correlation spectroscopy
cpm	counts per minute
crn1p	coronin like protein
CTL	cytotoxic T-cell
CTLA	cytotoxic T-cell associated
kDA	kiloDalton
DAB	diaminobenzidine
DC	dendritic cells
DCC	dicyclohexyl carbodiimide
dH ₂ O	distilled water
DNA	deoxyribonucleic acid
DMAP	4-(dimethylamino)-pyridine
DMEM	Dulbecco's modified Eagle's medium
DMSO	dimethylsulfoxide
DRiPs	defective ribosomal products
DSC	N',N'-disuccinimidylcarbonate
DTT	dithiothreitol
<i>E. coli</i>	<i>Escheria coli</i>
EBSS	Eagle's balanced buffered saline
ECL	enhanced chemiluminescence
EDTA	ethylenediamine tetraacetate
EGFP	enhanced green fluorescent protein
ER	endoplasmatic reticulum
ERAD	ER-associated degradation
ERAP	ER aminopeptidase
ERp57	ER protein 57
ESI	electron spray ionization
FACS	fluorescence assisted cell sorting
FCS	fetal calf serum
FF	fast flow
FITC	fluorescein-isothiocyanate
FP	filter paper
FPLC	fast performance liquid chromatography
GFP	green fluorescence protein
GM-CSF	granulocyte-macrophage colony-stimulating factor
GTPase	guanosintriphosphatase
HA	hemagglutinin
Hac	acetic acid
HB	homogenization buffer

HBBS	Hank's balanced buffered saline
HEK293	human embryonic kidney cell 293
HEPES	hydroxyethylpiperidine-ethanesulfonic acid
HIC	hydrophobic interaction chromatography
hDC	human dendritic cells
HLA	human leukocyte antigen
HMG	hydroxymethylglutaryl
HP	high performance
HPLC	high performance liquid chromatography
HR	high resolution
HRP	horseradish peroxidase
HSQC	Heteronuclear Single-Quantum Coherence
kan ^r	kanamycin resistance
IPTG	isopropyl-beta-D-thiogalactopyranoside
INF	interferon
Ig	immunoglobulin
Ii	invariant chain
IL	interleukin
IM	influenza matrix protein
IMDM	Iscoves Modified Dulbecco's Medium
ITAM	immunoreceptor tyrosine-based activatory motif
LatB	latrunculin B
LAMP	lysosomal associated glycoprotein
LB	Luria-Bertani
LC-MS	liquid chromatography/mass spectrometry
LMP	latent membrane protein
LPS	lipopolysaccharide
M	mol/l
MACS	magnetic cell sorting
MALDI	Matrix Assisted Laser Desorption Ionization
MART-1	Melanoma-associated antigen recognized by T cells
MAT	matrilin
MIIC	MHC class II compartment
MCD	methyl-β-cyclodextrin
MECL-1	multicatalytic endopeptidase complex
MEM	Minimum Essential Medium
MHC	major histocompatibility complex
M _r	molecular weight
MW	molecular weight
m/z	mass / charge
NADPH	nicotin-amide-adenine dinucleotide phosphate
NEB	New England Biolabs
neo ^r	neomycin resistance
NF-AT	nuclear factor of activated T-cells
NFκB	nuclear factor κB
NHS	N-hydroxysuccinimide
NLS	nuclear localization sequence
NMR	nuclear magnetic resonance
OD _{xnm}	optic density at x nm
O/N	overnight
PAGE	polyacrylamide gel electrophoresis
PAK	p21 activated kinase
PAMPs	pathogen-associated molecular patterns
PB	peripheral blood
PBMC	peripheral blood monocytes
PBS	phosphate buffered saline
PBST	phosphate buffered saline with Tween
PE	phycoerythrin
PEG	polyethylene glycol
PFA	paraformaldehyde

Appendix I: Abbreviations

pH	potentia hydrogenii
PI3K	phosphatidylinositol-3-kinase
PIPES	piperazine-1,4-bis(2-ethanesulfonic) acid
PMA	phorbol-1.2-myrisate,1.3-acetate
pMHC	peptide: MHC complex
PMSF	phenylmethylsulfonylfluoride
PNS	post nuclear supernatant
ppm	parts per million
PPR	pattern recognition receptor
rad	radiation absorbed dose
RNA	ribonucleic acid
RNAi	RNA interference
rpm	revolutions per minute
RT	room temperature
SAP	shrimp alkaline phosphatase
SAP+	Saponin/PBS/BSA
SB	sample buffer
SC	succinimidyl carbonate
SD	standard deviation
SDS	sodium dodecylsulfate
SLS	static light scattering
SMAC	supramolecular activation cluster
SP	sulfopropyl
TAP	transporter associated with antigen processing
TACO	tryptophane aspartate containing coat protein
TBE	Tris-Borate-EDTA
TCA	trichloroacetic acid
TCR	T-cell receptor
TEMED	N,N,N',N'-tetramethylethylenediamine
TFA	trifluoroacetic acid
TLC	thin layer chromatography
TOF	time of flight
Tris	tris(hydroxymethyl)aminomethane
TXR	texas red
U	unit
US	unique short
UV	ultra violet
V	volt
WASP	Wiskott-Aldrich syndrome protein
WD	tryptophan-aspartase
X-Gal	5-bromo-4-chloro-3-indolyl-beta-D-galactopyranoside
ZAP 70	ζ-associated protein-70

Appendix II: Acknowledgements

First I would like to thank my supervisor Prof. Dr. Jean Pieters for giving me the possibility to perform this work in his laboratory. His enthusiasm, creativity and perseverance created an invaluable Ph.D. experience.

I am grateful to Prof. Dr. Antonius Rolink for being the co-referent of my thesis and who, together with Prof. Dr. Martin Spiess accompanied me as my thesis committee throughout my time as a Ph.D. student. Thanks to both of you.

I thank Dr. John Gatfield for helping me in the lab, for the scientific discussions and his input into my work. I am very happy that our common project on coronin 1 could be finished so successfully.

I also want to thank Giorgio Ferrari for introducing me into fluorescence and confocal microscopy, for the good Italian food and evenings at his home.

Thanks to those people who helped me on a technical level by teaching me methods and providing guidance and technical support;

Thanks to

Bettina Zanolari for the generation of some of the constructs used in this work,
Dr. Michel Steinmetz (Paul Scherrer Institut, Villingen) for his guidance in protein expression,
Jörg Widmer and David Avila (Hoffmann LaRocheAG) for peptide synthesis,
Lotte Kuhn for performing the 2D gel electrophoresis,
and of course to all the former and the present members of our laboratory.

Furthermore I am very grateful to:

Thierry Mini, Thomas Aust and Dr. Paul Jenö for the mass spectrometry analysis of my proteins,

Reto Schumacher and Prof. Dr. Giulio Spagnoli (ZLF, Kantonsspital Basel) for their help and of course for their regular blood donations, which kept my IM project going,

Dr. Oliver Schwardt and Prof. Dr. Beat Ernst (Pharmazentrum, Universität Basel) for their assistance in the synthesis of the activated fatty acids,

Ulrich Schröder and PD Dr. Cora-Ann Schönenberger for providing me with samples of actin,
Wolfgang Oppliger for the usage of the FPLC,
Prof. Dr. Hans-Peter Hauri for providing me with the Na/K-ATPase antibody,
and to animal facility for their expert assistance with the mice.

I am grateful to Erika Meier who had the patience to proofread my thesis.
Thanks to all my friends for the time we spent together both at work and at play.

Finally I want to thank Markus, my sister Anke and my parents for their great support. Without them this thesis would not be possible.